LI

LABORATORY INVESTIGATION

THE BASIC AND TRANSLATIONAL PATHOLOGY RESEARCH JOURNAL

VOLUME 99 | SUPPLEMENT 1 | MARCH 2019

USCAP 2019

ABSTRACTS

HEAD AND NECK PATHOLOGY (1162-1233)

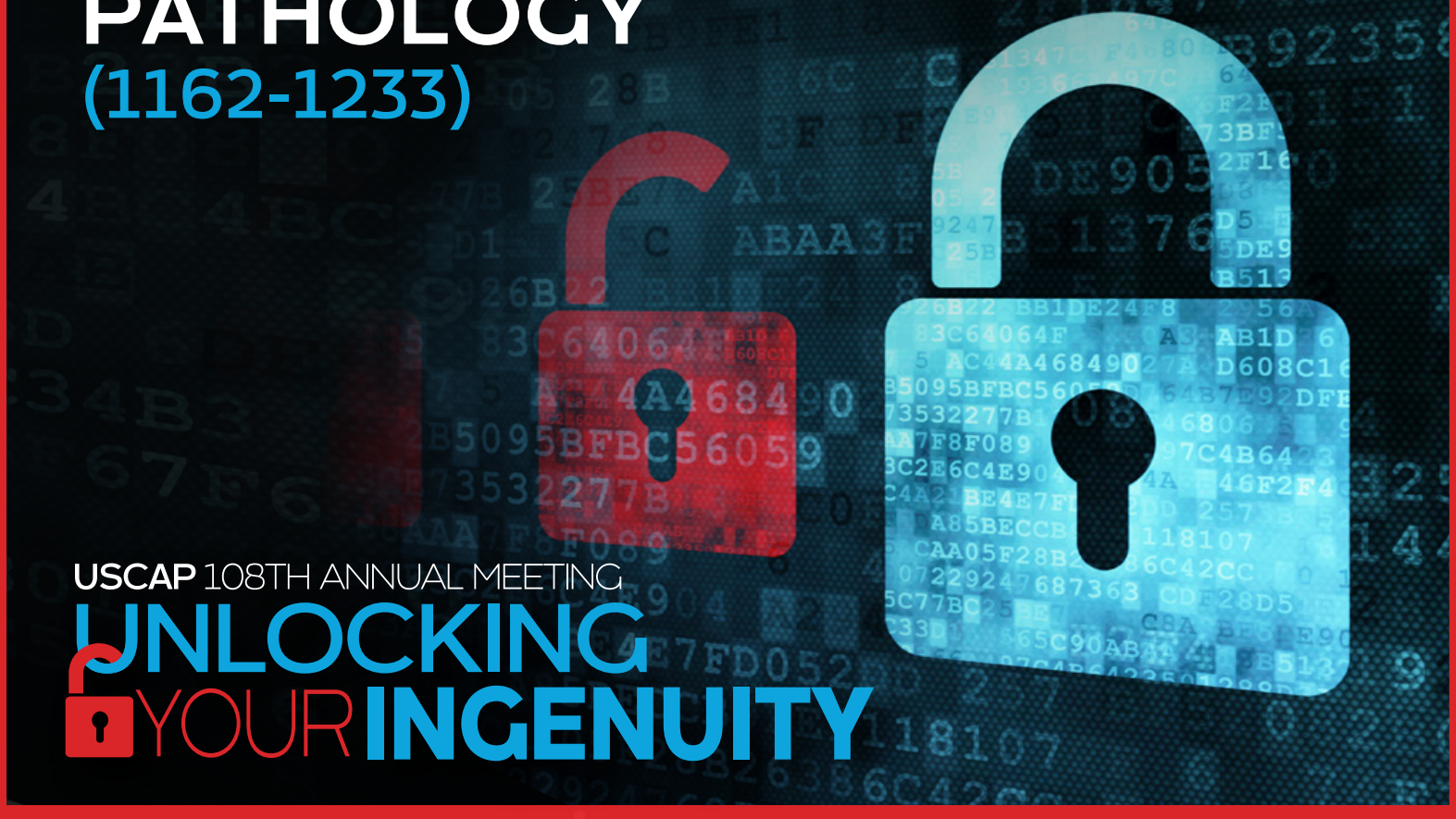

USCAP 108TH ANNUAL MEETING

UNLOCKING YOUR INGENUITY

MARCH 16-21, 2019

National Harbor, Maryland

Gaylord National Resort & Convention Center

Published by SPRINGER NATURE

www.ModernPathology.org

USCAP Creating a Better Pathologist

AN OFFICIAL JOURNAL OF THE UNITED STATES AND CANADIAN ACADEMY OF PATHOLOGY

EDUCATION COMMITTEE

Jason L. Hornick, Chair
Rhonda K. Yantiss, Chair, Abstract Review Board and Assignment Committee
Laura W. Lamps, Chair, CME Subcommittee
Steven D. Billings, Interactive Microscopy Subcommittee
Shree G. Sharma, Informatics Subcommittee
Raja R. Seethala, Short Course Coordinator
Ilan Weinreb, Subcommittee for Unique Live Course Offerings
David B. Kaminsky (Ex-Officio)
Aleodor (Doru) Andea
Zubair Baloch
Olca Basturk
Gregory R. Bean, Pathologist-in-Training
Daniel J. Brat
Ashley M. Cimino-Mathews
James R. Cook
Sarah M. Dry
William C. Faquin
Carol F. Farver
Yuri Fedoriw
Meera R. Hameed
Michelle S. Hirsch
Lakshmi Priya Kunju
Anna Marie Mulligan
Rish Pai
Vinita Parkash
Anil Parwani
Deepa Patil
Kwun Wah Wen, Pathologist-in-Training

ABSTRACT REVIEW BOARD

Benjamin Adam
Michelle Afkhami
Narasimhan (Narsi) Agaram
Rouba Ali-Fehmi
Ghassan Allo
Isabel Alvarado-Cabrero
Christina Arnold
Rohit Bhargava
Justin Bishop
Jennifer Boland
Elena Brachtel
Marilyn Bui
Shelley Caltharp
Joanna Chan
Jennifer Chapman
Hui Chen
Yingbei Chen
Benjamin Chen
Rebecca Chernock
Beth Clark
James Conner
Alejandro Contreras
Claudiu Cotta
Timothy D'Alfonso
Farbod Darvishian
Jessica Davis
Heather Dawson
Elizabeth Demicco
Suzanne Dintzis
Michelle Downes
Daniel Dye
Andrew Evans
Michael Feely
Dennis Firchau
Larissa Furtado
Anthony Gill
Ryan Gill
Paula Ginter
Tamara Giorgadze
Raul Gonzalez
Purva Gopal
Anuradha Gopalan
Jennifer Gordetsky
Rondell Graham
Alejandro Gru
Nilesh Gupta
Mamta Gupta
Krisztina Hanley
Douglas Hartman
Yael Heher
Walter Henricks
John Higgins
Mai Hoang
Mojgan Hosseini
Aaron Huber
Peter Illei
Doina Ivan
Wei Jiang
Vickie Jo
Kirk Jones
Neerja Kambham
Chiah Sui (Sunny) Kao
Dipti Karamchandani
Darcy Kerr
Ashraf Khan
Rebecca King
Michael Kluk
Kristine Konopka
Gregor Krings
Asangi Kumarapeli
Alvaro Laga
Cheng-Han Lee
Zaibo Li
Haiyan Liu
Xiuli Liu
Yan-Chun Liu
Tamara Lotan
Anthony Magliocco
Kruti Maniar
Jonathan Marotti
Emily Mason
Jerri McLemore
Bruce McManus
David Meredith
Anne Mills
Neda Moatamed
Sara Monaco
Atis Muehlenbachs
Bita Naini
Dianna Ng
Tony Ng
Ericka Olgaard
Jacqueline Parai
Yan Peng
David Pisapia
Alexandros Polydorides
Sonam Prakash
Manju Prasad
Peter Pytel
Joseph Rabban
Stanley Radio
Emad Rakha
Preetha Ramalingam
Priya Rao
Robyn Reed
Michelle Reid
Natasha Rekhtman
Michael Rivera
Michael Roh
Andres Roma
Avi Rosenberg
Esther (Diana) Rossi
Peter Sadow
Safia Salaria
Steven Salvatore
Souzan Sanati
Sandro Santagata
Anjali Saqi
Frank Schneider
Jeanne Shen
Jiaqi Shi
Wun-Ju Shieh
Gabriel Sica
Deepika Sirohi
Kalliopi Siziopikou
Lauren Smith
Sara Szabo
Julie Teruya-Feldstein
Gaetano Thiene
Khin Thway
Rashmi Tondon
Jose Torrealba
Evi Vakiani
Christopher VandenBussche
Sonal Varma
Endi Wang
Christopher Weber
Olga Weinberg
Sara Wobker
Mina Xu
Shaofeng Yan
Anjana Yeldandi
Akihiko Yoshida
Gloria Young
Minghao Zhong
Yaolin Zhou
Hongfa Zhu
Debra Zynger

1162 Ameloblastic Fibrosarcoma: Clinicopathological and Molecular Analysis of 7 Cases Highlighting Frequent BRAF and Rare NRAS Mutations

Abbas Agaimy[1], Alena Skalova[2], Alessandro Franchi[3], Rana Alshagroud[4], Robert Stoehr[5], Daniel Baumhoer[6], Sebastian Bauer[7]
[1]Erlangen, Germany, [2]Charles University, Faculty of Medicine in Plzen, Plzen, Czech Republic, [3]University di Pisa, Pisa, Italy, [4]Riyadh, Saudi Arabia, [5]Institute of Pathology, University Hospital, Erlangen, Erlangen, Germany, [6]University Hospital Basel, Basel, Switzerland, [7]University of Duisburg-Essen, University Hospital Essen, Essen, Germany

Disclosures: Abbas Agaimy: None; Alena Skalova: None; Alessandro Franchi: None; Rana Alshagroud: None; Robert Stoehr: None; Daniel Baumhoer: None; Sebastian Bauer: *Grant or Research Support*, Novartis; *Advisory Board Member*, Novartis; *Advisory Board Member*, Lilly; *Grant or Research Support*, Blueprint Medicines; *Consultant*, Deciphera

Background: Ameloblastic fibrosarcoma (AFS) is an aggressive neoplasm of odontogenic origin that features malignant mesenchymal spindle cell stroma in addition to ameloblastoma-like epithelial component. AFS is exceedingly rare with <100 cases reported so far. AFS is considered the malignant counterpart of ameloblastic fibroma (AF). Although frequent BRAF mutations have been recognized as driver mutations in ameloblastoma, the molecular pathogenesis of AFS remained elusive.

Design: We herein describe clinicopathological features of 7 unreported AFS cases and analyzed them for the first time for RAS/RAF alterations using NGS panels (TST15) and mutation site specific SNaPshot assay. Immunohistochemistry for mutant BRAF was done using the mutation-specific VE1 antibody.

Results: Patients were four females and three males aged 23 to 57 years (median, 26). Three tumors developed after one or multiple recurrences of ameloblastic fibroma (4 to 20 years after initial diagnosis), two showed transition from ameloblastic fibroma-like bland areas and two developed de novo. All patients were treated by surgery; adjuvant chemotherapy was given to one patient. At last follow-up, four patients were alive and well (13 to 344 months). One patient was a recent case and the remainder were lost to follow-up. Histological examination showed variable sarcomatous stromal overgrowth associated with varying degree of atypia and increased mitotic activity. The ameloblastoma-like epithelial component was invariably present in all cases but varied greatly depending on the degree of sarcomatous overgrowth. Of five cases tested successfully, four had BRAF V600E and one had NRAS p.Gln61Lys mutations. The components of one case were tested separately after manual microdissection and both showed V600E but VE1 IHC was positive only in the mesenchymal component suggesting possible contamination of the epithelial component.

Conclusions: To our knowledge, this is the first study reporting *RAF/RAS* gene mutations in ameloblastic fibrosarcoma. Given the activity of inhibitors against RAF and MEK across different cancers harboring V600E mutations our data strongly suggest to have all AFS genetically tested and to clinically investigate targeted treatment approaches in this extremely rare sarcoma subtype.

1163 Histologic Predictors of Treatment Response to Neoadjuvant PD-L1 Inhibitor Therapy in High-Risk HPV-Negative Head and Neck Squamous Cell Carcinomas

Zahra Alipour[1], Ian Hagemann[2], Paul Zolkind[3], Brian Nussenbaum[4], Ryan Jackson[2], Jason Rich[2], Pipkorn Patrik[2], Randal Paniello[2], Wade Thorstad[2], Loren Michel[5], Peter Oppelt[2], Douglas Adkins[6], Ravindra Uppaluri[7], Rebecca Chernock[6]
[1]Washington University in St. Louis, Clayton, MO, [2]Washington University in St. Louis, St. Louis, MO, [3]Barnes Jewish Hospital/Washington University, St. Louis, MO, [4]American Board of Otolaryngology, Houston, TX, [5]Memorial Sloan Kettering Cancer Center, New York, NY, [6]Washington University School of Medicine, St. Louis, MO, [7]Dana-Farber/Brigham and Women's Cancer Center, Boston, MA

Disclosures: Zahra Alipour: None; Ian Hagemann: None; Paul Zolkind: None; Brian Nussenbaum: None; Ryan Jackson: None; Jason Rich: None; Pipkorn Patrik: None; Randal Paniello: None; Wade Thorstad: None; Loren Michel: None; Peter Oppelt: *Speaker*, Bristol Myers Squibb; Douglas Adkins: *Grant or Research Support*, Merck & Co., Inc.; *Advisory Board Member*, Merck; Ravindra Uppaluri: *Advisory Board Member*, Merck & Co., Inc.; Rebecca Chernock: *Consultant*, Merck & Co., Inc.

Background: Pembrolizumab is an effective therapy in a subset of head and neck squamous cell carcinomas (HNSCC). An unmet need exists to define a biomarker-based approach to optimize patient selection. In lung cancer, limited evidence suggests that certain histologic features, such as solid type adenocarcinoma, may correlate with pathologic treatment response (PTR). Here, we perform an exploratory analysis to correlate histologic features in pre-treatment biopsies to PTR on subsequent resection specimens in surgically treated, high-risk HPV-negative HNSCC patients who received a single neoadjuvant dose (200 mg) of Pembrolizumab in a Phase II clinical trial.

Design: The following histologic features were evaluated in pre-treatment primary tumor biopsies from 33 enrolled patients: tumor grade, nuclear anaplasia (nucleus 3x the size of adjacent tumor cells), multinucleation, mitoses (per $2mm^2$), necrosis, LVI, PNI, infiltrating lymphocytes, neutrophils or eosinophils, tumor budding (nests of <5 cells), stromal desmoplasia and histologic type. Worst pattern of invasion and depth of invasion could not be assessed (biopsy material). Previously reported PTR (defined as percent of the tumor bed showing treatment effect manifested as giant cell reaction to keratinous debris and/or necrosis) on the post-pembrolizumab surgical resection specimens was grouped as follows: 1) minimal/no response (<10% PTR), 2) moderate response (10-50% PTR), 3) significant response (>50% PTR). PTR in lymph node metastases (LN) and primary tumors (P) were scored separately.

Results: PTR was observed in 30.3% in the P (4 moderate and 6 significant), in 27.3% in the LN (6 moderate and 3 significant) and in 45.5% in either site (7 moderate and 8 significant). All tumors were conventional HNSCCs except for 2 which were basaloid variants, both of which lacked PTR. Absence of stromal desmoplasia (seen in 12 cases, 60.0%) was the strongest predictor of PTR in both the P ($p<0.001$), LN ($p=0.0276$) or either site ($p=0.004$). Dense infiltrating lymphocytes (present in 9 cases, 28.1%) also correlated with PTR in the P and LN ($p=0.0668$ and $p=0.0037$, respectively). Low mitotic rate correlated with PTR in the P only ($p=0.0371$).

Conclusions: Absence of stromal desmoplasia in the pre-treatment tumor was the strongest histologic predictor of PTR to Pembrolizumab. While the mechanism is unknown, it is possible that stromal desmoplasia inhibits drug delivery or immune cell access to tumor thus limiting its effectiveness.

1164 Standalone p16 Immunohistochemistry is a Suboptimal Surrogate for HPV Status in Cervical Lymph Nodes: A Prospective Clinical Experience

Derek Allison[1], Maria Kryatova[2], Lisa Rooper[1]
[1]Johns Hopkins Hospital, Baltimore, MD, [2]Johns Hopkins University School of Medicine, Baltimore, MD

Disclosures: Derek Allison: None; Maria Kryatova: None; Lisa Rooper: None

Background: The 2018 College of American Pathologists Guidelines for Human Papillomavirus (HPV) Testing in Head and Neck Carcinomas state that p16 immunohistochemistry (IHC) can be used as a standalone surrogate marker of HPV status in metastatic squamous cell carcinoma (SCC) involving cervical lymph node levels II or III. Although the proclivity of oropharyngeal SCC to metastasize to levels II or III is well established, the specificity of p16 for transcriptionally active high-risk HPV has not been extensively evaluated in these levels. This study aims to assess the performance of p16 across cervical lymph node metastasis against the gold standard of HPV E6/E7 mRNA in-situ hybridization (ISH).

Design: All cervical lymph nodes biopsies evaluated for HPV at a large academic medical center between January 2015 and July 2018 were identified. A total of 104 metastatic SCC cases were included in this study, including suspected oropharyngeal or unknown primaries. HPV testing using both p16 IHC and HPV RNA ISH was performed prospectively at the time of diagnosis.

Results: The 104 biopsies were taken from 50 patients with a known oropharyngeal mass and 54 patients with an unknown primary; 73 biopsies targeted levels II or III and 31 sampled other or unknown levels. Across all levels, 78 metastatic SCC (75%) were p16 positive, of which 71 (91%) were also HPV positive. This included 52 p16-positive cases from levels II or III (71%), of which 48 (89%) were HPV positive, and 19 p16-positive cases from other or unknown levels (61%), of which 16 (84%) were HPV positive. The specificity of p16 for HPV involvement was 77% for cervical metastasis overall, ranging from 78% in levels II or III to 75% in other or unknown levels. Likewise, the positive predictive value of p16 for HPV positivity was 91%, ranging from 92% in levels II or III and 86% in other or unknown levels.

Conclusions: Even in a cohort enriched for patients with suspected oropharyngeal SCC, approximately 1 in every 5 patients with an HPV-negative SCC had p16-positive cervical lymph node samples, and 1 of every 10 p16-positive cervical lymph node biopsies were from HPV-negative SCC. The performance of p16 was not markedly better in levels II or III compared to other or unknown levels. In an era of therapeutic de-escalation, these results suggest a need for substantial caution in utilizing p16 as a standalone surrogate marker for HPV status in cervical lymph nodes.

1165 Clinicopathologic Features and Outcome of Head and Neck Spindle Cell Squamous Cell Carcinoma (SpC-SCC)

Bayan Alzumaili[1], Bin Xu[1], Carlos Prieto-Granada[2], Mohamed Rizwan Haroon Al Rasheed[3], Snjezana Dogan[1], Ronald Ghossein[1], Nora Katabi[1]
[1]Memorial Sloan Kettering Cancer Center, New York, NY, [2]University of Alabama at Birmingham, Birmingham, AL, [3]New York, NY

Disclosures: Bayan Alzumaili: None; Bin Xu: None; Carlos Prieto-Granada: None; Mohamed Rizwan Haroon Al Rasheed: None; Snjezana Dogan: None; Ronald Ghossein: None; Nora Katabi: None

Background: SpC-SCC is a rare variant of SCC, accounting for 0.5% of all Head and Neck (HN) SCCs. To date, little is known about SpC-SCC. We aimed to study the detailed clinicopathologic features of this tumor.

Design: A clinicopathologic review was conducted on 31 HN SpC-SCC by at least 2 HN pathologists.

Results: SpC-SCC occured most frequently in oral cavity (23/31, 74%), in particular oral tongue (15/31, 48%), followed by larynx (n=5, 16%), orpharynx (n=2, 6%) and sinonasal tract (n=1, 3%). It occured more commonly in non-smokers (17/31, 55%). Median patient's age was 64 (range 20-88). A slight male predominance was noted (M:F=1.4:1). Median tumor size, thickness and depth of invasion (DOI) were as follows: 18, 11 and 7 mm. Majority of tumors (25/31, 81%) was associated with conventional SCC (C-SCC), 22 were co-exisiting and 17

had C-SCC in prior materials, whereas 6 (19%) showed pure SpC-SCC. The C-SCC was keratininzing in most cases (20/22). In situ SCC and mild to moderate dysplasia were present in 27% and 10%, respectively.

Polypoid/exophytic growth and surface ulceration were seen 17/31 (61%) and 24/27 (89%), respectively. Histologically, the tumors showed sarcoma like pattern (23/31, 74%) or inflamed granulation like pattern (5/31, 16%). Tumor cells were spindled in 22/31 (71%) and epitheloid or pleomorphic in 15/31 (48%). One case (3%) showed heterologous malignant cartilage. Perineural and lymphovascular invasion were seen in 27% and 13%, respectively. Margins were positive for carcinoma in 6/26 (23%). By immunohistochemistry, tumors were positive for at least one keratin (AE1/3, Cam5.2, CK18, CK5/6 and 34BE12) in 10/17 (59%). P40 showed slightly higher immunopositivity (5/9) compared to p63 (3/7). Ki67 proliferation index ranged from 7% to 70% in 7 tested cases. Nine out of 19 patients (47%) had nodal metastasis in which the morphology was SpCC, C-SCC, or both (3 cases each).

Among the 29 patients with available follow up, 21 (72%) had recurrences (16 local, 11 regional, and 4 distant) and 11 (38%) died of their disease. Increased DOI but not tumor thickness was found to predict poorer overall survival (OS) (Log rank test, p=0.013). Compared to pure SpC-SCC, tumors associated with C-SCC showed a trend of improved OS (p=0.102).

Conclusions: HN SpC-SCC is an aggressive rare variant of SCC that is associated with variable morphology and proliferative rate which may create a diagnostic challenge. DOI and associated C-SCC appear to be prognostically relevant.

1166 Immunohistochemical Analysis of Respiratory Epithelial Adenomatoid Hamartomas/Seromucinous Hamartomas and Low-grade Tubulopapillary Adenocarcinomas: Related or Not?

Martina Baneckova[1], Alena Skalova[2], Michael Michal[3], Jan Laco[4], Michal Michal[5]
[1]Charles University, Faculty of Medicine in Plzen, Pilsen, Czech Republic, [2]Charles University, Faculty of Medicine in Plzen, Plzen, Czech Republic, [3]Charles University and Bioptic Laboratory Ltd. Pilsen, Plzen, Czech Republic, [4]The Fingerland Department of Pathology University Hospital Hradec Kralove, Hradec Kralove, Czech Republic, [5]Biopticka Laborator SRO, Plzen, Czech Republic

Disclosures: Martina Baneckova: None; Alena Skalova: None; Michael Michal: None; Jan Laco: None; Michal Michal: None

Background: Respiratory epithelial adenomatoid hamartoma (REAH) and seromucinous hamartoma (SH) are uncommon lesions of the sinonasal tract that are currently considered to be of hamartomatous nature and represent a morphological spectrum of one process. Low-grade tubulopapillary adenocarcinomas (LGTA) is a rare tumor belonging to the non-intestinal group of sinonasal adenocarcinomas. Based on our morphological observation, we hypothesized that REAH/SH could infrequently give rise to LGTA. Using a wide panel of antibodies, we attempted to corroborate our observations on the immunohistochemical (IHC) level.

Design: Ten cases of REAH and SH were retrieved from the authors' files. These cases were immunohistochemically analyzed by a mucin cocktail (MUC1, MUC2, MUC4, MUC5AC, MUC6), epithelial markers (CK7, CK20, CDX2, SATB2) and myoepithelial markers (S100 protein, p63, SOX10). Separate results were recorded for the serous, mucinous and respiratory component of REAH/SH. The same IHC panel was applied on 7 cases of LGTA.

Results: The serous component of REAH/SH was CK7 (10/10), MUC1 (9/10), MUC4 (5/10), SOX10 (9/10) and p63 (2/10) positive, other markers were negative. Respiratory component of REAH/SH was MUC1 (10/10), MUC4 (10/10), focally MUC5AC (10/10), p63 (10/10) and CK7 (4/10) positive, the remaining markers were not expressed. The mucinous component was negative with all markers. In all cases, all REAH/SH components were completely negative for CK20, CDX2, SATB2, MUC2, MUC6 and S100.- The LGTA expressed CK7 (7/7), MUC1 (4/7), focally MUC4 (7/7), SOX10 (6/7) and S100 (3/7) and was MUC2, MUC6, CK20, p63, and CDX2 negative. Only one LGTA was MUC5AC and SATB2 positive.

Conclusions: According to our results, all REAH cases were CK20 and CDX2 negative which clearly distinguishes them from intestinal-type lesions. Conversely, LGTA showed similar IHC profile to REAH/SH, particularly to its serous component. Therefore, it is possible that rather than hamartomas, REAH/SH represent a benign precursor of LGTA. Based on our observations, the neoplastic process follows the sequence REAH - SH – LGTA.

1167 Solitary Fibrous Tumors of The Head and Neck Region Revisited: Study of 20 Cases

Martina Baneckova[1], Petr Martinek[2], Alena Skalova[3], Marian Svajdler[2], Michal Michal[2]
[1]Charles University, Faculty of Medicine in Plzen, Pilsen, Czech Republic, [2]Biopticka Laborator SRO, Plzen, Czech Republic, [3]Charles University, Faculty of Medicine in Plzen, Plzen, Czech Republic

Disclosures: Martina Baneckova: None; Petr Martinek: None; Alena Skalova: None; Marian Svajdler: None; Michal Michal: None

Background: Solitary fibrous tumor (SFT) is a rare ubiquitous *NAB2-STAT6* fusion gene associated mesenchymal neoplasm that most commonly arises in the pleural site. SFTs of the head and neck region are rare, and were previously classified as hemangiopericytomas (HPC), giant-cell angiofibromas (of the orbit, GCA) and orbital fibrous histiocytomas.

Design: 20 cases of SFT of the head and neck region were retrieved from the authors' files. All cases were stained for STAT6 by immunohistochemistry and the next generation sequencing (NGS) was performed to verify the frequency of *NAB2-STAT6* fusion variants.

Results: The study included 11 females and 9 males, with no age predilection (range 13 - 77 years, median 51 years). The most common sites involved included posterior cervical (nuchal) region (7 cases), orbit (5 cases) and oral mucosa (4 cases). Two SFTs occurred in the sinonasal tract, one involved cheek and one was intradural at the level C7-Th1. Histologically, the growth pattern was cellular (HPC-like) in six cases, mixed SFT/HPC-like in 9, pure SFT in 3 and mixed SFT/GCA in two. Epithelioid morphology and areas of myxoid change were found in 2 and 9 tumors, respectively. Infiltrative growth pattern was noted in two cases. Based on histomorphology and follow-up, one case was classified as malignant. Intriguingly, in this malignant SFT, aberrant nuclear FLI1 expression was detected during the initial work-up. *NAB2-STAT6* fusion and nuclear STAT6 expression were confirmed in all cases. Three major fusion variants detected were *NAB2ex2-STAT6int1* (5/20, 25%), *NAB2ex6-STAT6ex16* (4/20, 20%), *and NAB2ex4-STAT6ex2* (3/20, 15%). No correlation was found between fusion variants, histological growth pattern and clinical behavior.

Conclusions: SFT is a potentially malignant tumor, which should be included in the differential diagnosis of spindle-cell and epithelioid lesions of the head and neck region. SFT may show several growth patterns that may be easily mistaken for other more common head and neck spindle-cell or epithelial lesions. STAT6 positivity and *NAB2-STAT6* fusion is present in all cases and represent useful ancillary markers in difficult cases.

1168 Microsecretory Adenocarcinoma: A Novel Salivary Gland Tumor Characterized by a Recurrent MEF2C-SS18 Fusion

Justin Bishop[1], Ilan Weinreb[2], David Swanson[3], Lisa Rooper[4], William Westra[5], Christina MacMillan[3], Brendan Dickson[6]
[1]University of Texas Southwestern Medical Center, Dallas, TX, [2]University Health Network, Toronto, ON, [3]Mount Sinai Hospital, Toronto, ON, [4]Johns Hopkins Hospital, Baltimore, MD, [5]Icahn School of Medicine at Mount Sinai, New York, NY,[6]Mount Sinai Health System, Toronto, ON

Disclosures: Justin Bishop: None; Ilan Weinreb: None; David Swanson: None; Lisa Rooper: None; William Westra: None; Christina MacMillan: None; Brendan Dickson: None

Background: Salivary gland adenocarcinoma not otherwise specified (NOS) is a heterogeneous group, likely containing distinct tumors not yet characterized. A growing number of low-intermediate grade tumors are known to harbor tumor-specific fusions; on occasion, identifying a novel fusion allows for recognition of a new salivary tumor type (e.g., secretory carcinoma). We sought to characterize a distinctive salivary adenocarcinoma that would previously have been regarded as adenocarcinoma NOS, and characterize its incidence among a group of other low-intermediate grade adenocarcinomas NOS.

Design: Based on the recognition of 3 morphologically distinct low-grade salivary carcinomas, we used targeted RNA sequencing (RNA-Seq) to determine whether these could be distinguished genetically from other fusion-associated salivary tumors. In addition to the index cases, RNA-Seq was performed on a cohort of 21 additional low-intermediate grade adenocarcinomas NOS from the authors' institutions (total N=24). Results were independently confirmed by RT-PCR.

Results: All 3 index cases harbored a *MEF2C-SS18* fusion. They arose in the oral cavity of 2 women and 1 man ranging from 21-80 years (mean 50) and shared near-identical histologic features: intercalated duct-like cells with eosinophilic to clear cytoplasm and small, uniform oval nuclei, infiltrative microcysts and cords, abundant intraluminal secretions, and cellular fibromyxoid stroma. Mitotic rates were low; necrosis was absent. *MEF2C-SS18* associated tumors were positive for S100 and p63, and negative for p40, SMA, calponin, and mammaglobin. The remaining cohort included a parotid tumor with overlapping features and a *SS18-ZBTB7A* fusion. In addition, single cases showed: *CRTC1-MAML2*, *CRTC3-MAML2*, *ETV6-NTRK3* and *MYB-NFIB* fusions; 4 contained other fusion genes of uncertain significance; 7 were negative by RNA-Seq; and 5 cases failed RNA extraction. Overall, 4 of 19 (21%) informative cases harbored *SS18* fusions.

Conclusions: Novel *MEF2C-SS18* fusions and unique histologic features characterize a new salivary gland adenocarcinoma for which we propose the term "microsecretory adenocarcinoma." This represented a small but significant fraction of adenocarcinoma NOS cases in this study. RNA-Seq helped to clarify this unique entity and identify 1 possibly related case with a different *SS18*-associated fusion. It also identified rare morphologic variants of other salivary neoplasms, as well as isolated fusion events that could represent altogether unique entities.

1169 Computing Dispersion - Distances of Cancer Satellites Are Associated with Disease Recurrence in Oral Cancer. Graphic-Based Analysis of Tumor Pattern of Invasion

Lauren Boehnke[1], Scott Doyle[2], Minhua Wang[3], Pooja Dhorajiya[4], Anna-Karoline Israel[5], Margaret Brandwein-Weber[6], Lei Zhang[7], Xulei Liu[4]

[1]University at Buffalo, Youngstown, NY, [2]University at Buffalo, Buffalo, NY, [3]The University of Texas MD Anderson Cancer Center, Houston, TX, [4]Mount Sinai Health System, New York, NY, [5]University of Rochester Medical Center, Rochester, NY,[6]Icahn School of Medicine at Mount Sinai, New York, NY, [7]The University of Texas MD Anderson Cancer Center, Gainesville, FL

Disclosures: Lauren Boehnke: None; Scott Doyle: None; Minhua Wang: None; Poojaben Dhorajiya: None; Anna-Karoline Israel: None; Margaret Brandwein-Weber: None; Lei Zhang: None; Xulei Liu: None

Background: Patients with early-stage (Stage I/II) oral cavity cancer (OCC) are typically treated with surgery alone. However, 25-37% of these patients will develop loco-regional recurrence (LRR), indicating the need for aggressive multi-modal therapy. A previously validated Histological Risk Model (HRM) is capable of predicting LRR risk with a positive predictive value 10% higher than other risk factors. The HRM is based on architectural features of histology such as worst pattern of invasion (WPOI), which characterizes the spatial dispersion of tumor "satellites" separated from the main tumor mass. Here, our goal is to improve the performance of the HRM using a quantitative computational pathology approach of extracting features at the tumor advancing edge to build a tissue architectural model that is predictive of LRR. Our features are modeled after the WPOI used in the HRM. We evaluate our model by predicting LRR status from patient histological images.

Design: Our dataset consists of digitized hematoxylin and eosin (H&E) tissue images from 48 OCC patients, 31 males, 17 females, ages 27 to 89 (mean 61 years) (See Table 1). Manual annotation of the digital slides is performed by a pathologist on a region of interest (ROI) depicting WPOI using three classes: main tumor, satellites, and background. Graphs are calculated based on this annotation, quantifying the spatial dispersion of the satellites. Architectural features are then extracted from the graphs, turning tissue architecture into a feature vector which is then used to train a simple decision tree classifier to recognize ROIs at risk of LRR. We calculate the true positive rate (TPR) and false negative rate (FNR) of the classifier, as well as the accuracy over 1000 rounds of 5-fold cross-validation.

Results: We obtain a TPR of 47% for identifying LRR and 83% for non-LRR. Our average classification accuracy is 64.6%. Figure 2 shows class separation of patients with LRR (green) and without (red).

Table 1. Characteristics of 48 OCC Patients

Variable	Number of Patients
AJCC Tumor Stage	
T1	27
T2	21
Cervical Lymph Node Status	
N_0	42
Occult metastasis	6
Worst Pattern of Invasion (WPOI)	
WPOI3	1
WPOI4	24
WPOI5	23
Disease Progression	
Yes	22
No	26

Figure 1 - 1169

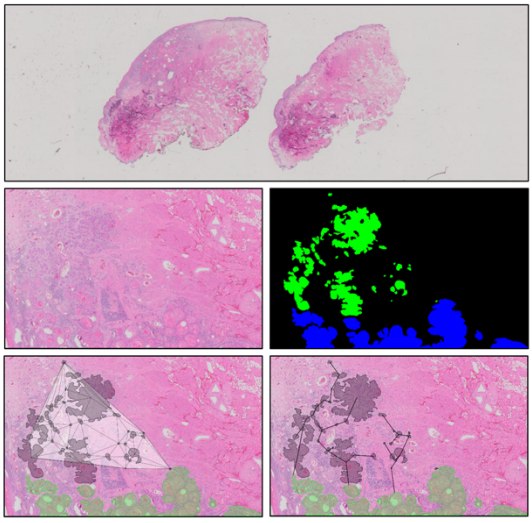

Figure 1: Example of a whole-slide image (top), along with an ROI depicting worst pattern of invasion (middle left) and the associated manual annotation (middle right). Also shown are examples of Delaunay triangulation (bottom left), and wave-graph (bottom right) used to extract quantitative architecture features.

Figure 2 - 1169

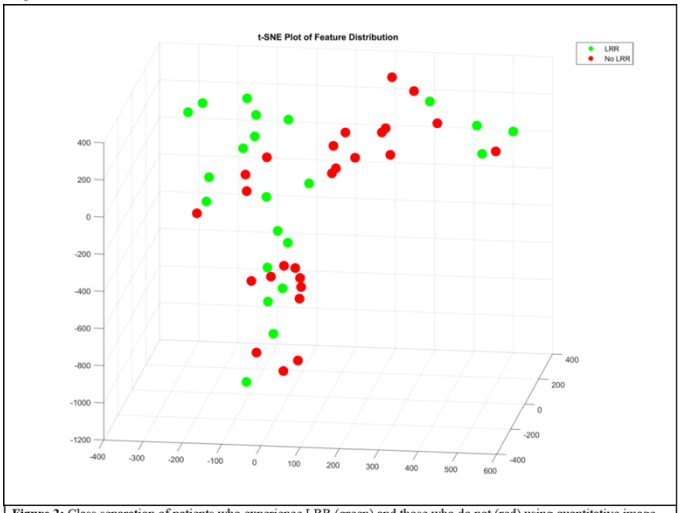

Figure 2: Class separation of patients who experience LRR (green) and those who do not (red) using quantitative image features. Each point is a region of interest characterized by quantitative architectural features; the axes of the scatter plot are obtained by reducing the high-dimensional feature space down to three dimensions using t-distributed Stochastic Neighborhood Embedding (t-SNE).

Conclusions: Our quantitative approach to predicting risk of LRR compliments the previously established HRM. Extracting features based on satellite distances is able to predict LRR. These results are encouraging as this small cohort is not yet adequately powered. The graph-based approach is a robust model for quantitatively assessing tissue architecture at the tumor boundaries. In future work, we will accrue a larger dataset to build a statistically-significant validation cohort for the classifier.

1170 Reappraisal of Epithelial-Myoepithelial Carcinoma Using Translocation-Associated Immunohistochemical Markers

Tiffany Chen[1], Jeffrey Mito[2], Jeffrey Krane[2], Vickie Jo[3]
[1]Brookline, MA, [2]Brigham and Women's Hospital, Boston, MA, [3]Brigham and Women's Hospital, Harvard Medical School, Boston, MA

Disclosures: Tiffany Chen: None; Jeffrey Mito: None; Jeffrey Krane: None; Vickie Jo: None

Background: Epithelial-myoepithelial carcinoma (EMCA) is a rare biphasic salivary gland malignancy that shows a broad morphologic spectrum. Recent studies indicate that a significant proportion of EMCA arise from pleomorphic adenoma (PA), with at least 50% having *PLAG1*or *HMGA2* rearrangement. Furthermore, hybrid carcinomas showing mixed patterns of EMCA and adenoid cystic carcinoma (AdCC) have also been recognized. We examined the immunohistochemical expression of PLAG1, HMGA2, and MYB in EMCA to better characterize the pathogenesis of EMCA, and assess the potential diagnostic utility of these translocation-associated markers.

Design: In-house and consultation cases diagnosed as EMCA (including 2 cases with hybrid EMCA-AdCC features and 1 EMCA which appeared as AdCC on recurrence) with material available for immunohistochemistry from 2006-2018 were retrieved from the surgical pathology archives. Immunohistochemistry for PLAG1, HMGA2, and MYB was performed, and nuclear expression was scored semi-quantitatively for extent (0; 1+, 1-10%; 2+, 11-50%; 3+, >50%) and intensity (weak, moderate, strong).

Results: Fifteen cases of EMCA were identified, including 9 males and 6 females with an age range of 34-83 years (median, 57). Tumor sites included: parotid (11), cavernous sinus (1), maxillary sinus (1), suprahyoid (1), and submandibular gland (1). Two EMCAs showed PLAG1 expression (1-2+ extent, moderate and weak intensity). HMGA2 expression was seen in 2 cases (both 1+ extent, moderate intensity). Four cases showed MYB expression ranging from 2+ (N=2; strong intensity) and 1+ (N=2; moderate and weak intensity); this included 2 hybrid EMCA-AdCC tumors, 1 EMCA metastasis to the cavernous sinus, and 1 EMCA which later recurred as AdCC (and subsequently found to have *MYB* rearrangement). No cases showed overlapping expression of translocation markers.

Conclusions: Immunohistochemical expression of translocation-associated markers PLAG1, HMGA2, and MYB is heterogeneous in EMCA and likely reflects the diverse pathogenetic mechanisms within this entity, including tumors that arise secondarily from PA and tumors showing hybrid features with AdCC. In conjunction with morphologic features, PLAG1, HMGA2, and MYB immunohistochemistry may serve as useful diagnostic adjuncts, particularly for cases that are better classified as AdCC or hybrid AdCC-EMCA, which show more aggressive behavior than classic EMCA.

1171 Gal-3 Expression in High-Risk HPV-Positive and Negative Head & Neck Squamous Cell Carcinomas

Joseph Coppock[1], Anne Mills[1], Edward Stelow[2]
[1]University of Virginia, Charlottesville, VA, [2]University of Virginia Health System, Charlottesville, VA

Disclosures: Joseph Coppock: None; Anne Mills: None; Edward Stelow: None

Background: Despite their higher stage at presentation, patients with high-risk (HR) HPV-related head and neck squamous cell carcinomas (HNSCCs) have better survival rates compared to those with non-HPV-related disease. While treatment is successful in at least 80% of patients, significant comorbidity and the number of patients who suffer failed treatment, recurrent disease, late metastasis, and death are increasing due to the rapidly increasing incidence of HPV-related HNSCCs. A CD8-positive T-cell-dependent immune response is required for clearance of this antigenic cancer subtype, providing a unique opportunity for the clinical employment of immune modulators in therapy. Galectin-3 (Gal-3) is a mammalian lectin and glycoprotein with numerous intra- and extracellular functions. It has been demonstrated to induce apoptosis of lymphocytes, decrease anti-tumor natural killer cell action, and suppress T-cell function and expansion, including of CD8-positive T-cells. Gal-3 inhibitors are currently available and under clinical investigation for various cancers.

Design: A tissue microarray (TMA) of primary and metastatic (lymph node) HNSCC was constructed containing 17 primary HR-HPV-positive (HPV+), 36 primary HPV-negative (HPV-), 11 metastatic HPV+, and 14 metastatic HPV- HNSCCs. HR-HPV status was determined by RNA in situ hybridization (RNA Scope, Advanced Cell Diagnostics). Gal-3 expression was compared by immunohistochemistry (IHC) (Cell Marque, 255-M15). At least 5% Gal-3 tumor cell staining was considered positive.

Results: Overall, HR-HPV+ cases were more likely to be Gal-3-positive (Gal+) [54% (15/28)] than HPV- cases [26% (13/50), p=0.03]. No significant difference in the overall number of Gal+ cases was identified between primary [42% (22/53)] and metastatic [24% (6/25)] cancers (p=0.2). 59% (10/17) of primary HPV+ cancers were Gal+ and 45% (5/11) of metastatic HPV+ cancers were Gal+ (p=0.06). 33% (12/36) of primary HPV- cancers were Gal+ and 7% (1/14) of metastatic HPV- cancers were Gal+ (p=0.08).

5% GAL-3		HPV RNA ISH + (28)	HPV RNA ISH - (50)
Primary (53)	GAL+	10	12
	GAL-	7	24
Metastasis (25)	GAL+	5	1
	GAL-	6	13

Conclusions: Gal-3 positivity is observed in a subset of HNSCC, suggesting a potential role for therapeutic Gal-3 inhibition in this tumor type. The significantly higher rates of expression seen in HR-HPV+ versus HPV- HNSCC suggest particular promise in the setting of HPV infection. The relatively consistent Gal-3 expression rates observed between metastases and primaries argues against progressive Gal-3 expression in metastasis.

1172 Sinonasal non-keratinising squamous cell carcinoma: high prevalence of HPV infection and impact on the outcome

Valerie Costes Martineau[1], Mathieu Gallo[1], Louis Crampette[1], Nathalie Boulle[1], Morgan le Balch[1]
[1]CHU Montpellier, Montpellier, France

Disclosures:
Valerie Costes Martineau: None

Background: High risk human papillomavirus (HPV) is recognized as a driver for oropharyngeal non-keratinizing squamous cell carcinoma (NK-SCC) with a tremendous clinical significance due to their improved outcomes. Several studies have suggested that HR-HPV may also play a role in the pathogenesis of sinonasal NK-SCC. We studied a group of 29 sinonasal SCC for HPV positivity correlated with outcome.

Design: Twenty nine NK-SCC were studied (2002 – 2016) comprised 20 males and 9 females with a mean age of 62 (35 – 86 years). Six cases were associated with an inverted papilloma story (2 with metachronus and 4 with synchronous malignancy). The mean folow up was 69.12 months. HPV DNA testingwas performed by PCR using INNO-LIPA HPV genotyping (16, 18, 31, 33, 35, 39, 45, 51, 52, 56, 58, 59, 68, 26, 53, 66, 70, 73, 82, 6, 11, 40, 42, 43, 44, 54, 61, 81, 62, 67, 83, 89) . In situ hybridization was performed with the Roche INFORM HPV probes HIS (probes for genotypes 16, 18, 31, 33, 35, 39, 45, 51, 52, 56, 58, 66 and probes for genotypes 6, 11). Standard immunochemistry for p16 was performed on all cases. Strong cytoplasmic and nuclear staining in more than 70% of the tumor was considered as a positive result

Results: Results: sixteen cases were HPV ADN positive (55%). The more prevalent genotype were HPV18 (4) and HPV 16 (3). We found others genotypes: 26 (2), 33 (1), 39 (1), 56 (1) and 61 (1) with co-infection in 3 cases. All these cases except one (HPV11+) were p16 positive. 3/4 of the synchronous cases and ½ of the metachronous cases were HPV positive with the same genotype in the papilloma and the carcinoma. The HIS was positive only in 6/16 cases with very few punctate nuclear signals.Comparing the 2 HPV + and HPV- groups we did not observed any significant difference concerning the sex ratio, the age or the histology. However the outcome was significantly different. Eigh on 13 patients were well without disease in the HPV+ group (61%) compared to only 5/13 patients in the HPV- group (38%).

Conclusions: This study confirm a high prevalence of HPV in sinonasal NK-SCC (55%) but with limited genomic integration in HIS. Interestingly, HPV positive NK-SCC seem to have a more favorable outcome than their HPV negative counterpart.

1173 Genomic Analysis of 134 Squamous Cell Carcinomas Arising in the Base of Tongue Diagnosed From 1985 to 2017

Snjezana Dogan[1], Bin Xu[1], Mohsin Jamal[1], Sumit Middha[1], Chad Vanderbilt[2], Anita Bowman[3], Venkatraman E. Seshan[1], Michael Berger[1], Lara Dunn[1], Sean M. McBride[1], Ian Ganly[1]
[1]Memorial Sloan Kettering Cancer Center, New York, NY, [2]Memorial Sloan Kettering Cancer Center, Denver, CO, [3]Memorial Sloan Kettering Cancer Center, Yeadon, PA

Disclosures: Snjezana Dogan: None; Bin Xu: None; Mohsin Jamal: None; Sumit Middha: None; Chad Vanderbilt: None; Anita Bowman: None; Venkatraman E. Seshan: None; Michael Berger: *Consultant*, Roche; *Grant or Research Support*, Illumina; Lara Dunn: None; Sean M. McBride: *Consultant*, Bristol-Myers Squibb; *Grant or Research Support*, Janssen; Ian Ganly: None

Background: The incidence of HPV-driven oropharyngeal squamous cell carcinomas (SCC) is on the rise over the past 30 years. Here we studied a large retrospective cohort of squamous cell carcinomas (SCC) arising exclusively in the base of tongue (BOT). We aimed (1) to explore the temporal trends in frequency of HPV-positive (HPV-P) SCC in this location, (2) to examine the mutational profile relative to the HPV status, and (3) to compare mutational profile of HPV negative (HPV-N) BOTSCC to that of HPV-N oral (OSCC) and laryngeal SCC (LSCC).

Design: A total of 134 BOTSCC (89 primary tumors, 43 metastases and 2 local recurrences) were subjected to hybridization capture sequencing of 341-468 cancer-related genes by the MSK-IMPACT assay, including 68 research cases diagnosed from 1985-2005 ("old cohort", OC) and 66 clinical cases diagnosed from 2008-2017 ("new cohort", NC). HPV/p16 status was determined by HPV *in situ* hybridization, p16 immunohistochemistry, and/or by using a bioinformatics algorithm based on mapping of off-target MSK-IMPACT sequencing reads to the HPV genome.

Results: BOTSCC was overall more common in men (N=107, 80%) than in women; they presented at median age 61 years (range 33-79 years), and 62 years (range 27-84 years), respectively. HPV-P SCC was more frequent in NC than in OC (82% vs 54%, p=0.0008). The proportion of HPV-P SCC among women was similar in NC and OC (56% and 61%) but was significantly higher among men in NC (86% vs 52%, p=0.0002). In HPV-P SCC, the most frequently mutated gene was *PIK3CA* (32%). HPV-N SCC had significantly more alterations in *TP53* (81% vs 12%), *FGF3/FGF4/FGF19/CCND1* (28% vs 2%), *SOX2* (33% vs 15%) and *TP63* (33% vs 13%). HPV-N BOTSCC had fewer *CDKN2A* alterations than HPV-N OSCC and LSCC (6% vs 56% vs 56%, respectively) and more *NOTCH3* mutations (16% vs 5% vs 4%, respectively); had fewer *FAT1* (34% vs 14%), and more *SOX2* and *TP63* alterations than HPV-N OSCC, and fewer *PIK3CA* mutations than HPV-N LSCC (21% vs 51%; **Table 1**).

Table 1. Mutational profile of BOTSCC by HPV status. P values compare the mutational frequencies between HPV-P and HPV-N BOT SCC (left), HPV-N BOTSCC and HPV-N OSCC (middle), and HPV-N BOTSCC and HPV-N LSCC (right).

	Current study					TCGA, Nature 2015					
Gene	BOT SCC, HPV-P (N=91)		BOT SCC, HPV-N (N=43)			Oral SCC, HPV-N (N=160)			Larynx SCC, HPV-N (N=71)		
	N	%	N	%	p value	N	%	p value	N	%	p value
TP53	11	12.0%	35	81.0%	0.0001	129	81%	ns	66	93%	0.07
CDKN2A	0	0.0%	2	5.0%	0.0001	90	56%	0.0001	40	56%	0.0001
CDKN2B	1	1.1%	7	16.0%	ns	44	28%	ns	22	31%	ns
FAT1	7	8.0%	6	14.0%	ns	54	34%	0.01	19	28%	ns
PIK3CA	29	32.0%	9	21.0%	ns	44	28%	ns	36	51%	0.002
SOX2	14	15.0%	14	33.0%	0.004	20	13%	0.005	26	38%	ns
TP63	12	13.0%	14	33.0%	0.01	22	14%	0.007	26	37%	ns
NOTCH1	9	10.0%	9	21.0%	ns	36	23%	ns	16	23%	ns
FGF3	2	2.2%	13	30.0%	0.0001	41	26%	ns	26	37%	ns
FGF4	2	2.2%	12	28.0%	0.0001	41	26%	ns	26	37%	ns
FGF19	2	2.2%	12	28.0%	0.0001	43	27%	ns	26	37%	ns
CCND1	2	2.2%	13	30.0%	0.0001	43	27%	ns	26	37%	ns
KMT2D	7	8.0%	7	16.0%	ns	22	14%	ns	17	24%	ns
EGFR	1	1.1%	3	7.0%	0.097	25	16%	ns	10	15%	ns
MYC	4	4.0%	2	5.0%	ns	20	13%	ns	12	18%	0.076
CASP8	2	2.2%	2	5.0%	ns	25	16%	0.075	4	6%	ns
NFE2L2	4	4.0%	2	5.0%	ns	20	13%	ns	9	14%	ns
CUL3	2	2.2%	2	5.0%	ns	4	3%	ns	9	14%	ns
KEAP1	3	3.0%	1	2.3%	ns	8	5%	ns	7	10%	0.086
TERT	7	8.0%	6	14.0%	ns	17	11%	ns	4	6%	ns
NOTCH2	5	5.0%	5	12.0%	ns	12	8%	ns	7	10%	ns
NOTCH3	5	5.0%	7	16.0%	0.054	8	5%	0.02	2	4%	0.03
FGFR1 amp	3	3.0%	1	2.3%	ns	15	9%	ns	8	11%	ns
FBXW7	10	11.0%	1	2.3%	ns	11	7%	ns	4	6%	ns
EP300	9	10.0%	4	9.0%	ns	12	8%	ns	1	3%	0.07
ATM	3	3.0%	1	2.3%	ns	8	5%	ns	1	3%	ns
ERBB2	2	2.2%	3	7.0%	ns	4	3%	ns	5	8%	ns
FOXA1 amp	2	2.2%	4	9.0%	ns	2	1%	0.02	3	4%	ns
NKX2-1	3	3.0%	4	9.0%	ns	2	1%	0.02	4	6%	ns

Abbreviations: BOT=base of tongue, SCC=squamous cell carcinoma, HPV-P=HPV positive, HPV-N=HPV negative.

Conclusions: The increasing frequency of HPV-P BOTSCC is due to an increasing frequency of these tumors in men but not in women. HPV-P and HPV-N BOTSCC are genetically distinct. HPV-N BOTSCC has also a different genetic profile compared to HPV-N OSCC and LSCC indicating that HPV-N SCC of the head and neck is a genetically heterogenous disease.

1174 Novel Rearrangements in Salivary Gland Tumors Detected by an RNA-based, Targeted Next-Generation Sequencing Assay

Snjezana Dogan[1], Kerry Mullaney[1], James Solomon[1], Maria Arcila[1], Jennifer Cracchiolo[1], Alan Ho[1], Nora Katabi[1], Marc Ladanyi[1], Ryma Benayed[1]
[1]Memorial Sloan Kettering Cancer Center, New York, NY

Disclosures: Snjezana Dogan: None; Kerry Mullaney: None; James Solomon: None; Maria Arcila: *Speaker*, archer; *Speaker*, Raindance Technologies; *Speaker*, invivoscribe; Jennifer Cracchiolo: None; Alan Ho: *Advisory Board Member*, Ayala; *Advisory Board Member*, Kura Oncology; *Advisory Board Member*, Regeneron; *Consultant*, Ignyta; *Advisory Board Member*, Sun Pharmaceuticals; Nora Katabi: None; Marc Ladanyi: *Grant or Research Support*, LOXO Oncology; Ryma Benayed: None

Background: Salivary gland tumors (SGT) are a histologically diverse group of tumors, many of which are driven by gene fusions. Emerging next-generation sequencing (NGS) methodologies utilized for a routine molecular profiling of clinical samples often lead to genetic discoveries, help identify novel molecular markers, and elucidate tumor pathogenesis. Here we provide our institutional experience on the SGT cohort examined for gene rearrangements by our clinical RNA-based targeted NGS assay.

Design: A clinical cohort of >1700 tumors subjected to a custom Archer® FusionPlex® assay interrogating a panel of 62 cancer fusion genes was searched for SGT. Patients' demographics, tumor characteristics and specimen type data were collected.

Results: A total of 37 SGT cases from 19 women and 18 men, diagnosed at a median age 56 years (range 14-84) included 23 (62%) major salivary glands tumors arising in parotid (n=13), submandibular (n=6) and 4 sublingual gland (n=4), and 14 (38%) minor salivary glands tumors originating in the palate (n=3), upper lip (n=2), nasopharynx (n=2), trachea (n=2), base of tongue, gingiva, buccal mucosa, maxillary sinus and thyroid. Sequenced specimens were metastases (49%), primary (38%) or recurrent tumors (13%). Most commonly tested were adenoid cystic carcinoma (AdCC, n=15), myoepithelial carcinoma (MyoepC, n=4), and secretory carcinoma (SC, n=3). Gene fusions were detected in 21 (57%) cases **(Table 1)**. Most notable findings were novel rearrangements in these tumor types: *SEC16A-NOTCH1* in AdCC with high-grade transformation, *MALAT1-PLAG1* in basal cell adenocarcinoma, *PTCH1-GLI1* in a carcinoma with myoepithelial features, and *FRMD6-PLAG1* in MyoepC ex pleomorphic adenoma (PA). *ETV6-NTRK3* was confirmed in all 3 SCs, including one late lung metastasis from an initially unrecognized thyroid primary, and rendered patients eligible for targeted therapy.

Table 1. Gene fusions detected in salivary gland tumors by Archer assay.

#	Age/Sex	Diagnosis	Primary site	Tested sample (site)	Gene fusion
1	63F	Adenoid cystic carcinoma	Parotid gland	met (lung)	*MYB-NFIB*
2	36F	Adenoid cystic carcinoma	Maxillary sinus	primary	*MYB-NFIB*
3	61M	Adenoid cystic carcinoma	Sublingual gland	met (lung)	*MYB-NFIB*
4	66M	Adenoid cystic carcinoma	Submandibular gland	met (spine)	*MYB-NFIB*
5	22F	Adenoid cystic carcinoma	Submandibular gland	met (liver)	*MYB-NFIB*
6	31F	Adenoid cystic carcinoma	Trachea	recurrence	*MYB-NFIB*
7	44F	Adenoid cystic carcinoma	Upper lip	recurrence	*MYB-NFIB*
8	84M	Adenoid cystic carcinoma	Upper lip	primary	*MYB-NFIB*
9	71F	Adenoid cystic carcinoma with HGT	Parotid	primary	*SEC16A-NOTCH1*
10	45M	Basal cell adenocarcinoma	Submandibular gland	met (ln)	*MALAT1-PLAG1*
11	55F	Clear cell carcinoma	Nasopharynx	primary	*EWSR1-ATF1*
12	56F	Clear cell carcinoma	Nasopharynx	recurrence	*EWSR1-ATF1*
13	60F	HG carcinoma with basaloid features	Buccal mucosa	met (lung)	*HMGA2-WIF1*
14	54M	Secretory carcinoma	Parotid gland	met (lung)	*ETV6-NTRK3*
15	57M	Secretory carcinoma	Submandibular gland	met (lung)	*ETV6-NTRK3*
16	49M	Secretory carcinoma	Thyroid gland	met (lung)	*ETV6-NTRK3*
17	31F	Carcinoma with myoepithelial features	Submandibular gland	met (lung)	*PTCH1-GLI1*
18	35M	Myoepithelial carcinoma XPA	Parotid gland	met (lung)	*LIFR-PLAG1*
19	68F	Myoepithelial carcinoma XPA	Parotid gland	primary	*FRMD6-PLAG1*
20	26M	Pleomorphic adenoma (?)	Parotid gland	met (kidney)	*CTNNB1-PLAG1*
21	71F	Pleomorphic adenoma with atypical features	Parotid gland	primary	*FGFR1-PLAG1*

Abbreviations: HG=high-grade, HGT=high=grade transformation, XPA=ex pleomorphic adenoma, met=metastasis, ln=lymph node.

Conclusions: The spectrum of gene rearrangements in SGT is broader than currently recognized. Further studies on a larger number of cases are needed to determine the frequency and biological/clinical significance of *PTCH1-GLI1, MALAT1-PLAG1, FRMD6-PLAG1* and *SEC16A-NOTCH1* in their respective histologic types. In addition to novel findings, routine molecular testing identifies cases amenable to targeted therapies and can serve as an adjunct diagnostic tool in under-recognized entities such as SC of the thyroid gland.

1175 Acinic Cell Carcinoma with High-Grade Transformation: β-Catenin and Cyclin D1 Data

Sedef Everest[1], Lauren Yue[2], Muhammad Qazi[3], Todd Stevens[4], Kayvon Sharif[1], Fred Baik[5], Pooja Dhorajiya[1], Xulei Liu[1], Margaret Brandwein-Weber[6]
[1]Mount Sinai Health System, New York, NY, [2]THANC (Thyroid, Head and Neck Cancer Foundation), New York, NY, [3]Bergenfield, NJ, [4]University of Alabama at Birmingham, Birmingham, AL, [5]Stanford Hospital and Clinics, Stanford, CA, [6]Icahn School of Medicine at Mount Sinai, New York, NY

Disclosures: Sedef Everest: None; Lauren Yue: None; Muhammad Qazi: None; Todd Stevens: None; Kayvon Sharif: None; Fred Baik: None; Poojaben Dhorajiya: None; Xulei Liu: None; Margaret Brandwein-Weber: None

Background: Acinic cell carcinoma (ACC) is salivary tumor characterized by serous acinar cell differentiation with cytoplasmic zymogen secretory granules. It is considered to have low malignant potential and is usually associated with good outcome. High-grade transformation of ACC (de-differentiated ACC) is a rare variant associated with a significantly poorer prognosis and has been increasingly recognized and reported. Neither of the commonly used markers (Ki67 and p53) are adequate for identifying high-grade transformation of ACC. We discuss the application of β-catenin and cyclin D1 (CD1) IHC stains.

Design: Seven patients were identified at Mount Sinai Beth Israel and University of Alabama at Birmingham. Immunostaining was accomplished with a fully automated, random access, open system immunostainer using a polymer approach. The following primary antibodies were used: beta-catenin (Leica, RTU), CD1 (Neomakers, 1:10), p53 (Leica, RTU), and Ki67 (Leica, RTU). The tissue was counterstained with hematoxylin.

Results: The degree and distribution of nuclear pleomorphism varied from moderate to severe, and focal to diffuse, respectively. Figure 1 shows an example of severe pleomorphism. Typical regions of cytoplasmic acinar differentiation are always present, seen as distinct cytoplasmic basophilic granules. Necrosis was seen in all cases, usually as a distinct nodule (Figure 2). All tumors demonstrated strong membranous β-catenin and nuclear CD1 expression (Figure 2, bottom left and right, respectively).

Table 1 demonstrates outcome for this group of seven patients. Two patients had positive lymph nodes at initial surgery, one patient was N0, and four were Nx. Two of the five patients with follow-up developed regional and distant metastases.

Table 1. Cases of acinic cell carcinoma lesions with high-grade transformation.

Age	Sex	Location	Staging	Treatment	Radiology	Distant metastasis	Outcome
53	M	Left parotid	**pT3N2bMx**	Total parotidectomy, ALT free flap, facial nerve repair; post-op chemoradiation	Poorly defined mass	Highly suspicious pulmonary nodules; Left pterygoid plate highly suspicious for malignancy at 18 months	Under treatment for metastatic disease
53	F	Right parotid	**pT2NxM0**	Total parotidectomy; adjuvant radiotherapy	Well-defined	Lost to follow up	
37	M	Right parotid	**pT2NxM0**	Superficial parotidectomy, adjuvant radiotherapy	Well-defined	No	Disease-free after 6 months
59	M	Left parotid	**pT2NxMx**	Total parotidectomy, adjuvant radiotherapy	Well-defined	Treated for metastases to calvarium, mastoid, mandible	Alive 18 months
59	M	Left superficial and deep lobe parotid	**pT4aN3Mx**	Total parotidectomy adjuvant radiotherapy	Infiltrative	No	Disease-free after 14 months
58	F	Left parotid	**pT3NxMx**	Total parotidectomy adjuvant radiotherapy	Well-defined	No	Disease-free after 43 months
69	M	Left parotid	**pT3N0Mx**	Total parotidectomy adjuvant radiotherapy	Unknown	Lost to follow-up	

Figure 1 - 1175

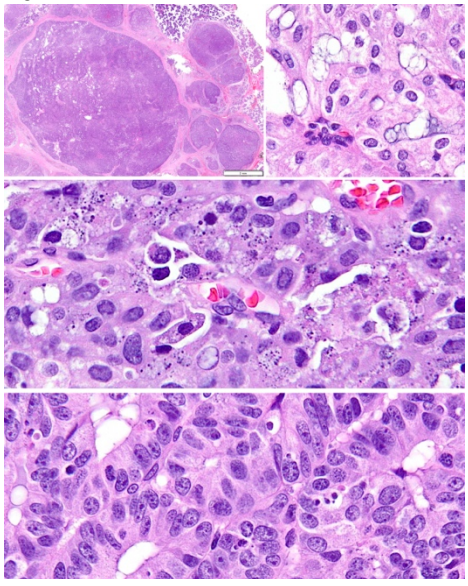

Figure 2 - 1175

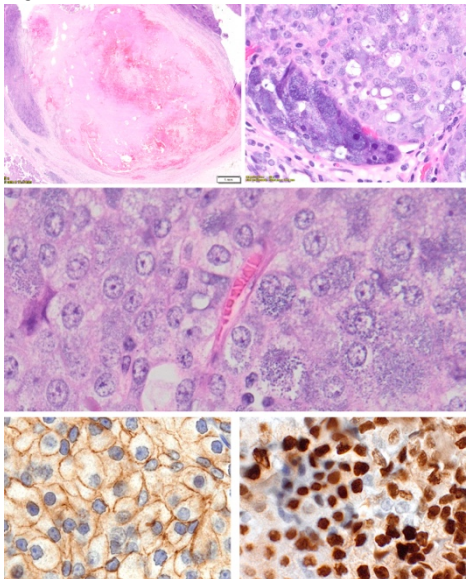

Conclusions: The diagnosis of high-grade ACC may be subtle in the face of moderate pleomorphism; a necrotic nodule may be mistaken for infarction after fine needle aspiration. Two of the five patients with follow-up data developed regional and distant metastases, supporting the idea that high-grade ACC has a more aggressive clinical course. The weight of the published evidence regarding β-catenin and nuclear CD1 for ***typical ACC*** begs for further studies (which are in progress) before conclusions can be drawn regarding their predictive value.

1176 HPV Testing in Head and Neck Squamous Cell Carcinomas - Impact of New CAP Guidelines Among Referral Cases at a Large Academic Institution

Donna Ferguson[1], Kim Ely[1], Mitra Mehrad[2], James Lewis[2]
[1]Nashville, TN, [2]Vanderbilt University Medical Center, Nashville, TN

Disclosures: Donna Ferguson: None; Kim Ely: None; Mitra Mehrad: None; James Lewis: None

Background: Human papillomavirus (HPV) related oropharyngeal squamous cell carcinoma (SCC) is common and HPV status is of utmost importance. Testing practices are widely variable, however, so the College of American Pathologists (CAP) published a guideline statement on 12/18/17 regarding appropriate testing for head and neck SCC. Our goal was to evaluate for use of these recommendations among referral cases before and after the guidelines were released.

Design: Referral cases from outside institutions were reviewed (1/1/2017 to 12/18/2017– and 12/18/2017 to 8/1/2018 - 206 total cases, 103 from each time period). Patients with a diagnosis of SCC of the nasal cavity, nasopharynx, oral cavity, oropharynx, hypopharynx, or larynx were included. All cases had been reviewed by at least one of three specialist head and neck pathologists at the time of referral. Cases were judged based whether they followed (or deviated from) the recently published CAP guidelines.

Results: HPV testing was ordered incorrectly in 42 patients (40.8%) before the guidelines were released and 47 (45.6%) after (p=0.57). For oropharyngeal SCCs, 5 cases (20%) before and 2 (8.7%) after the guidelines were ordered incorrectly (p=0.43). Of these cases, 60% had HPV DNA PCR ordered instead of p16 IHC. For non-oropharyngeal SCCs, 30 cases (45.5%) before and 35 (54.7%) after the guidelines were ordered incorrectly (p=0.65). Immunohistochemistry for p16 was ordered the unnecessary test in 96.7% and 91.4% of cases before and after, respectively. In particular, 19/42 (45.2%) and 24/42 (57.1%) of oral cavity SCCs before and after, respectively, had incorrect ancillary testing performed, all of which was unnecessary p16 immunohistochemical staining. Lastly, neck metastasis biopsies were incorrectly handled in 7/12 (58.3%) before and 9/16 (56.3%) cases after guidelines (p=1.00), with marked variability the testing performed. There was a trend toward higher compliance with CAP recommendations for oropharyngeal SCC patients in the final 3 months of the study, after the guidelines had been formally published.

	1/1/2017 to 12/18/2017	12/19/2017 to 8/1/2018
Total Cases	103	103
Incorrect Testing Or Omission	42 (40.8%)	47 (45.6%)

Conclusions: This study shows only a slight increase in appropriate HPV/ancillary testing for oropharyngeal SCC patients since CAP guideline publication. However, it also shows no improvement in the high rate of inappropriate ancillary testing for non-oropharyngeal

primaries, primarily in oral cavity SCC but also in neck specimens and other primary sites. More education and efforts to improve uptake of consensus guidelines are needed.

1177 Artificial Intelligence Generation of Multiclass Cancer Maps for Oral Cavity Cancer

Jonathan Folmsbee[1], Scott Doyle[1], Xulei Liu[2], Margaret Brandwein-Weber[3], Sedef Everest[2], Pooja Dhorajiya[2]
[1]University at Buffalo, Buffalo, NY, [2]Mount Sinai Health System, New York, NY, [3]Icahn School of Medicine at Mount Sinai, New York, NY

Disclosures: Jonathan Folmsbee: None; Scott Doyle: None; Xulei Liu: None; Margaret Brandwein-Weber: None; Sedef Everest: None; Poojaben Dhorajiya: None

Background: Computational pathology has been shown to improve pathology workflows by identifying regions of interest (ROIs) & quantifying patterns of tissue. In particular, deep learning is a computational approach to machine learning that has led to peak performance on many complex tasks. Unfortunately, high performance requires large & well-annotated dataset sizes, which are time consuming & costly to generate. In particular, tissue mapping tasks (**Fig 1**) require hand-annotated maps of training data. Algorithms to identify carcinoma also need to identify other tissue groups that might confound accurate cancer identification. We aim to reduce the time needed to generate large annotated pathology datasets by developing a "**human-in-the-loop"** active learning (AL) approach, whereby the algorithm is evaluated on new digitized cases to identify misclassification. In this way, the computer is able to improve the classifier via human interaction, & pathologists are able to "correct" the classifier.

Design: 143 whole slides were digitally scanned on an Olympus scanner, resized to 2 µm/pixel, & cropped to ROIs of 2000x2000 pixels. 5 images were randomly chosen for manual annotation & used to train a classifier to map pixels to various tissue groups (Version 1). This classifier then generates tissue maps on new ROI, which are then sent to our pathology team for QA. The QA team compared the generated tissue maps with the original ROIs, & scored each sample 0-5, where 0 is poor & 5 is accurate. The worst performing samples are selected for annotation & re-training (Version 2). This "train-QA-annotate-retrain" loop is then repeated until accuracy no longer improves. At each iteration, the classifier accuracy is evaluated (**Fig 2**).

Results: Table 1 shows classifier accuracy as assessed "patch by patch". The drop in accuracy with version 2 of the classifier is expected, as the classifier is applied to new cases. After 2 iterations of AL, we see that AL is more stable. **Figure 1**compares manually annotated maps with our computer generated maps. The manually annotated maps are smoother & more accurate. However, the computer generated maps were faster to generate.

Type of Classifier	Initial Classifier Average Accuracy (n=5 images, #patches = 173709)	Version 2 Average Accuracy (n=10 images, #patches = 269751)	Version 3 Average Accuracy (n=15 images, #patches=366160)
Active Learning (AL)	**96.4%±0.10**	**95.7%±0.13**	**96.4%±0.11**
Random Learning (RL)		92.0%±0.21	93.5%±0.17

Table 1: Average accuracy for subsequent versions of the patch based tissue classifier. As you can see, Active Learning attains higher accuracies than random learning as subsequent versions are created. The reason there is a dip between the initial classifier and version 2, is due to the adding of underrepresented samples to the dataset. Like the maps in Figure 1, AL is more stable, whereas RL is more volatile

Figure 1 - 1177

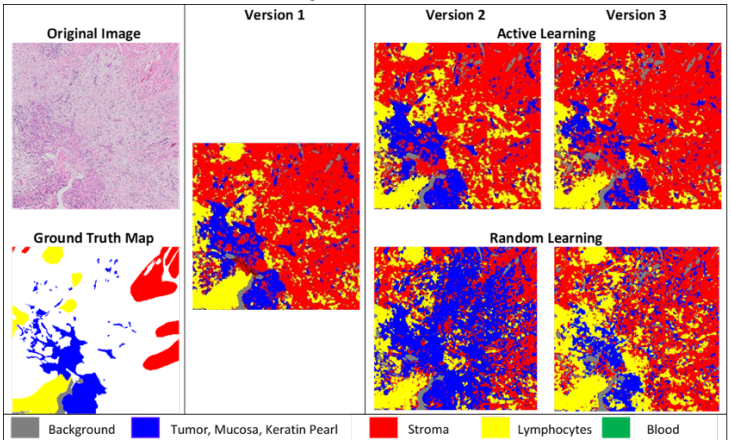

Figure 1: Shown are the progression of the computer's output through Version 3. The most noticeable difference AL and RL, is the stability of AL as compared to RL. The AL algorithm improves constantly while the RL is volatile in its classification

Figure 2 - 1177

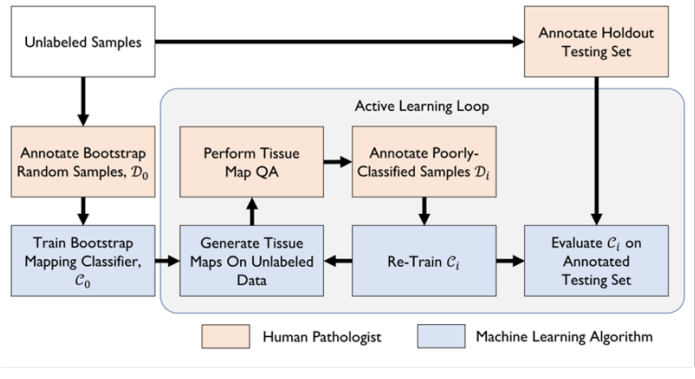

Figure 2: Flowchart of the active learning experimental design

Conclusions: The human-in-the-loop training paradigm improves classifier performance vs a randomly-generated training set. This training loop leads to an improved modeling of tissue groups by the classifier, & demonstrates how pathologist feedback through QA is crucial. Future work will demonstrate the AL pipeline in a multi-site, multi-reader environment.

1178 Comprehensive Molecular Profiling of Salivary Duct Carcinomas

Stacey Gargano[1], Wijendra Senarathne[2], Rebecca Feldman[3], Elena Florento[3], Jeffrey Swensen[3], Semir Vranic[4], Zoran Gatalica[3]
[1]Thomas Jefferson University Hospital, Haddonfield, NJ, [2]Phoenix, AZ, [3]Caris Life Sciences, Phoenix, AZ, [4]College of Medicine, Qatar University, Doha, Qatar

Disclosures: Stacey Gargano: None; Wijendra Senarathne: None; Rebecca Feldman: *Employee*, Caris Life Sciences; Elena Florento: None; Jeffrey Swensen: *Employee*, Caris Life Sciences; Semir Vranic: None; Zoran Gatalica: *Employee*, Caris Life Sciences

Background: Salivary duct carcinomas (SDC) are aggressive malignancies currently managed with surgery followed by radiation- and/or conventional (empirical) chemotherapy. Targeted anti-Her2 and anti-androgen therapies are being tested, however these options have not been standardized or clinically validated. In the present study, we explored novel molecular targets and biomarkers of immuno-oncology (I-O) therapies.

Design: Tumor samples from twelve patients (10 males and 2 females; mean age 66 years, range, 50-91) were profiled using next-generation sequencing (NGS), and immunohistochemistry (IHC) assays for androgen receptor (AR) [positive defined as nuclear staining ?10% tumor cells], ERBB2 (Her2) [positive defined as ?3+ staining in >10% tumor cells], PDCD1 (PD-1; number of positive tumor infiltrating lymphocytes [TILs] per 10 hpf), CD274 (PD-L1; clone 28-8; ?1+ tumor cell expression in ?1% cells) and CD8 (number of positive TILs per 10 hpf).

Results: Primary tumors originated in parotid gland (10/12) submandibular gland and lip (one case each); all patients presented with metastatic disease (at least pN2b). All 12 cases expressed androgen receptor (AR) by IHC, and six harbored splice variant AR-V7 (RNA seq). Her2 was overexpressed in 58% of the cases. Genetic alterations were detected in all 12 cases, most commonly *TP53* (7 cases), *HRAS* (6), *PIK3CA* and *MLL3* (3 each), ERBB2, *NF1* and *NOTCH1* (2 each). Two cases exhibited low (1-5%) tumor cells PD-L1 expression (Ab clone 28-8) while one case showed *PD-L1/JAK2* gene co-amplification (but negative for PD-L1 expression). Tumor infiltrating lymphocytes showed varying ratios of PD-1+ to CD8+ (range, 0-73.1%; average: 12%). All tested samples (n=6) were microsatellite stable and had a low tumor mutational burden (TMB<10/Mb). Two patients (one male, one female) showing responses to anti-androgen therapy (enzalutamide) had no ARv7 detected in their tumor samples.

Conclusions: Comprehensive molecular profiling of SDCs can refine selection of patients for targeted therapies including AR, Her2, MAPK and PIK3CA pathways. Additionally, some patients with SDC may benefit from immune checkpoint inhibitors. Presence of AR-V7, a biomarker predictive of resistance to anti-androgen therapy, in 50% of cases indicates a potential role of this testing for refining patient selection for hormonal therapies.

1179 Basaloid Squamous Cell Carcinoma: Novel SOX10-Expressing Subset Correlates with Specific Histopathology and Behavior

Natalya Hakim[1], David Dueber[2], Virgilius Cornea[1], Julie Dueber[3], Therese Bocklage[1]
[1]University of Kentucky College of Medicine, Lexington, KY, [2]University of Kentucky College of Education, Lexington, KY, [3]University of Kentucky, Lexington, KY

Disclosures: Natalya Hakim: None; David Dueber: None; Virgilius Cornea: Nonel; Julie Dueber: None; Therese Bocklage: None

Background: Basaloid squamous cell carcinoma (BSCC) is a variant of squamous cell carcinoma (SCC) composed of a prominent basaloid component with squamous differentiation. It is typically considered more aggressive than keratinizing SCC. Studies of BSCC behavior are hampered by interobserver variability in identifying BSCC and distinguishing it from poorly differentiated SCC. SOX10 immunohistochemical (IHC) expression is touted as a marker of basaloid tumors such as some salivary gland tumors. In fact, strong SOX10 expression is proposed as a diagnostic clue at biopsy for salivary carcinoma. However, we recently noted a BSCC diffusely expressing SOX10. We hypothesized that this novel SOX10 expression may be a diagnostic marker of a subset of BSCC. We further postulated that SOX10-positive BSCC may exhibit specific morphologic and behavioral features.

Design: We searched our pathology records from 2009 to mid-2018 and captured SCCs described as basaloid. We identified 81 cases from multiple body sites with most deriving from the head and neck region (n= 54). After initial group review, four pathologists independently scored basaloid features including comedonecrosis, basement membrane (BM)-like matrix and pseudoglands. We correlated SOX10 expression with histologic BSCC features and with: age, gender, body site, AJCC TNM stage, margin status, treatment, and behavior (any recurrences, metastases, and time of death). Statistical analyses were performed to evaluate kappa values for scoring of basaloid features and correlation of SOX10 expression with specific histology, body site, stage, and behavior.

Results: SOX10 expression was found in 29% of cases (24/81). Presence of at least two of three features (comedonecrosis, BM-matrix and pseudoglands) were significantly associated with diffuse SOX10 expression (p <.001). SOX10 positive tumors showed a higher rate of lymph node metastases compared to non-SOX10 expressing basaloid SCC (p < .001; Sens. 0.82, Spec.0.90). SOX10 positive BSCC were found in multiple body sites including Waldeyer Ring mucosa (tonsil etc.).

Figure 1 - 1179

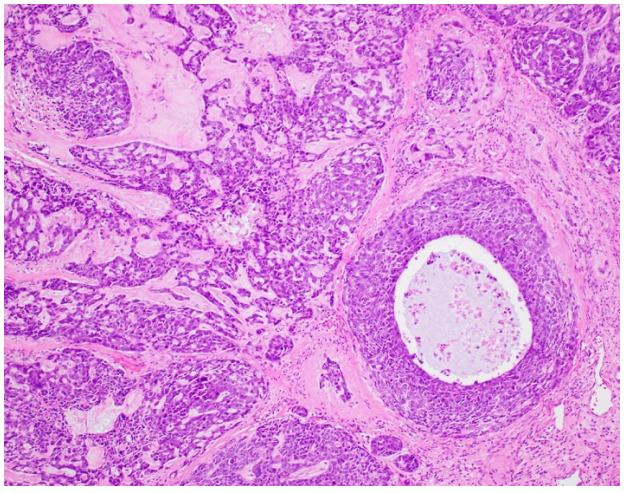

Figure 2 - 1179

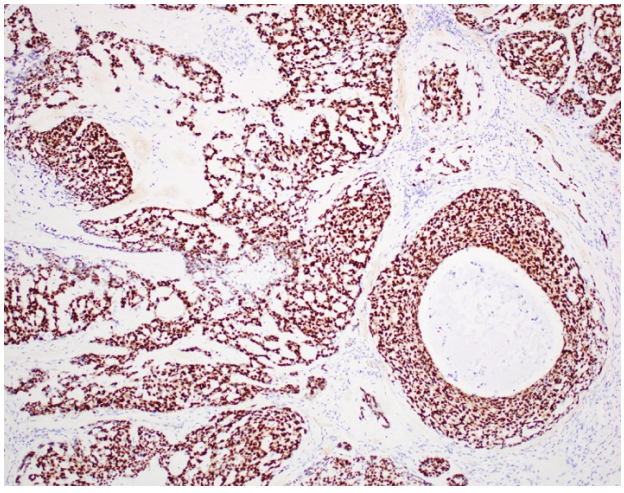

Conclusions: We have identified a novel subset of BSCC that diffusely, strongly express SOX10 by IHC. These tumors typically show distinct histologic features including comedonecrosis **with** basement membrane matrix **and/or** pseudogland formation. SOX10-expressing BSCC occur throughout the head and neck. Compared to SOX10 negative BSCC, SOX10 positive tumors are more aggressive. Whole exome and RNA sequencing of this distinct group are underway.

1180 Utility of Pan-TRK Immunohistochemistry (IHC) as an Ancillary Tool in Diagnosing Secretory Carcinoma (SC) of Salivary Gland and Detecting ETV6-NTRK3 fusion

Mohamed Rizwan Haroon Al Rasheed[1], Bin Xu[2], Cristina Antonescu[2], Deepu Alex[3], Denise Frosina[2], Ronald Ghossein[2], Achim Jungbluth[2], Nora Katabi[2]
[1]New York, NY, [2]Memorial Sloan Kettering Cancer Center, New York, NY, [3]BC Cancer, Vancouver, BC

Disclosures: Mohamed Rizwan Haroon Al Rasheed: None; Bin Xu: None; Cristina Antonescu: None; Deepu Alex: None; Denise Frosina: None; Ronald Ghossein: None; Achim Jungbluth: None; Nora Katabi: None

Background: SC is a salivary carcinoma that harbors a signature *ETV6-NTRK3* fusion in a majority of cases, which can be utilized to assist with diagnosis. Targeted therapy using pan-TRK inhibitor entrectinib has resulted in drastic response in patients with metastatic SC. Recently, pan-TRK IHC has emerged as a sensitive and specific tool in detecting *NTRK1/2/3* fusions in various cancers. We aimed to establish the specificity and sensitivity of pan-TRK IHC as an affordable and feasible tool to diagnose SC, detect *ETV6-NTRK3* fusion, and differentiating it from its mimickers especially acinic cell carcinoma (AciCC).

Design: Pan-TRK IHC using monoclonal antibody EPR17341 was performed on 24 SCs and 13 AciCCs, diagnosed histologically. Staining pattern (nuclear, cytoplasmic, or both), intensity (weak, moderate, or strong), and percentage of positive tumor cells (TC) were documented. Less than 5% pan-TRK immunostaining in TCs was considered as negative. *ETV6-NTRK3* fusion status was established in 18/24 SCs using *ETV6* FISH (n=13), *NTRK3* FISH (n=5) or next generation sequencing (NGS, n=5).

Results: 20/24 SCs and 2/13 AciCCs were positive for pan-TRK IHC rendering a sensitivity and specificity of pan-TRK IHC in diagnosing SC of 83% and 85%, respectively. The staining intensity in SCs was strong in 4/20 (20%), moderate in 12/20 (60%), and weak in 4/20 (20%) cases. The majority of SCs (70%, 14/20) had both cytoplasmic and nuclear staining pattern and the two positive AciCCs for pan-TRK showed only cytoplasmic staining (90% weak to moderate in one case and 10% weak in the other).

ETV6 fusion was detected in 14/18 (78%) SC cases. The fusion partner was determined in 9 cases and found to be *NTRK3* in all. The sensitivity and specificity in detecting the fusion were 93% and 25%, respectively: 13 of 14 cases with *ETV6*translocation were positive for pan-TRK IHC. Three of four *ETV6* negative but morphologically typical SCs exhibited pan-TRK immunopositivity (one with 10% weak cytoplasmic, one with 75% weak to moderate cytoplasmic, and one with 70% weak cytoplasmic and nuclear).

Conclusions: Majority of histologically diagnosed SCs (83%) showed pan-TRK immunopositivity (mostly nuclear and cytoplasmic and with moderate to strong intensity) whereas merely 15% of AciCCs exhibited immunostaining and only cytoplasmic. Only 1/14 *ETV6* positive SCs was negative for pan-TRK IHC. Pan-TRK IHC may serve as an affordable sensitive tool for SC and *NTRK3* fusion in salivary gland tumors, with a sensitivity of 83% and 93%.

1181 Impact of Thyroseq® Performance on Indeterminate Thyroid nodules: An Institutional Experience

Katherine Huenerberg[1], Peter Abader[2], Shanna Colletti[3], Aziza Nassar[2]
[1]Mayo Clinic Jacksonville, Ponte Vedra Beach, FL, [2]Mayo Clinic, Jacksonville, FL, [3]Mayo Clinic Florida, Jacksonville, FL

Disclosures: Katherine Huenerberg: None; Peter Abader: None; Shanna Colletti: None; Aziza Nassar: None

Background: Approximately 10-30% of thyroid nodules biopsied by fine needle aspiration biopsy (FNAB) are considered indeterminate by the Bethesda system for classifying thyroid nodules. The risk of malignancy for indeterminate thyroid nodules ranges from 5–15%. In these nodules, the most common genetic abnormality is a RAS mutation; which carries a malignancy risk of approximately 80%. An encapsulated non-invasive follicular thyroid neoplasm with papillary-like nuclear features (NIFTP) is by far the most common tumor that exhibits RAS mutation.

Thyroseq® is a next-generation sequencing test that pre-operatively analyzes multiple mutational markers associated with thyroid cancer.This test is routinely performed on patients who are diagnosed on FNAB as indeterminate thyroid nodules (Bethesda Categories III and IV).

In this study, we are seeking to identify our institutional experience with Thyroseq® testing in patients with indeterminate thyroid nodules.

Design: We retrieved all patients with Thyroseq® testingfrom January 1st, 2015 to September 7th, 2018. We annonnated all significant clinical and pathologic data, and reviewed any available resection.

Results: A total of 81 cases were retrieved from our pathology database. The age ranged from 19-85 years (mean – 59.5); with 50 (61.0%) females and 32 (39.0%) males. The average nodule size was 2.1 cm (range 0.5 – 6.5 cm). The most common ultrasonographic feature was a hyoechoic solid nodule (38.3%). The diagnostic categories included AUS (31/81 – 38.3%), suspicious for follicular neoplasm (39/81 – 48.1%) and suspicious for Hurthle cell neoplasm (11/81 – 13.6%). Almost two thirds of the PTC (8/13 – 61.5%) and of the NIFTP cases (3/5 – 60.0%) were classified as “suspicious for follicular neoplasm”. The majority of patients did not have surgical resection (54/81-66.7%). Of these, 51(94.4%) had no molecular alteration. The most frequent neoplasm was PTC (13/24 - 54.2%) followed by NIFTP (5/24 - 20.8%). The most frequent molecular alteration was NRAS (14/30 - 46.7%); 5 (35.7%) of which were detected in PTC and 3 (21.4%) in NIFTP. HRAS (5/30 – 16.7%) was the second most common mutation detected, mostly in NIFTP cases (2/5-40.0%).

	Surgical diagnosis							
Molecular Alteration	**Benign Thyroid Nodule**	**Follicular Adenoma**	**Follicular Carcinoma**	**Hurthle Cell Adenoma**	**Hurthle Cell Carcinoma**	**No surgical specimen**	**NIFTP**	**Papillary Thyroid Carcinoma**
Negative (51) - 63.0%	1	2	0	0	0	47	0	1
NRAS (14) - 17.3%	0	1	0	1	0	4	3	5
HRAS (3) - 3.7%	0	0	0	0	0	1	2	0
HRAS/EIF1AX (2) - 2.5%	0	0	0	0	1	0	0	1
BRAF (1) - 1.2%	0	0	0	0	0	0	0	1
DICER1 (1) - 1.2%	1	0	0	0	0	0	0	0
EIF1AX (1) - 1.2%	0	0	0	0	0	0	0	1
KRAS (1) - 1.2%	0	0	0	0	0	0	0	1
KRAS/TERT (1) - 1.2%	0	0	0	0	0	0	0	1
NRAS/TERT/TSHR (1) - 1.2%	0	0	0	0	0	0	0	1
PAX-8/PRARG (1) - 1.2%	0	0	1	0	0	0	0	0
PTEN (1) - 1.2%	1	0	0	0	0	0	0	0
THADA/IGF2BP3 (1) - 1.2%	0	0	0	0	0	0	0	1
TSHR (1) - 1.2%	0	0	0	0	0	1	0	0
Multiple chromosomes (1) - 1.2%	0	0	0	0	0	1	0	0

Conclusions: Surgical resection was eliminated in at least 47 (58.0%) patients due to lack of molecular alteration on Thyroseq® testing. NRAS mutation (17.3%) was by far the most common alteration detected in both PTC (35.7%) and NIFTP (21.4%). NIFTP cases exhibited only RAS mutations.

1182 Utility of p16 and HPV in Oropharyngeal Squamous Cell Carcinoma: An Institutional Review

Katherine Huenerberg[1], Shanna Colletti[2], Aziza Nassar[3]
[1]Mayo Clinic Jacksonville, Ponte Vedra Beach, FL, [2]Mayo Clinic Florida, Jacksonville, FL, [3]Mayo Clinic, Jacksonville, FL

Disclosures: Katherine Huenerberg: None; Shanna Colletti: None; Aziza Nassar: None

Background: According to the CDC, there are more than 16,000 cases of oropharyngeal squamous cell carcinoma (OPSCCs) in the USA. Of these, approximately 60-80% of OPSCCs are associated with HPV. HPV-associated OPSCCs have better treatment responses and prognoses than HPV negative tumors. A positive p16 result in a cervical lymph node can strongly point to an occult primary tumor in the oropharynx.

The College of American Pathologists recently published a guideline addressing HPV testing in head and neck carcinomas. Prior to this guideline, there was no consensus as to when to test for HPV or which test to choose. The goal was to standardize testing across diverse pathology practice settings. Our objective was to evaluate the use of p16 and HPV testing at our own institution and to better understand the distribution of HPV positive OPSCC in our patient population.

Design: We retrieved all cases of squamous cell carcinoma (SCC) of the head and neck with a concurrent p16 result from our Anatomic pathology database spanning from 1/1/2013 to 8/31/2018. The patients' demographics, tumor characteristics, p16 result and any HPV result (DNA ISH and E6/E7 RNA ISH) were captured and statistical analysis performed.

Results: We identified 104 cases of primary and metastatic SCC with a concurrent p16 immunostain over a period of 68 months. Our p16 IHC performance increased from 5 in 2013 to 28 in 2017.The average age of the p16 negative patient was 68.9 years; while the average age of the p16 positive patient was 64.6 years. The majority of p16 positive cases were in men (83/93 – 89.2%). In about one third of cases (37/104 – 35.6%), reflex high-risk (HR) HPV testing was performed. In 17.1% (6/35) of p16-positive cases tested for HR HPV, the results were discrepant (p16-positive, HR HPV negative). The majority of primary tumors (53/57 – 93%) and metastases (40/47 – 85.1%) were positive for p16. The majority of metastases (SCC of unknown origin) were cytology cases (34/47 – 77.3%). Tumor differentiation was not predictive of p16 status (LR 0.51). Tumor subtype (basaloid vs. keratinizing) did correlate with p16 positivity or negativity (LR 0.0004).

	p16 Positive	p16 Negative
no HR HPV testing	58	9
HR HPV positive	29	0
HR HPV negative	6	2
known primary	53	4
node metastasis with no known primary	40	7
males	83	7
females	10	4
Basaloid	20	0
Keratinizing	1	4
Non-Keratinizing	5	2
Poorly Differentiated	21	1
Moderately Differentiated	16	3
Well-Differentiated	3	0

Conclusions: When used in the proper context, p16 IHC can accurately identify HPV-positive OPSCC. Cytology specimens play an important role in SCC of unknown origin. HR HPV testing is not routinely required and may cause discrepancy. Subjective analysis of tumor differentiation has little role in predicting p16 status, but tumor subtype can be predictive.

1183 PD-L1 Expression in Salivary Duct Carcinoma: Does the Scoring System Matter?

Anna-Karoline Israel[1], Jennifer Findeis-Hosey[1], David Hicks[1], Abberly Lott Limbach[1]
[1]University of Rochester Medical Center, Rochester, NY

Disclosures: Anna-Karoline Israel: None; Jennifer Findeis-Hosey: None; David Hicks: None; Abberly Lott Limbach: None

Background: Salivary duct carcinoma (SDC) is <10% of all salivary gland malignancies, with morphologic similarities to high-grade invasive and in situ ductal carcinoma of the breast. It is well characterized that 30-60% of SDCs can have amplification of HER-2/neu making patients eligible for specific targeted-therapy options. Recently therapeutic options that block the programmed death 1 pathway have become available and determining programed death ligand 1 (PD-L1) expression by immunohistochemistry (IHC) can help stratify patients for treatment with those drugs. While use of these treatment options are agnostic of site, the site of origin and tumor type impacts the scoring system and threshold used. In this study we compare PD-L1 expression using a TPS score and CPS score, as well as HER2 amplification status.

Design: The pathology LIS was searched for diagnoses of SDC in the last 10 years. H&E-stained slides were reviewed and a single block was stained for HER2 (if not previously done) and PD-L1 (22C3 PharmDx Agilent/Dako). HER2 IHC was graded as 0, 1+, 2+, or 3+ using established breast criteria. TPS and CPS scores were determined from PD-L1-stained slides using established lung criteria for TPS (percentage of membranous-staining tumor cells), and established CPS criteria (percentage of PD-L1 staining tumor cells, lymphocytes, and macrophages, divided by the total number of viable tumor cells), with a CPS threshold of 1%.

Results: Fifteen cases of SDC were identified with tissue available for IHC. There were 6 (40%) females and 9 (60%) males, with average age of 67.33 years. Table 1 details case-specific HER2 and PD-L1 results. HER2 amplification (3+) was identified in 7 (46.7%) cases. Utilizing the TPS criteria, 11 (73.3%) cases demonstrated a TPS of 1% or greater. In comparison, 14 (93.3%) demonstrated a CPS of 1% or greater (p = 0.3295). The 3 cases with a TPS of 0% but CPS of greater than 1% demonstrate significant PD-L1 staining in tumor-associated mononuclear inflammatory cells without staining of any tumor cells.

Case	HER2 IHC Grade	PDL1 TPS	PDL1 CPS	CPS
1	3+	1%	22.2	>1
2	1+	0%	20	>1
3	2+	0%	7	>1
4	1+	10%	30	>1
5	0+	0%	6	>1
6	2+	5%	6.66	>1
7	3+	1%	3	>1
8	2+	50%	70	>1
9	0+	0%	0	0
10	3+	1%	12	>1
11	3+	1%	37.5	>1
12	3+	10%	40	>1
13	1+	1%	23	>1
14	3+	1%	31	>1
15	3+	1%	30	>1

Conclusions: The rate of HER2 amplification in our study was consistent with reported literature. All of the examined HER2 positive tumors expressed PD-L1 by both the TPS and CPS criteria, giving patients multiple chemotherapeutic options. However, taking into account the immune cell staining and using the CPS score with a 1% threshold would have allowed more patients (93.3%) to be eligible for treatment then with use of the TPS score (73.3%).

1184 p16 Immunoexpression in Sinonasal Adenoid Cystic Carcinomas

Deepali Jain[1], Vijay Mariadas Antony[1], Aanchal Kakkar[2], Alok Thakar[1], Deo SVS[1], Justin Bishop[3]
[1]All India Institute of Medical Sciences, New Delhi, India, [2]New Delhi, India, [3]University of Texas Southwestern Medical Center, Dallas, TX

Disclosures: Deepali Jain: None; Vijay Mariadas Antony: None; Aanchal Kakkar: None; Alok Thakar: None; Deo SVS: None; Justin Bishop: None

Background: Sinonasal adenoid cystic carcinoma (SNACC) is a rare malignancy which is clinically characterized by worse prognosis due to proximity to vital structures, inherent tendency for perineural invasion and difficulty to achieve complete resection. Human papilloma virus (HPV) related multiphenotypic sinonasal carcinoma (HMSC) has been described recently with a histopathological appearance markedly similar to that of adenoid cystic carcinoma. At times in small biopsies, it may be difficult to distinguish SNACC from HMSC. Due to clear-cut clinical and pathogenetic differences, it is crucial to make a correct diagnosis. A limited number of studies with a smaller number of cases have investigated the p16 expression in SNACC. We aim to study p16 expression in all previously reported SNACC in an attempt to identify possible cases of HMSC.

Design: All cases, during the last 8 years (2009-2017), diagnosed as adenoid cystic carcinomas arising from sinonasal region were included in the series. Slides were reviewed, and the diagnosis of adenoid cystic carcinoma was confirmed. Each case was graded on the basis of the predominant histological pattern: low-grade (tubular), intermediate-grade (cribriform) and high grade (solid). All cases were tested by immunohistochemistry for p16 (E6H4 clone, CINtec, Roche) expression. Overall, a semiquantitative scoring was also performed ranged from 0 to 4+. p16 immunostaining was considered positive only if present in ≥70% of the tumor cells with both nuclear and cytoplasmic expression. HPV testing was performed by RNA *in-situ* hybridization (RNA ISH) via the RNAscope method in positive cases.

Results: A total of 113 SNACC cases were retrieved. p16 was negative in 3 cases (score 0). One hundred cases showed patchy expression including 1+ (1-29%), 2+ (30-49%) and 3+ (50-69%) positivity in 73, 20 and 7 cases respectively. Six cases showed >70-100% positivity. In 4 cases, tumor tissue was scant on IHC slide for interpretation. Histomorphologically, 3 out of 6 positive cases showed solid pattern. HPV RNA ISH was negative in all p16 positive (>70 -100% positivity) cases.

Conclusions: P16 immunoexpression in SNACC is quite a common finding with approximately 90% of them show patchy positivity. Even diffuse and strong p16 expression in SNACC is not a reliable surrogate for coexisting HPV infection. These findings are especially important to consider in cases where the differential diagnosis includes both SNACC and HMSC as the latter are always HPV positive.

1185 The Mutational Profile of 50 Squamous Cell Carcinomas of the Soft Palate

Mohsin Jamal[1], Bin Xu[1], Sumit Middha[1], Anita Bowman[2], Chad Vanderbilt[3], Venkatraman E. Seshan[1], Michael Berger[1], Lara Dunn[1], Sean M. McBride[1], Ian Ganly[1], Snjezana Dogan[1]
[1]Memorial Sloan Kettering Cancer Center, New York, NY, [2]Memorial Sloan Kettering Cancer Center, Yeadon, PA, [3]Memorial Sloan Kettering Cancer Center, Denver, CO

Disclosures: Mohsin Jamal: None; Bin Xu: None; Sumit Middha: None; Anita Bowman: None; Chad Vanderbilt: None; Venkatraman E. Seshan: None; Michael Berger: *Consultant*, Roche; *Grant or Research Support*, Illumina; Lara Dunn: None; Sean M. McBride: *Consultant*, Bristol-Myers Squibb; *Grant or Research Support*, Janssen; Ian Ganly: None; Snjezana Dogan: None

Background: The majority (>70%) of oropharyngeal squamous cell carcinomas (OP-SCC) are driven by high-risk HPV, most arise in the palatine tonsils and base of tongue (BOT) and the most frequent genetic alterations are *PIK3CA* mutations detected in about one third HPV positive (HPV-P) OP-SCC. SCC of the soft palate (SP-SCC) is relatively rare. Although anatomically a part of the oropharynx, in contrast to tonsils and BOT, soft palate mucosa is lymphoid stroma-poor and as such may be relatively less susceptible to HPV infection.

Design: Fifty resected SP-SCC, including 49 primary and one locally recurrent tumor were subjected to a targeted hybridization capture-based massive parallel sequencing of 341-468 genes by MSK-IMPACT assay as research (N=43) or clinical diagnostic (N=7) samples. HPV/p16 status was determined by RNA *in situ* hybridization/immunohistochemistry and/or by using the bioinformatics algorithm for detection of HPV sequence reads in MSK-IMPACT sequencing data.

Results: SP-SCC was more common in men (36/50, 72%). Most (93%) patients were smokers. Minority of SP-SCC were HPV positive (HPV-P; 20%), all occurred in men (p=0.045) at median age 56 years (range 45-83), and harbored *SOX2*(50%), *TP53* (40%), *TP63* (30%), *FGF3/FGF4/FGF19/CCND1* (20%), and *RB1* (20%) mutations; no *PIK3CA* mutations were detected in HPV-P SP-SCC. HPV negative (HPV-N) SP-SCC patients presented at a median age 62 years (range 39-77) harboring tumors with alterations in *TP53* (70%), *FGF3/FGF4/FGF19/CCND1* (30%), *NOTCH1* (28%), *KMT2D* (25%), *CDKN2A/2B* (25%), *SOX2* (20%), *PIK3CA* (15%), *FAT1* (15%), *NFE2L2* (8%), *TERT* (8%), and *FGFR1* (5%). *PIK3CA* mutations in HPV-N cases were associated with worse outcome (Log rank test, p=0.051).

Conclusions: This is the largest genomic study on SP-SCC as a single oropharyngeal subsite to date. A relatively lower frequency of HPV-P SP-SCC may be due to a different anatomy of SP from other oropharyngeal subsites. HPV-P SP-SCC is uncommon in women. In contrast to tonsil or BOT, *PIK3CA* mutations in HPV-P SP-SCC are rare, and in HPV-N SP-SCC may indicate a more aggressive tumor biology.

1186 Genotype profiling of Uveal melanoma reveals novel variant mutations

Susan Kennedy[1], Sinead Toomey[2], Bryan Hennessy[3], Nicolas Deeney[4], Annemarie Larkin[5]
[1]Royal Victoria Eye and Ear Hospital, Dublin, Ireland, [2]Royal College Surgeons in Ireland (RCSI), Dublin, Ireland, [3]Royal College Surgeons in Ireland, Dublin, Ireland, [4]Trinity College Dublin, Dublin, Ireland, [5]Dublin City University, Dublin, Ireland

Disclosures: Sinead Toomey: None; Bryan Hennessy: None; Annemarie Larkin: None

Background: Uveal melanoma (UM) is a highly aggressive malignancy which displays a high propensity for metastasis for which there are no effective therapies. The aim of this study was to profile the mutations present in primary and metastatic tumours in a cohort of Irish UM patients diagnosed between 2008 and 2015 to add to our knowledge of the gene mutation spectrum of UM.

Design: Patients which had previously received enucleations were selected from the archives of The National Ophthalmic Laboratory, Royal Victoria Eye & Ear Hospital. Four matched primary and metastatic UM formalin-fixed paraffin embedded tissue tumour blocks together with 32 primary UM blocks underwent microdissection to extract DNA ahead of high-throughput Genotyping (OncoCarta panel Vi) for interrogation of 238 known mutations in 42 key cancer related genes

Results: High throughput Genotyping using a custom designed Sequenome panel revealed that a high proportion of cases (91%) in this UM cohort harboured GNAQ / GNA11 mutations which were present in a mutually exclusive pattern. Novel variant mutations; PHLPP2 L1016S and PIK3R1 M3261 were identified in 12 and 6 primary UM tumours, respectively. IDH-1 V1781, and MET variant mutations, N375S, E168D and T10101 were less frequently identified. A discordant pattern of mutations was revealed between primary and metastatic tumours from 2 patients.

Conclusions: Our mutation profiling confirms the distinct molecular profile and low mutational burden of UM. In addition, our findings also highlight a number of novel mutation variants in genes implicated in cancer which have not been previously associated with UM. There is limited knowledge regarding the potential pathogenic nature of these variants, thus future functional studies are warranted to investigate these novel mutation variants further in UM.

1187 Primary and Recurrent Head and Neck Squamous Carcinomas are Strikingly Different Regarding their Immune Microenvironment

Rosemarie Krupar[1], Christian Watermann[2], Helen Pasternack[1], Julika Ribbat-Idel[3], Christian Idel[4], Mark Philipp Kuehnel[5], Danny Jonigk[5], Sven Perner[3]
[1]Pathology of the University Medical Center Schleswig-Holstein, Campus Lübeck and Research Center Borstel, Leibniz Lung Center, Luebeck, Germany, [2]Pathology of the University Medical Center Schleswig-Holstein, Campus Lübeck and Research Center Borstel, Leibniz Lung Center, Lübeck, Germany, [3]University Medical Center Schleswig-Holstein, Leibniz Center for Medicine and Biosciences, Luebeck, Germany, [4]University Hospital Schleswig-Holstein, Luebeck, Germany,[5]Biomedical Research in Endstage and Obstructive Lung Disease (BREATH), German Center for Lung Research, Institute for Pathology, Hannover Medical School, Hannover, Germany

Disclosures: Rosemarie Krupar: None; Christian Watermann: None; Helen Pasternack: None; Julika Ribbat-Idel: None; Christian Idel: None; Mark Philipp Kuehnel: None; Danny Jonigk: None; Sven Perner: None

Background: The tumor immune microenvironment (TIME) has a crucial impact on cancer progression and patients´ survival for various cancer entities. In head and neck squamous cell carcinoma (HNSCC) the development of recurrences in up to 60% is one main factor leading to poor prognosis. We aimed to reveal changes in the TIME of primary tumours and their corresponding recurrences, hypothesising that recurrent HNSCC have successfully escaped anti-tumor immune response.

Design: The TIME of 70 formalin fixed paraffin embedded (FFPE) tissue samples of HNSCC primary tumours and their corresponding local recurrences was characterised via immunohistochemical staining for the markers CD4, CD8, CD20, FOXP3, CD1A, PD1, CD68 and CD56 and semi-automated quantification with *Definines* software. RNA was extracted using the *Maxwell® 16 LEV RNA FFPE Purification Kit* for a subgroup of 18 patients, who underwent (chemo-)radiation therapy between the resection of the primary tumour and the development of a local recurrence. RNA expression levels of 770 immune related genes were identified by *nanostring nCounter® PanCancer Immune Profiling Panel* and assessed with the *nSolver™ Analysis Software*.

Results: The immunohistochemical TIME analysis demonstrated a loss of CD20+ B lymphocytes (p= 0.0006), an increase in CD1A+ dendritic cells (p= 0.017) and a decrease in the CD8/FOXP3 T-cell ratio (p= 0.106) in HNSCC recurrences compared to their corresponding

primary tumours. *Nanostring* analysis confirmed the depletion of B lymphocytes and additionally revealed a strong decrease in the total number of tumor infiltrating lymphocytes (TILs) as well as an increase in dendritic cells, mast cells, neutrophils and macrophages in HNSCC recurrences. In summary, 141 genes of the *nanostring panel* were identified to be significantly differentially expressed with the majority being downregulated in HNSCC recurrences. Significantly downregulated chemokines included CXCL13 and CXCR5, which are involved in B lymphocyte chemotaxis. In contrast, one of seven upregulated genes, Osteopontin, plays a major role in myeloid cell chemotaxis.

Figure 1 - 1187

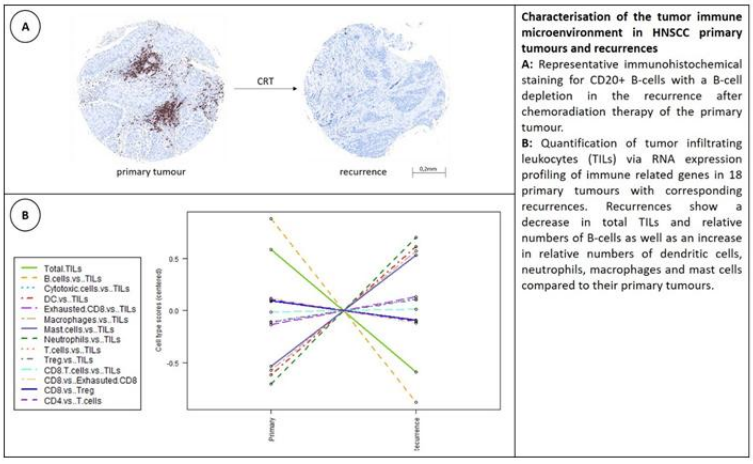

Characterisation of the tumor immune microenvironment in HNSCC primary tumours and recurrences
A: Representative immunohistochemical staining for CD20+ B-cells with a B-cell depletion in the recurrence after chemoradiation therapy of the primary tumour.
B: Quantification of tumor infiltrating leukocytes (TILs) via RNA expression profiling of immune related genes in 18 primary tumours with corresponding recurrences. Recurrences show a decrease in total TILs and relative numbers of B-cells as well as an increase in relative numbers of dendritic cells, neutrophils, macrophages and mast cells compared to their primary tumours.

Conclusions: Our results reveal significant differences in the TIME of HNSCC primary tumours and recurrences, characterised by a loss of B lymphocytes and an overall shift from anti-tumor immune response to an increase in pro-tumor immune factors in recurrences.

1188 Cam5.2 Immunostaining for Extrafollicular Reticulum Cells is an Effective Means of Separating Salivary Gland Tumor-Associated Lymphoid Proliferation From True Lymph Node Involvement

Elizabeth Kurian[1], Rodney Miller[2], Bahram Oliai[2], Justin Bishop[3]
[1]Dallas, TX, [2]ProPath, Dallas, TX, [3]University of Texas Southwestern Medical Center, Dallas, TX

Disclosures: Elizabeth Kurian: None; Rodney Miller: None; Bahram Oliai: None; Justin Bishop: None

Background: Tumor-associated lymphoid proliferation (TALP) is a well-recognized lymphoid reaction that is commonly associated with certain salivary gland carcinomas. A salivary carcinoma with TALP may be confused with true lymph node involvement, a potential pitfall in tumor staging that may result in erroneous prognostication or unnecessary surgical intervention. True lymph nodes harbor populations of extrafollicular reticulum cells, which can be highlighted by low molecular weight cytokeratin Cam5.2 immunostaining. We sought to determine whether Cam5.2 imunostaining this can be utilized to differentiate true lymph node involvement from TALP.

Design: The surgical pathology database of a large medical center was searched from 2015-2018 for cases of salivary gland lesions exhibiting TALP or true lymph node involvement, classified by the presence or absence of a definitive lymph node capsule and subcapsular sinus by routine histology. Cam.2 immunostaining was performed on all cases.

Results: 26 cases were identified, including 19 salivary gland carcinomas with TALP (10 acinic cell carcinomas, 8 mucoepidermoid carcinomas, 1 myoepithelial carcinoma), 4 metastatic carcinomas to regional lymph nodes (3 mucoepidermoid carcinomas, 1 squamous cell carcinoma), 2 carcinomas arising from benign lymph node inclusions (1 intraductal carcinoma and 1 secretory carcinoma), and 1 benign salivary lymph node inclusion. Cam5.2 immunostaining highlighted extrafollicular reticulum cells within the lymph node tissue of all 7 true lymph nodes (100%), and none of the tumors exhibiting TALP (0%), for a 100% concordance with the histologic classification.

Conclusions: In this series, employment of Cam5.2 staining of extrafollicular reticulum cells correctly distinguished true lymph node involvement from salivary gland carcinomas with TALP in 100% of cases. This strategy may be useful in histologically ambiguous cases to avoid upstaging cases as false positive nodal metastasis and the resulting prognostic and therapeutic implications. Moreover, Cam5.2 immunostaining may also be useful in identifying rare examples of salivary gland tumors arising from intranodal salivary gland inclusions.

1189 No or aberrant expression of E-cadherin in salivary duct carcinoma with rhabdoid features (SDCRF) is associated with CDH1 gene mutation: Multi-institutional retrospective study

Kimihide Kusafuka[1], Haruhiko Sugimura[2], HIdetaka Yamada[2], Takuya Kawasaki[3], Matsuyoshi Maeda[4], Koji Yamanegi[5], Satoshi Baba[6], Tomoyuki Ohuchi[7], Akira Ishihara[8], HIroshi Inagaki[9], Takashi Nakajima[10], Takashi Sugino[11]
[1]Sunto-gun, Shizuoka, Japan, [2]Hamamatsu University School of Medicine, Hamamatsu, Japan, [3]Shizuoka Cancer Center, Sunto-gun, Japan, [4]Toyohashi Municipal Hospital, Toyohashi, Japan, [5]Hyogo College of Medicine, Nishinomiya, Japan,[6]Hamamatsu University School of Medicine Hospital, Hamamatsu, Japan, [7]Keiyukai Sapporo Hospital, Sapporo, Japan, [8]Miyazaki Prefectural Nobeoka Hospital, Nobeoka, Japan, [9]Nagoya City University, Nagoya, Japan, [10]Shizuoka Cancer Center, Nagaizumi, Shizuoka, Japan, [11]Shizuoka Cancer Center, Nagaizumi-cho, Japan

Disclosures: Kimihide Kusafuka: None; Haruhiko Sugimura: None; HIdetaka Yamada: None; Takuya Kawasaki: None; Matsuyoshi Maeda: None; Koji Yamanegi: None; Satoshi Baba: None; Tomoyuki Ohuchi: None; Akira Ishihara: None; HIroshi Inagaki: None; Takashi Nakajima: None; Takashi Sugino: None

Background: Salivary duct carcinoma (SDC) is high-grade malignancy of the salivary glands. Salivary duct carcinoma with rhabdoid features (SDCRF) is extremely rare. We elucidate the morphological, immunohistochemical and genetic characteristics of SDCRF.

Design: We extracted SDCRF cases from pathology files of our institutions during 1995-2018. We examined them histologically and immunohistochemically. Immunostains were performed for cytokeratin (CK), Gross cystic disease fluid protein (GCDFP)-15, androgen receptor (AR), Her-2, EGFR, CK5/6, vimentin, SMARCB1, E-cadherin, Beta-catenin and Ki-67. We also examined the mutation status of E-cadherin (*CDH1*) gene in six cases, using PCR and direct sequence method with DNA extract from FFPE samples and analyzed with Mutation Taster software.

Results: Fifteen cases of SDCRF were selected. Eleven cases were male with a mean of 65 years (range: 36-85 years), which included ten parotid gland cases, including one accessory parotid gland case, and five submandibular gland cases. Nine cases died of disease. Histologically, the carcinoma components showed diffuse proliferation of less-coherent large ovoid atypical cells (rhabdoid-like cells) with eosinophilic cytoplasm and eccentric nuclei. Immunohistochemically, the rhabdoid-like cells were positive for GCDFP-15 and AR in all cases except for one case. All cases were positive for CK, but negative for vimentin. Intact nuclear expression of SMARCB1 was seen in all cases. No or decreased/cytoplasmic expression of E-cadherin was seen in 7 or 6 cases of 15 cases, respectively. No or decreased/cytoplasmic expression of beta-catenin was seen in 4 or 5 of 13 cases, respectively. In 6 cases which could be examined genetically, *CDH1* gene showed the non-sense or missense mutations in 4 or 4 of 6 cases, respectively. Three or one of four missense mutations were estimated as “disease causing” or “polymorphism” with Mutation Taster analysis, respectively.

Figure 1 - 1189

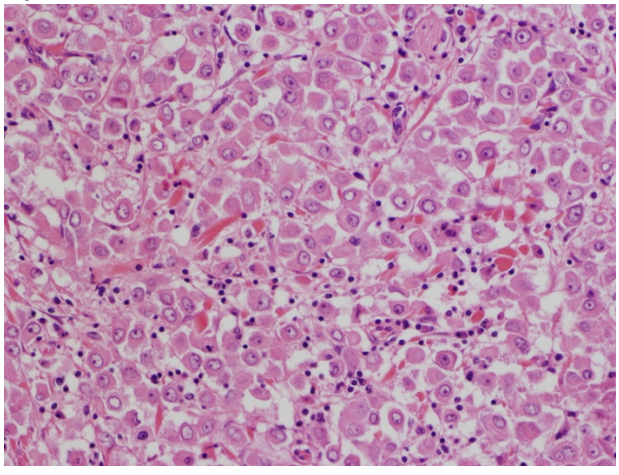

Figure 2 - 1189

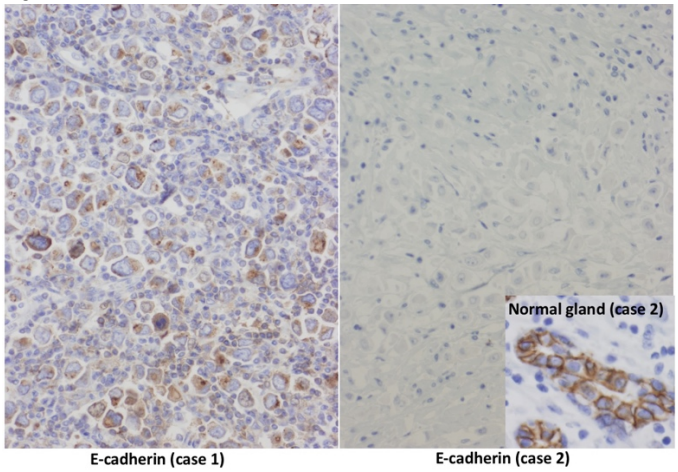

Conclusions: The morphogenesis of “rhabdoid-like cells” in SDCRF is related to the down-regulation of E-cadherin expression, which is induced by the *CDH1* gene mutation. Because of no co-expression of CK and vimentin, the tumor cells should not be called true “rhabdoid cells” but “rhabdoid-like cells”.

1190 Race-ethnicity Associated Disparities of Molecular Genotyping in Classical Papillary Thyroid Carcinoma, Follicular Variant Papillary Thyroid Carcinoma, and Noninvasive Follicular Thyroid Neoplasm with Papillary-Like Nuclear Features (NIFTP): An Institutional Experience, 162 Patients

Israa Laklouk[1], Gedik Reyhan[2], Sandra Cerda[2]
[1]Boston University Medical Center, Somerville, MA, [2]Boston University Medical Center, Boston, MA

Disclosures: Israa Laklouk: None; Gedik Reyhan: None; Sandra Cerda: None

Background: Recent studies have reported the evidence of racial disparities of clinical behavior, and long-term outcomes in of papillary thyroid carcinoma variants, but molecular prolife in different racial/ethnic populations has been understudied. The aim of this study was to update our prior findings and to evaluate racial differences in the expression of oncogenic driver mutations associated with classical papillary thyroid carcinoma (PTC), follicular variant papillary thyroid carcinoma (FVPTC), and Noninvasive Follicular Thyroid Neoplasm with Papillary-like Nuclear Features (NIFTP).

Design: We identified 162 resected thyroid nodules with corresponding ThyroSeq next generation result performed at our institute between February 2015 -June 2018. The race/ethnicity of all candidates included in this study was designated as white (31%), black (31%), Hispanic (19%), Asian (6%), and Other (13%).

Results: Of 162 resected thyroid nodules, 90 were neoplastic lesions. PTC was the most prevalent neoplastic diagnosis in whites (15/29, 52%) and Hispanics (10/21,48%), FVPTC was the most prevalent in blacks (10/19, 53%), and NIFTP in Asians (4/8, 50%) [P=0.01]. The molecular testing was positive in 25 of 37 PTCs. In white 14/15 PTCs had mutations (57% BRAF V600E, 43% RAS), 2/3 PTCs were positive for mutation in blacks (50% BRAF V600E, 50% PAX8/PPARG), 2/3 PTCs in Asians had RAS mutations (100%), 5/10 PTCs were positive in Hispanic (40% BRAF V600E, 60% RAS), in others 2/4 PTCs had only BRAF V600E (100%) [p= 0.029]. Of 25 FVPTCs, 20 FVPTCs had positive molecular testing; in whites 5/7 FVPTCs were positive (60% RAS, 20% PAX8/PPARG, 20% THADA fusion); in blacks, 10/10 FVPTCs were positive for RAS mutations (100%); Hispanic had 2/3 positive FVPTCs (50% THADA fusion, 50% RAS), others had 3/4 FVPTCs with positive mutations (66% BRAF K601, 33% RAS); no FVPTC was diagnosed in Asian [p= 0.012]. All NIFTPs had positive molecular testing, NIFTPs were associated with 50%TSHR and 50% RAS in Asians, Hispanics had 50%THADA fusion, 50% RAS, one NIFTP had RAS mutation in white, while others had 66% RAS and 33% THADA fusion. No NIFTP was diagnosed in Backs [p= 0.46]. See figure1.

Figure 1 - 1190

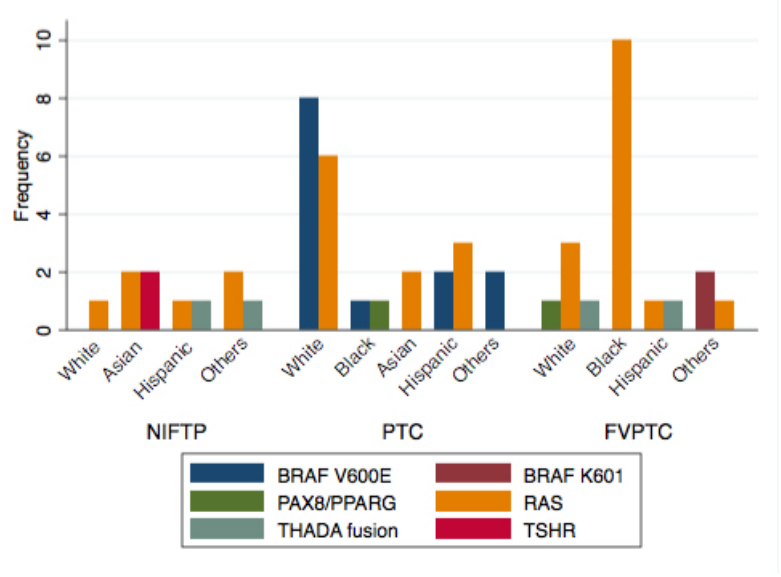

Conclusions: We found a significant difference in molecular profile of PTC and FVPTC in different race/ethnicity subgroups, however it was not significant in NIFTP. Even though, we cannot generalize our results, our findings emphasis the racial/ethnic differences may impact the diagnostic value of molecular testing.

1191 Computerized Quantitation of Tumor Cell Multinucleation is Strongly Prognostic for p16-Positive Oropharyngeal Squamous Cell Carcinoma

James Lewis[1], Zelin Zhang[2], Jun Xu[2], Cheng Lu[3], Justin Bishop[4], Anant Madabhushi[3]
[1]Vanderbilt University Medical Center, Nashville, TN, [2]Nanjing University of Information Science and Technology, Nanjing, China, [3]Case Western Reserve University, Cleveland, OH, [4]University of Texas Southwestern Medical Center, Dallas, TX

Disclosures: James Lewis: None; Zelin Zhang: None; Jun Xu: None; Cheng Lu: None; Justin Bishop: None; Anant Madabhushi: *Advisory Board Member*, Inspirata Inc.; *Consultant*, Inspirata Inc.

Background: Human papillomavirus (p16) positive oropharyngeal squamous cell carcinoma (OPSCC) has a generally favorable prognosis. However, 10 to 15% of patients develop recurrent disease and surviving patients can have significant morbidity from treatment. Better knowledge about which patients have more aggressive tumors versus more indolent ones is critical. Tumor cell multinucleation (MN) appears to be associated with disease recurrence. The current work detects and quantitates tumor cell MN both visually and by computer-aided image analysis, tests the p16 and HPV RNA status of these multinucleated cells, and correlates findings with patient outcomes.

Design: 240 p16 positive OPSCC patients was gathered from two institutions with robust clinical follow up. Best representative whole slides were digitally scanned. An experienced head and neck pathologist reviewed each slide for tumor cell MN (3 or more nuclei in one cell) and quantitated it by finding a hot spot and counting 10 consecutive HPFs. Image analysis to detect all nuclei on the slide and and to detect MN was performed based on human annotation. Raw tumor MN counts were normalized to total nuclei on the slide. Time-to-event data were analyzed using Kaplan-Meier method and Cox modeling. Lymph node slides from 9 separate patients with extensive anaplasia and MN were immunostained for p16 and underwent high risk HPV RNA in situ hybridization.

Results: 219 patients had sufficient tumor for visual quantitation and 229 for image analysis. Visually,106 (48%) had no MN. MN index positive patients ranged from 1 to 71 cells/HPF. Computerized MN quantitation normalized to total nuclei ranged from 0.0032 to 0.044% and was strongly correlated with survival (see Table). In particular, by KM analysis, patients with MN to total nuclei ratios > median had poorer overall and disease specific survival (p=0.002 and 0.0002, respectively), including just among the 180 AJCC Stage I/II patients (p=0.007 and 0.002, respectively - 4 year DFS 90% versus 65%). In all 9 separate patients, MN tumor cells showed p16 expression (although commonly of reduced intensity) in both nuclei and cytoplasm and retained positive for high risk HPV mRNA.

Cox PH Analysis	Overall Survival: HR (95% CI)	Disease Free Survival: HR (95% CI)
Visual MN Index (per index increase)	0.99 (0.94, 1.05); p=0.706	0.98 (0.94, 1.03); p=0.446
Computer-Aided MN/Total Nuclei (per 0.1% increase)	29.29 (0.72, 1191.79); p=0.074	142.15 (8.23, 2454.03); **p=0.0006**

Conclusions: Computerized detection and quantitation of MN is strongly prognostic for overall and disease free survival in p16+ OPSCC, including in low and intermediate risk (AJCC I and II) patients, further setting the stage for its possible use as a risk stratification test in routine clinical practice.

1192 Computational Histomorphometric Classifier Identifies Higher Risk Patients Who Might Benefit from Adjuvant Radiation within Clinically Defined "Low-Risk" Oral Cavity Squamous Cell Carcinomas

Cheng Lu[1], Kaustav Bera[1], Xiangxue Wang[2], James Lewis[3], Anant Madabhushi[1]
[1]Case Western Reserve University, Cleveland, OH, [2]Cleveland, OH, [3]Vanderbilt University Medical Center, Nashville, TN

Disclosures: Cheng Lu: None; Kaustav Bera: None; Xiangxue Wang: None; James Lewis: None; Anant Madabhushi: *Advisory Board Member*, Inspirata Inc.; *Consultant*, Inspirata Inc.

Background: Oral cavity squamous cell carcinoma (OC-SCC) is the most common head and neck malignancy (38%) in the United States (US) and worldwide. In 2018, the American Cancer Society estimates about 33,950 new OC-SCC cases in the US with an expected 6800 deaths. The prognosis remains relatively poor, with worldwide 5-year overall survival of only 50%. In addition to TNM stage, factors such as perineural and lymphovascular invasion, and depth of invasion play a role in the clinical classification of these tumors as low-, intermediate-, or high risk. While low risk tumors are overwhelmingly treated by surgical removal alone, many patients' tumors still recur. Studies have shown the benefit of adjuvant radiation in appropriately selected patients, and there is a major need for a clinically validated test that can help to identify patients with low risk OC-SCC who might benefit from post-operative adjuvant radiation.

Design: A retrospective chart review of the Radiation Oncology and Otolaryngology databases at a single large institution was performed to continuously select N=115 OC-SCC patients seen between 1997-2010. Out of these N=44 cases were clinically defined as "low-risk"

(8th ed. AJCC), who were all treated by surgical excision alone. H&E stained TMAs were obtained and digitized for these cases along with clinical and outcome data. A set of histomorphometric features pertaining to the local nuclear diversity in terms of nuclear morphology was extracted from the digitized TMA at 40x magnification. A Wilcoxon rank sum feature selection algorithm was then used to pick out the top 10 features predicting DFS. These top features were used to train a model under a leave one out cross-validation scheme to generate a risk score.

Results: OHbIC generated a risk assessment for every patient in the low-risk cohort. Subsequently log-rank test was used to calculate the HR and generate the KM curves stratifying patients based on DFS. OHbIC found two distinct groups as illustrated in Figure 1. On univariate analysis, higher OHbIC scores also had a HR of 2.9 (p=0.027) as compared to the lower OHbIC for potentially worse outcomes. None of the clinicopathological variables were found to be statistically significant predictors of outcome in this selected group of patients.

Variable	DFS HR(95% CI)	p-value
Age (>60 vs <60)	1.2 (0.659-2.17)	0.54
T-stage (T1 vs T2)	1.06 (0.502-2.22)	0.88
N-stage (N1 vs N0)	1.96 (0.496-7.78)	0.18
Histologic grade (moderately/poorly differentiation vs well differentiation)	1.46 (0.61-3.49)	0.33
Histologic grade (well/moderately differentiation& vs poorly differentiation)	1.7 (0.894-3.23)	0.14
OHbIC prediction (positive vs negative)	2.9 (1.23-6.86)	0.03

Figure 1 - 1192

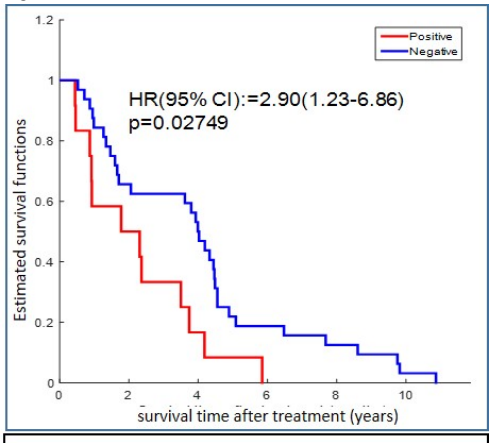

Kaplan-Meier survival curve of the low-risk OC-SCC cohort (n=44) using OHbIC to stratify the patients based off DFS. OHbIC found two distinct groups (HR=2.90; p=0.027) within the AJCC defined "low-risk" group.

Figure 2 - 1192

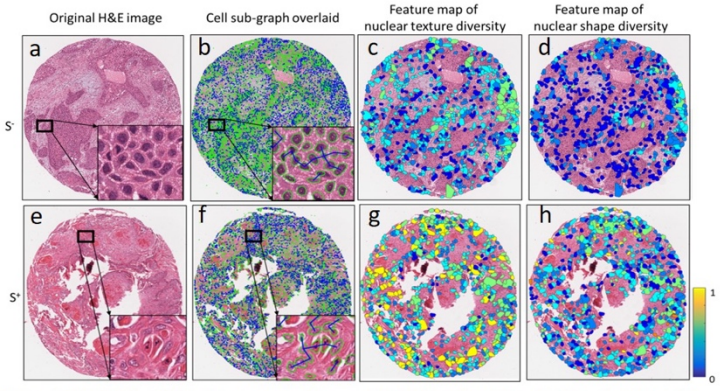

Figure 2: Quantitative histomorphometry feature map illustration. The first column (a, e) shows H&E-stained images of tumors from S- (no disease-specific death) and S+ (disease-specific death) patients from the low risk group. The segmented nuclei contours (shown with green boundaries) are shown in the second column (b, f) with cell cluster graphs. The lines represent connecting edges between nuclei. The third (c, g) and fourth (d, h) columns show quantitative histomorphometric features that capture the local cellular diversity in terms of nuclear texture and shape, respectively. Each small color patch represents different local cell sub-graph. The blue and yellow colors represent low and high diversity, respectively. The S+ case shows a larger range of cellular diversity, shown as brighter color, than that in the S- case.

Conclusions: OHbIC has the potential to be a validated and non-invasive imaging biomarker to predict which traditional "low-risk" OC-SCC patient might derive benefit from post-operative radiotherapy after routine surgical resection.

1193 Lymph Node Characteristics and Their Prognostic Significance in Oral Squamous Cell Carcinomas

Namrata Maity[1], Pattatheyil Arun[1], Prateek Jain[1], Saranya Venkatesh[1], Indu Arun[1]
[1]Tata Medical Center, Kolkata, India

Disclosures: Namrata Maity: None; Pattatheyil Arun: None; Prateek Jain: None; Saranya Venkatesh: None; Indu Arun: None

Background: Oral squamous cell carcinomas are by far the most common malignancy of the head and neck region accounting for 90% of the cases. In spite of its wide prevalence and refinement of diagnostic and treatment modalities with time, the survival of oral squamous cell carcinoma patients is still elusive and depends on a large number of factors. Lymph node (LN) metastasis is one such factor that is associated with significant poor prognosis. Characteristic of LN involvement, including the number of nodes involved, level of nodal involvement, size of metastatic deposit and extranodal extension can predict tumour behaviour, progression and survival.

Design: A retrospective analysis of LN characteristics of 213 oral squamous cell carcinoma patients from 2011 to 2015 from a single institution was performed. LN characteristics including number (no.) of positive nodes, LN ratio (ratio of no. of LNs positive for metastasis

and no. of LNs harvested), size of metastatic deposit, presence of extranodal extension (ENE), extent of ENE, lowest level of LN involvement and their association with overall (OS) and disease free survival (DFS) and other clinico-pathological variables was determined.

Results: DFS using Kaplan Meier curves showed LN ratio, size of the deposit, ENE and lower level of node positivity to be predictors of poor DFS. However, none of the factors assessed had an impact on OS. Multivariate Cox regression analysis of factors showed significance for LNR and low level of positive nodes only.

LEVEL OF LYMPH NODE INVOLVEMENT				
	Frequency	**Percent**	**Valid Percent**	**Cumulative Percent**
Level I	70	32.9	32.9	32.9
Level II	82	38.5	38.5	71.4
Level III	37	17.4	17.4	88.7
Level IV	14	6.6	6.6	95.3
Level V	10	4.7	4.7	100.0
Total	213	100.0	100.0	
EXTRANODAL EXTENSION				
	Frequency	**Percent**	**Valid Percent**	**Cumulative Percent**
Absent	102	47.9	47.9	47.9
Present	111	52.1	52.1	100.0
Total	213	100.0	100.0	
PATHOLOGICAL NODAL STAGE (pN)				
	Frequency	**Percent**	**Valid Percent**	**Cumulative Percent**
N1	83	39.0	39.0	39.0
N2a	3	1.4	1.4	40.4
N2b	103	48.4	48.4	88.7
N2c	20	9.4	9.4	98.1
N3	4	1.9	1.9	100.0
Total	213	100.0	100.0	
Total 213 treatment naive for oral cancer patients were included in the study				
Median No of nodes harvested are 46 (22-168)	Median number of positive nodes are 3 (0-17)	Lymph node ratio (LNR) is 0.06 (0.01-0.48)	Median size of deposit is 18 mm (5-68 mm)	Median extent of extranodal extension is 1.9mm (0.1-9 mm)

Figure 1 - 1193

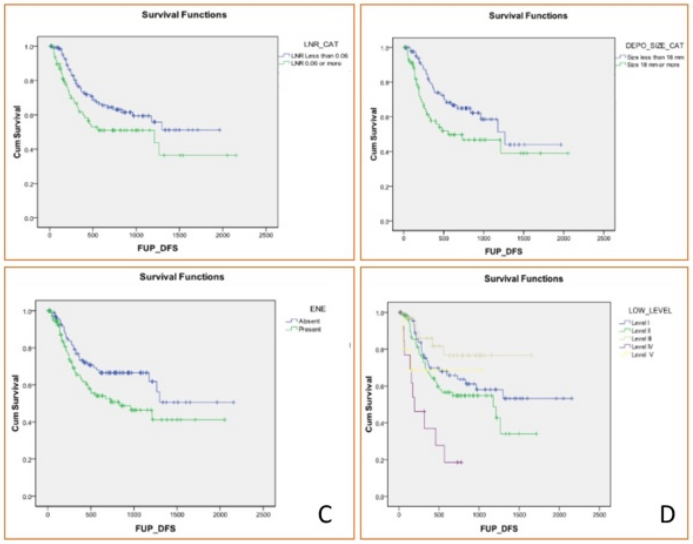

A. Survival curve for lymph node ratio (p=0.032)

B. Survival curve for deposit size category (p=0.028)

C. Survival curve for extranodal extension (p=0.036)

D. Survival curve for level of lymph node involvement (p=<0.001)

Conclusions: Lymph node ratio and location of positive nodes were the only predictors of DFS in squamous cell carcinomas of oral cavity.

1194 Real-Time PCR Testing of Fine Needle Aspirations of Metastatic Head and Neck Squamous Cell Carcinoma: Exposing the Limitations of Conventional p16 Immunostaining

Mena Mansour[1], William Westra[2], Fadi Salem[2]
[1]*Washington University Medical Center, St. Louis, MO,* [2]*Icahn School of Medicine at Mount Sinai, New York, NY*

Disclosures: Mena Mansour: None; William Westra: None; Fadi Salem: None

Background: Given the propensity for HPV-positive head and neck squamous cell carcinoma (HPV-HNSCC) to metastasize to cervical lymph nodes, fine needle aspiration (FNA) plays an important diagnostic role in their initial detection. Indeed, there is now an unwavering commitment to HPV testing of FNAs even in the absence of clear guidelines for methodology and threshold criteria. A particular difficulty pertains to the interpretation of p16 staining of cell blocks.

Design: Data was collected for 210 patients with suspected regionally metastatic HNSCC that had undergone FNA as part of standard clinical care. Initial HPV screening was performed on cell blocks with real-time PCR using primers designed to target the L1 region of high-risk HPV types. Additional genotyping was performed on HPV positive cases. The results were compared to p16 staining and subsequent excisions when available.

Results: Of the 207 samples with sufficient DNA, 175 (85%) were HPV positive. HPV-16 was the most commonly detected genotype (90%). Of these positive cases, the primary tumor site was the oropharynx (n=154, 88.0%), supraglottic larynx (n=2, 1.1%), nasal cavity (n=1, 0.6%), hypopharynx (n=1, 0.6%) or unknown (n=17, 9.7%). On comparison with 31 paired surgical excisions, HPV status was concordant in all cases (100% correlation). Of 142 HPV-positive cases with matching p16 stains, p16 staining was reported as positive (n=85, 60%), focal (n=27, 19%), negative (n=24, 17%) or non-contributory (n=6, 4%); and only 33% reached the standard threshold limit (i.e. 70%) for HPV positivity.

Conclusions: For patients with metastatic HNSCC, real-time PCR of FNAs reliably reflects HPV status, and is superior to conventional p16 immunostaining.

1195 Histologic Spectrum of Polymorphous Adenocarcinoma of the Salivary Gland Harbor Genetic Alterations Affecting PRKD Genes

Ana Paula Martins Sebastiao[1], John Lozada[1], Fresia Pareja[1], Bin Xu[1], Arnaud Da Cruz Paula[1], Ronald Ghossein[1], Felipe Geyer[1], Ilan Weinreb[2], Britta Weigelt[1], Jorge Reis-Filho[1], Nora Katabi[1]
[1]*Memorial Sloan Kettering Cancer Center, New York, NY,* [2]*University Health Network, Toronto, ON*

Disclosures: Ana Paula Martins Sebastiao: None; John Lozada: None; Fresia Pareja: None; Bin Xu: None; Arnaud Da Cruz Paula: None; Ronald Ghossein: None; Felipe Geyer: None; Ilan Weinreb: None; Britta Weigelt: None; Jorge Reis-Filho: *Advisory Board Member*, Volition Rx; *Advisory Board Member*, Paige.AI; *Consultant*, Goldman Sachs; Nora Katabi: None

Background: Polymorphous adenocarcinoma (PAC), cribriform adenocarcinoma of the salivary gland (CASG) and tumors with a predominant papillary pattern (TPPP) display overlapping histologic features, such as papillary arrangement, and cribriform and solid areas, posing challenges to their differential diagnosis. Over 70% of classical PACs harbor recurrent *PRKD1* E710D hotspot mutations. Conversely, CASG has shown rearrangements involving *PRKD1*, *PRKD2* or *PRKD3* in 80% of cases. Approximately one third of cases are difficult to classify and have been labeled tumors with indeterminate features (TIFs). Moreover, there is controversy about whether CASG and PAC are related, and no single molecular study has incorporated all these alterations to stratify this differential diagnosis.

Design: Thirty-five tumors in the morphologic spectrum of PAC were retrieved from the files of the authors' institutions. After a consensus review by three Head and Neck pathologists (NK, BX, RG), the tumors were classified as i) PAC, ii) CASG, iii) TIF and iv) TPPP (? 50% papillary pattern). The majority of cases were included in a prior histologic study on PACs. Tumor DNA from all cases was subjected to a new Sanger sequencing analysis of *PRKD1* hotspot loci. Fluorescence *in situ* hybridization (FISH) analysis for *PRKD1, PRKD2* and *PRKD3* was performed using dual-color break-apart probes.

Results: Of the thirty-five cases, all were successfully subjected to *PRKD1* sequencing and 33 for FISH analysis. The tumors affected 11 males (31%) and 24 females (69%). The majority (33/35; 94%) of tumors originated from minor salivary glands, and the most frequent site was the palate (21/41, 51%). Sanger sequencing analysis revealed *PRKD1* E710D hotspot mutations in 56% (5/9), 20% (2/10) and 43% (6/14) of PACs, CASGs and TIFs, respectively, whereas the two TPPPs were wild-type for *PRDK1*. FISH analysis conducted in all *PRKD1* wild-type cases revealed *PRKD1*/*PRKD2*/*PRKD3* rearrangements in 25% (1/4), 88% (7/8) and 63% (5/8) of the PACs, CASGs and TIFs respectively, and in both TPPP cases.

Conclusions: PACs, CASG, TPPP and TIF are underpinned by genetic alterations affecting *PRKD* genes. Although*PRKD1* E710D hotspot mutation are numerically more frequent in classic PACs and *PRKD1, PRKD2* and *PRKD3* rearrangements are more frequently found in CASGs, there is significant overlap at the genetic level. These findings support the notion that these tumors represent a spectrum of lesions driven by PRKD gene alterations rather than two separate entities.

1196 Recurrences and High-Grade Forms of Polymorphous Adenocarcinoma are Underpinned by Genetic Alterations Affecting PRKD Genes

Ana Paula Martins Sebastiao[1], Fresia Pareja[1], Rahul Kumar[1], Ju Youn Lee[1], Catarina Silveira[1], Edaise Da Silva[1], David Brown[1], Nora Katabi[1], Simon Chiosea[2], Britta Weigelt[1], Jorge Reis-Filho[1], Raja Seethala[3]
[1]Memorial Sloan Kettering Cancer Center, New York, NY, [2]University of Pittsburgh, Pittsburgh, PA, [3]University of Pittsburgh School of Medicine, Pittsburgh, PA

Disclosures: Ana Paula Martins Sebastiao: None; Fresia Pareja: None; Rahul Kumar: None; Ju Youn Lee: None; Catarina Silveira: None; Edaise Da Silva: None; David Brown: None; Nora Katabi: None; Simon Chiosea: None; Britta Weigelt: None; Jorge Reis-Filho: *Advisory Board Member*, Volition Rx; *Advisory Board Member*, Paige.AI; *Consultant*, Goldman Sachs; Raja Seethala: None

Background: Although most polymorphous adenocarcinomas (PACs) are low-grade and follow an indolent course, some cases may be high-grade *de novo*, or display recurrences. Classic PACs harbor recurrent *PRKD1* E710D somatic hotspot mutations in >70% of cases. *PRKD1* wild-type PACs often show cribriform/papillary glomeruloid growth and tend to harbor *PRKD1*, *PRKD2* or *PRKD3* rearrangements. Here we sought to define whether high-grade PACs, either *de novo* or recurrences, would be driven by the same somatic genetic alterations previously described in classic primary PACs. We also sought to define the repertoire of somatic genetic alterations in a PAC where materials from the primary tumor and recurrence were available.

Design: Two recurrent PACs with high-grade morphology and one *de novo* high grade PAC were microdissected. DNA was extracted from microdissected tumor and normal areas and subjected to whole-exome (n=2) or MSK-IMPACT sequencing (i.e. the primary and recurrent lesions of one patient). The presence of the *PRKD1* E710D hotspot mutation was also investigated in all samples by Sanger sequencing analysis. Fluorescence *in situ* hybridization (FISH) for *PRKD1, PRKD2* and *PRKD3* using dual-color break-apart probes was conducted in the case that was wild-type for *PRKD1*.

Results: Two high-grade PACs (n=2; 67%), including a recurrence and *de novo* case, harbored *PRKD1* E710D hotspot mutations. One recurrent high-grade PAC was wild-type for *PRKD1* and displayed rearrangements in *PRKD2* (n=1; 33%), as demonstrated by FISH. Whole-exome or MSK-IMPACT analysis revealed no additional recurrent genetic alterations in the PACs analyzed. A clonal decomposition analysis of a matched primary and recurrent PAC revealed that a minor sub-clone from the primary tumor, which harbored a *PIK3CA* missense mutation (D350G) and a frameshift mutation affecting *SETD2* (L2012Wfs*7) became dominant in the recurrent tumor, which in addition acquired likely-pathogenic mutations in *ZFHX3* (G3527dup) and *ERBB2* (V839M). These findings suggest that the PAC recurrence stemmed from a minor sub-clone of the primary PAC.

Conclusions: Our findings support the notion that the *PRKD1* E710D hotspot mutation and the rearrangements involving members of the PRKD gene family are early events and drivers of high-grade PACs, either *de novo* or in recurrences. The recurrences of PACs may be driven by clonal selection of preexisting sub-clones of the primary tumor.

1197 Transcriptionally-Active Low-Risk HPV in Sinonasal Inverted Papillomas; Closing the Chapter

Mitra Mehrad[1], Edward Stelow[2], James Lewis[1]
[1]Vanderbilt University Medical Center, Nashville, TN, [2]University of Virginia Health System, Charlottesville, VA

Disclosures: Mitra Mehrad: None; Edward Stelow: None; James Lewis: None

Background: Inverted papilloma (IP) is the most common type of sinonasal papilloma. Recurrences are common and malignant progression occurs in ~10% patients. Recent studies have shown that IPs, including those with carcinoma, are not driven by transcriptionally-active high-risk human papillomavirus (hrHPV). However, low risk HPV (lrHPV) is sometimes identified in IPs and head and neck carcinomas, but its role is not clear and no one to date has evaluated for transcriptionally-active lrHPV in these lesions.

Design: IP cases and carcinomas developing from them over a ten-year period were identified and re-reviewed. The tumors had been previously assessed for p16 by immunohistochemistry with a 70% staining cutoff and for hrHPV mRNA by RT-PCR capable of identifying 12 of the most common types. Low-risk HPV RNA (cocktail probe) was performed using RNAscope (Advanced Cell Diagnostics) for 6 lrHPV types (6,11, 40, 42, 43, and 44). Brown dot signals were considered positive as follows: 3+ easily visualized at 100x; 2+ easily visualized at 200x; and 1+ visualized at 400x. Seven cases of non-keratinizing and papillary squamous cell carcinoma (NKSCC), as defined by the WHO, with “papilloma-like” (papillary and inverted) growth patterns were included as controls.

Results: Overall, 40 IPs were identified, including 5 (12.5%) with associated SCC. All IPs and associated carcinomas were negative for p16 and hr HPV RNA by RTPCR. RNA ISH for lrHPV ISH failed in 2 cases due to lack of specimen RNA integrity. Of the remaining 38, lrHPV RNA was detected in 6 (15.8%) cases, including 3 of the 5 (60%) associated with SCC. This difference was statistically significant ($p = 0.02$) All seven nonkeratinizing SCCs not associated with IP were negative for lrHPV RNA while 5 of them were positive for p16 and hrHPV RNA.

Conclusions: Although DNA data in the past has been highly variable, our HPV RNA data shows that a small subset of IPs are related to transcriptionally-active lrHPV. It also shows that lrHPV is enriched in specimens with malignant transformation, suggesting that they may have a role in this progression.

1198 Sinonasal Teratocarcinosarcoma: A Single Institution Clinic-Pathological Study

Neha Mittal[1], Munita Bal[2], Swapnil Rane[2], Asawari Patil[2]
[1]Tata Memorial Hospital, Mumbai, Maharashtra, India, [2]Tata Memorial Centre, Mumbai, India

Disclosures: Neha Mittal: None; Munita Bal: None; Swapnil Rane: None; Asawari Patil: None

Background: Sinonasal teratocarcinosarcoma (SNTCS) is a rare tumour with a unique combination of teratomatous and malignant epithelial and mesenchymal elements. Our aim was to study the clinical and pathological findings of SNTCS cases diagnosed at our center.

Design: A detailed retrospective review of the clinical and histological parameters of SNTCS cases diagnosed from 2008 onwards was undertaken.

Results: A total of 35 patients (34 male, 1 female) diagnosed as SNTCS (including 4 recurrent and 4 cases with distant metastasis) with an age range of 16-68 years (mean,48; median, 47 years) were evaluated. The most notable clinic-radiological findings were symptoms of nasal obstruction and bleeding in 72.8%, nose and ethmoid sinus as the origin in 90%, cribriform plate erosion in 59.1%, and intracranial extension in 40.1% patients. On histology, SNTCS showed a very characteristic triphasic pattern of epithelial, mesenchymal and primitive undifferentiated component. Epithelial elements were seen as benign and malignant glandular and/or squamous components; at places exhibiting a hybrid squamo-glandular units frequently containing fetal-type immature squamous elements. Mesenchymal component was seen as immature cellular mesenchyme with loose stroma. Primitive undifferentiated tumor cells seen as cellular blue round cells in sheets or nodules (positive for epithelial and neuroendocrine markers) formed the third and frequently the dominant component. Teratomatous components were seen in 75% of recurrent and 55.6% of metastatic cases. Nodal metastasis was seen in 5 cases (14.3%). Mucin-secreting adenocarcinoma (2cases), undifferentiated malignant tumour (1 case), osteogenic sarcoma (1 case), and vascular tumour like areas (4 cases) were the unusual histological findings. Rhabdomyoblastic differentiation is better highlighted on immunohistochemistry(2 cases on histology, and 8 cases on IHC). Multimodality (NACT, Surgery, CTRT) therapy was completed in 15 patients, 12 of whom are alive without disease(NED), and three are alive with disease(AWD), with a follow up of 2-84 months.

Parameter	Primary (N=30)	Residual/Recurrent(N=4)	Distant and nodal metastasis(N=9)
Epithelial component			
A. **Benign glands**	30 (100%)	3(75%)	5(55.6%)
B. **Benign fetal-like squamous cells**	29(96.7%)	3(75%)	2(22.2%)
C. **Malignant round cell component(RC)**	30(100%)	3(75%)	9(100%)
Mesenchymal component			
A. **Immature mesenchyme-like**	28(93.3%)	2(50%)	Not seen
B. **Rhabdomyosarcomatous differentiation**	8 (2 on histology, rest only on IHC)	-	1 case
C. **Cartilage**	2 (6.7%)	-	-
D. **Smooth muscle**	2 (6.7%)	-	-
E. **Osteosarcoma-like**	1(3.3%)	1 case(same as primary)	-
F. **Glial areas**	2 (6.7%)	2(50%)(post-chemo)	-
G. **HPC/ Vascular tumour like**	4 (13.3%)	1 case (also in primary)	-
Immunohistochemistry			
A. **CK/AE1/AE3- RC component**	27(90%) (dot–like positivity)	3(75%)	2/4(50%)
B. **P40 in RC component**	2 (10%, <5%of tumour cells)	-	-
C. **Neuroendocrine marker positivity in RC (synapto, chromo, CD56)**	29(96.7%)	3(75%)	2/4(50%)
D. **NUT IHC**	0/5	0/2	0/2
E. **Desmin in mesenchymal component**	7	1	1
F. **Myogenin in mesenchymal component**	6	0	1
Treatment details			
A. **On treatment**	2	1	NA
B. **DOD (on treatment)**	2	NA	NA
C. **Multimodality completed**	13	2	
D. **AWD**	2/13	1/13	NA
E. **NED**	11/13	1/13	NA

Conclusions: SNTCS is a multiphenotypic tumour of naso-ethmoid region with a distinct male preponderance, divergent differentiation on histology and/or immunohistochemistry in primary as well as metastatic tumours, and a significant risk of recurrence, nodal and distant metastasis. Tri-modality therapy in a tertiary care oncology set-up, with aggressive follow-up can significantly affect the outcome.

1199 INI-1-deficient Sinonasal Undifferentiated Carcinomas Are Morphologically Diverse Yet Show Significantly Worse Survival Outcomes

Jeremy Molligan[1], Chandala Chitguppi[1], Voichita Bar-Ad[1], James Evans[1], Jennifer Johnson[1], Gurston Nyquist[1], Mindy Rabinowitz[1], Marc Rosen[1], Stacey Gargano[2]
[1]Thomas Jefferson University, Philadelphia, PA, [2]Thomas Jefferson University Hospital, Haddonfield, NJ

Disclosures: Jeremy Molligan: None; Chandala Chitguppi: None; Stacey Gargano: None

Background: Undifferentiated and poorly differentiated carcinomas of the sinonasal tract are a diagnostic challenge for the practicing pathologist. This group of tumors includes poorly differentiated adenocarcinoma and squamous cell carcinoma (SCC), sinonasal undifferentiated carcinoma (SNUC), NUT-midline carcinoma, neuroendocrine carcinoma, among others. A distinct entity has emerged from this group defined by loss of SMARCB1 (INI-1) by immunohistochemistry. We conducted a clinicopathologic review of undifferentiated and poorly differentiated sinonasal carcinomas at our institution, evaluated the INI-1 status of these tumors, and sought to correlate INI-1 status with patient outcomes.

Design: A natural language search was conducted at a single institution between 2006 and 2018 for all undifferentiated or poorly differentiated neoplasms of the sinonasal tract. Cases were retrospectively reviewed for histomorphology, immunohistochemical profile, treatment strategy, and clinical outcome. INI-1 status was evaluated by immunohistochemical staining.

Results: Fifty seven cases of poorly or undifferentiated sinonasal carcinoma were identified, consisting of 20 SCC, 2 adenocarcinoma, 16 SNUC, 1 NUT midline carcinoma, and 10 poorly differentiated carcinoma, NOS and 8 "Other" diagnosis. Eight of the 47 cases (17%) with available blocks were aberrantly INI-1 deficient. The INI-1 deficient cases consisted of 7 SNUC and 1 poorly differentiated SCC. There were no statistically significant differences in growth pattern, cytomorphology, presence of necrosis, and mitotic rate between the INI-1 retained and INI-1 deficient groups. The INI-1 deficient SNUCs showed diverse cytomorphology (3 squamoid, 3 basaloid, 2 plasmacytoid/rhabdoid) (Figure 1). Overall survival was 46.75 months and 11.75 months for INI-1 retained and INI-1 deficient SNUCs, respectively (p=0.05) (Figure 2). Disease-free survival was 31.75 months and 8.5 months for INI-1 retained and INI-1 deficient SNUCs, respectively (p=0.03).

Figure 1 - 1199

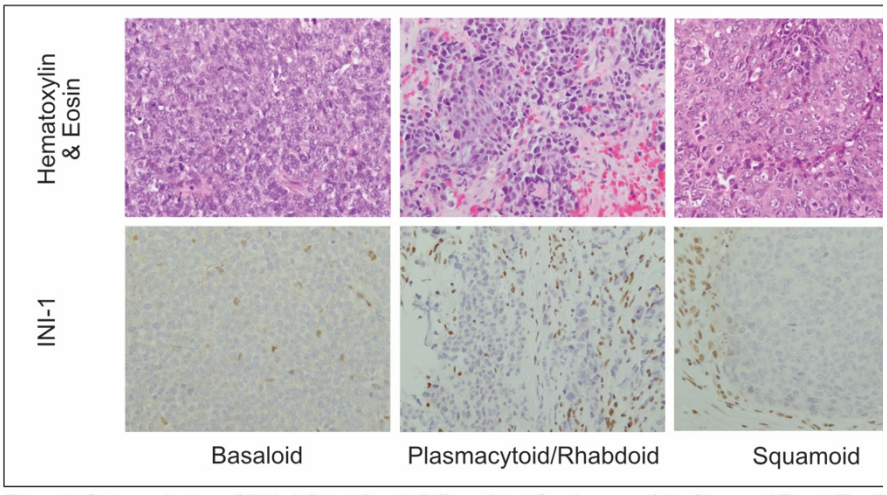

Figure 1. Cytomorphology of INI1-deficient Poorly Differentiated Carcinomas of the Sinonasal Tract. The II deficient SNUCs showed diverse cytomorphology (3 basaloid, 2 plasmacytoid/rhabdoid, 2 squamoid)

Figure 2 - 1199

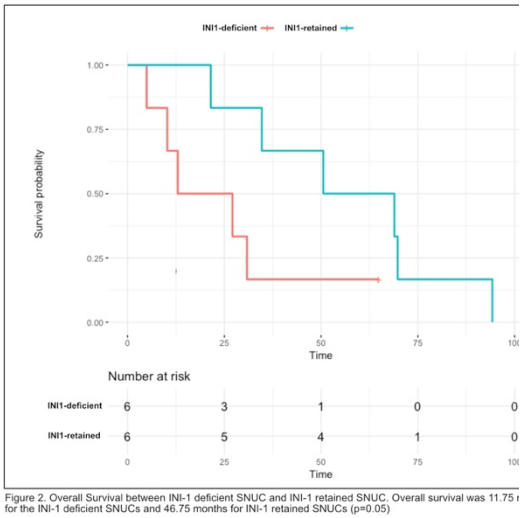

Figure 2. Overall Survival between INI-1 deficient SNUC and INI-1 retained SNUC. Overall survival was 11.75 for the INI-1 deficient SNUCs and 46.75 months for INI-1 retained SNUCs (p=0.05)

Conclusions: INI-1 status should be evaluated in all undifferentiated and poorly differentiated carcinomas of the sinonasal tract. In our study, INI-1 deficiency in a tumor otherwise meeting diagnostic criteria for SNUC confers a significantly worse clinical prognosis. The subcategorization of sinonasal carcinomas harboring a unique molecular finding of SMARCB1 (INI-1) inactivation will help facilitate better understanding of the pathogenesis, clinical behavior, and potential therapeutic options for these tumors.

1200 Tumour Cell Anaplasia and Multinucleation as Prognosticators in Oropharyngeal Squamous Cell Carcinoma

Peter Molony[1], Linda Feeley[2], Cynthia Heffron[2], Patrick Sheahan[3], Gerard O'Leary[4], Reiltin Werner[2], Christine White[5], Cara Martin[6]
[1]Smithfield, Ireland, [2]Cork University Hospital, Cork, Ireland, [3]South Infirmary Victoria University Hospital, Cork, Ireland, [4]South Infirmary Hospital Cork, Cork, Ireland, [5]Trinity College Dublin, Dublin, Ireland, [6]Trinity St. James's Cancer Institute, Dublin, Ireland

Disclosures: Peter Molony: None; Linda Feeley: None; Cynthia Heffron: None; Patrick Sheahan: None; Gerard O'Leary: None; Reiltin Werner: None; Christine White: None; Cara Martin: None

Background: Tumour cell anaplasia and multinucleation have previously been shown to be prognostically significant in human papilloma virus (HPV) related oropharyngeal squamous cell carcinoma (OPSCC). We sought to further investigate the potential utility of these 2 parameters in OPSCC as markers of high grade disease.

Design: Retrospective review of 58 patients who underwent primary resection of OPSCC with or without lymph node dissection. Slides of both the primary and nodal metastatic disease where present were reviewed and assessed for the presence of tumour cell anaplasia and multinucleation using the criteria devised by Lewis et al. The impact of anaplasia and multinucleation on survival outcomes and disease recurrence were evaluated according to HPV status.

Results: Of the 58 patients comprising the final study population 32 were HPV-positive and 26 were HPV-negative. Amongst the entire cohort neither anaplasia nor multinucleation were significant for survival outcomes. Within the HPV-positive cohort anaplasia or multinucleation was not significant for recurrence free survival (p=0.91, p=0.75 respectively) or disease specific survival (p=0.28, p=0.23 respectively). Within the HPV-negative group anaplasia or multinucleation at the primary site again was not significant for recurrence free survival (p=0.70, p=0.54 respectively) or disease specific survival (p=0.62, p=0.19 respectively). However, anaplasia or multinucleation in nodal metastatic disease was significant for recurrence free survival (p=0.03, p=0.001 respectively) and multinucleation alone was significant for disease specific survival (p=0.001).

Conclusions: Anaplasia and multinucleation in nodal metastases may be significant predictors of poor outcome in HPV negative OPSCC. Anaplasia and multinucleation were not found to be prognostically significant in HPV positive cases in this study. Further investigation in sufficiently large patient cohorts will be required to definitively ascertain the potential utility of anaplasia and multinucleation as grading parameters in HPV positive and negative OPSCC.

1201 Immunostains are Required to Identify Intraepithelial Melanocytic Proliferations in Sinonasal Mucosal Melanoma

Gustavo Moreno[1], Shira Ronen[2], Bryan Hunt[2], Tamar Giorgadze[2]
[1]Medical College of Wisconsin, Brookfield, WI, [2]Medical College of Wisconsin, Milwaukee, WI

Disclosures: Gustavo Moreno: None; Shira Ronen: None; Bryan Hunt: None; Tamar Giorgadze: None

Background: Sinonasal mucosal melanoma (SNMM) is a rare malignancy, comprising up to 4% of all sinonasal tumors. It is usually a fatal disease with high rates of local recurrence and metastasis. SNMMs have different pathophysiologic features than cutaneous melanomas and are thought to be due to the migration of melanocytes into regional ectodermal tissue. The literature evaluating the presence and significance of intraepithelial melanocytic proliferations associated with SNMM is scant and inconsistent. Our goal was to evaluate those lesions with a variety of melanocytic immunohistochemical (IHC) markers.

Design: Consecutive cases of SNMM diagnosed between 2007-2018 were retrieved from our files. 21 specimens from 8 patients were identified with at least focal histologically unremarkable surface epithelium (SE) or submucosal glands (SG) present for evaluation. 15 control cases of unremarkable sinonasal mucosa were also reviewed. IHC staining for the melanocytic markers SOX10, HMB45, and melanoma cocktail (S100 [red], Melan-A [brown], and tyrosinase [brown]) were performed in all cases. We examined all slides for melanocytic proliferations within the SE (confluent staining and/or upward spread) and SG.

Results: All control cases showed similar IHC staining (figure 1) with no melanocytes seen within SE or SG and myoepithelial cells of SG highlighted by SOX10 and S100. In 14 of 21 specimens (66.7%), the IHC stains highlighted melanocytes that were not observed on H&E slides (figure 2). Melanoma in situ (MIS) was seen in 8/14 specimens while an atypical melanocytic proliferation was seen in 6/14. IHC from the margin of one case showed MIS that was not recognized on H&E stained slides.

Figure 1 - 1201

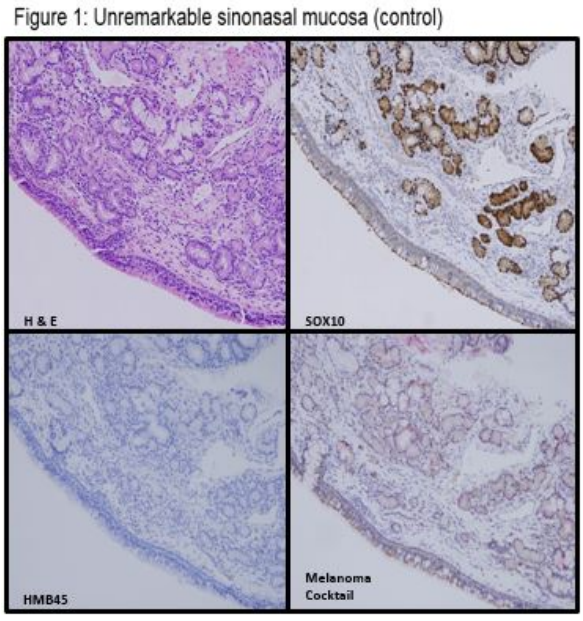

Figure 2 - 1201

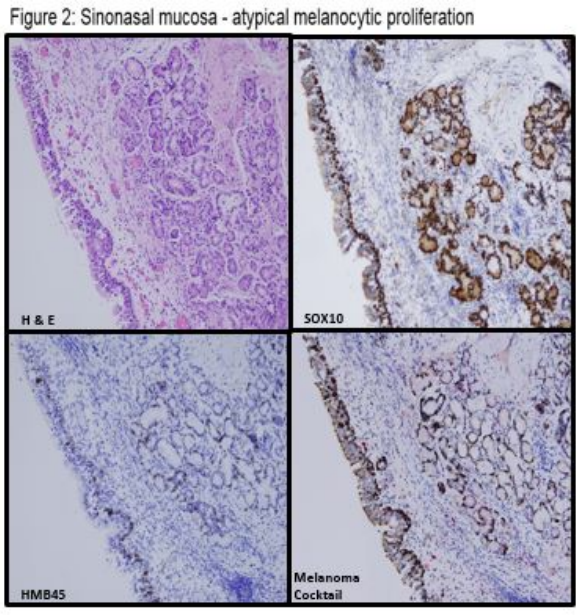

Conclusions: Staining at our laboratory showed that HBM45 and Melan-A stains were more specific but less sensitive in identifying melanocytes in both SE and SG. SOX10 and S100 were less specific because they also highlight myoepithelial cells in SG. Our results also show that the incidence of intraepithelial melanocytic proliferations in cases of SNMM is greater than reported in the literature, likely due to difficulties in identifying intraepithelial melanocytes on H&E. Therefore, IHC panels should be done on all surgical margins to identify intraepithelial melanocytic proliferations, especially in cases where melanocytes are not seen on H&E sections. Additional studies are needed to determine the clinical significance of these findings.

1202 Prognostic Significance of Venous Invasion in Node Negative Head and Neck Squamous Cell Carcinoma

Aysha Mubeen[1], Roi Dagan[1], Ahmad Alkhasawneh[2], Raafat Makary[1], Rui Fernandes[1], Anthony Bunnell[1], Phillip Pirgousis[3], Erica Hoy[2], Arun Gopinath[1]
[1]University of Florida College of Medicine, Jacksonville, FL, [2]UF Health Jacksonville, Jacksonville, FL, [3]Mayo Clinic Florida, Jacksonville, FL

Disclosures: Aysha Mubeen: None; Roi Dagan: None; Ahmad Alkhasawneh: None; Raafat Makary: None; Rui Fernandes: None; Anthony Bunnell: None; Phillip Pirgousis: None; Erica Hoy: None; Arun Gopinath: None

Background: Lymphovascular invasion (LVI) in head and neck squamous cell carcinomas (HNSCCs) has been associated with poor outcomes and propensity for lymph node metastasis. Venous invasion is not frequently evaluated for on routine histologic examination of HNSCC. Studies have shown that extramural venous invasion is an adverse prognostic factor in colorectal carcinoma and is currently included in the CAP cancer protocol. However, the prognostic significance of venous invasion (VI) in HNSCC is largely unknown. In this study we are evaluating the prognostic significance of venous invasion in node negative (without evidence of lymph node involvement) HNSCC, utilizing elastic stain.

Design: A total of 120 consecutive node negative (N0) HNSCC were studied, 11 cases were excluded as no follow up data was available. Slides were reviewed for presence of VI. Verhoeff-Van Gieson stain for elastic fibers was done on a selected slide from each case to confirm/detect VI. Clinical and demographic data was recorded. Statistical analysis was done using Graphpad prism 7 software. Additionally 5 cases with less than 6 months follow up were excluded from the survival analysis.

Results: The clinico-pathologic and demographic data are summarized in Table1. 38 patients had venous invasion, and 18% of these patients had loco-regional recurrence. Univariate analysis revealed statistically significant decreased recurrence free survival in the presence of venous invasion (log-rank (mantel-Cox) test p value 0.0087)

	Positive VI (n=38)	Negative VI (71)
Mean age (yrs)	63.4	57.6
Male/Female	23/15	51/20
Pathologic T stage	T1: 11 T2: 11 T3: 6 T4: 10	T1: 24 T2:16 T3: 8 T4: 23
Histological Grade	G1:7 G2: 25 G3: 6	G1: 11 G2: 38 G3: 22
Perineural invasion	22	19
LVI	Positive: 5 Negative: 33	Positive: 8 Negative: 61 Indeterminate: 2
Positive margins	5	5
Average Follow up (months)	23.5	46.6
Loco-regional recurrence	7/38	8/71

Figure 1 - 1202

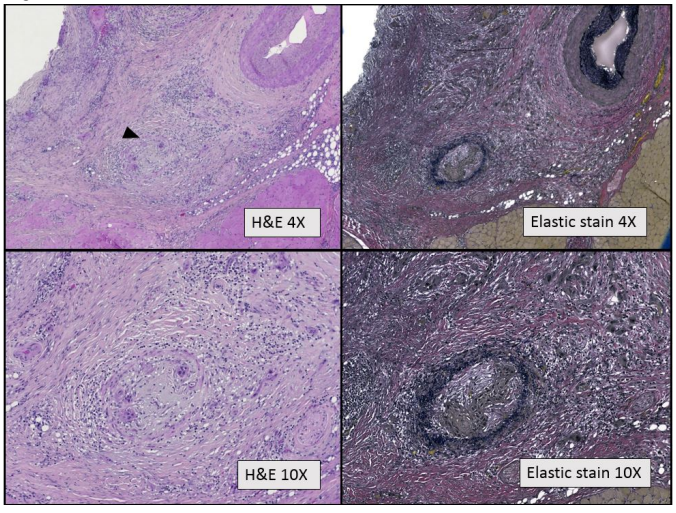

Figure 2 - 1202

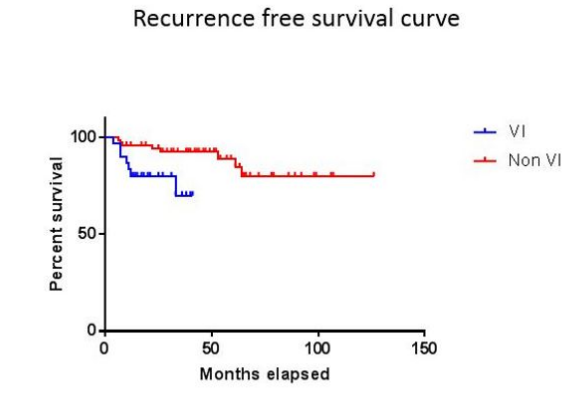

HR=3.38(95% CI, 0.97-11.82)
Log-rank *P*=0.0087

Conclusions: Identification of venous invasion is greatly aided by elastic stain (Fig 1). Our study shows that presence of VI in node negative HNSCC resulted in a decreased recurrence free survival (Fig 2). The impact of venous invasion as a prognostic marker for HNSCC needs to be further investigated.

1203 High Rate of BRAF V600E Mutation in Sialadenoma Papilliferum and Its Diagnostic Significance

Masato Nakaguro[1], Makoto Urano[2], Ikuko Ogawa[3], Yoshinari Yamamoto[4], Mayumi Yokotsuka[4], Toshitaka Nagao[5]
[1]Nagoya University Hospital, Nagoya City, Japan, [2]Fujita Health University, Toyoake, Japan, [3]Hiroshima University Hospital, Hiroshima, Japan, [4]Tokyo Medical University, Shinjuku-ku, Japan, [5]Tokyo Medical University, Tokyo, Japan

Disclosures: Masato Nakaguro: None; Makoto Urano: None; Ikuko Ogawa: None; Yoshinari Yamamoto: None; Mayumi Yokotsuka: None; Toshitaka Nagao: None

Background: Sialadenoma papilliferum (SP) is a rare benign minor salivary gland tumor characterized by a combination of exophytic papillary growth of surface squamous epithelium and intraductal papillary-cystic structures. SP was named based on its histological resemblance to syringocystadenoma papilliferum of the skin. Recently, the *BRAF* V600E mutation was reported in syringocystadenoma papilliferum, but the molecular characteristics of SP have not been clarified due to the rarity of SP. Here, we analyzed genetic alterations in 10 SP cases and compared the results with those obtained from tumors histologically mimicking SP.

Design: Ten cases of SP, comprising eight and two SPs that arose in the intraoral area and bronchus, respectively, were retrieved from our institution cases and consultation files. We also selected 29 tumors representing various histological differential diagnoses of SP, including intraductal papilloma (2 cases), cystadenoma (5 cases), cystadenocarcinoma (2 cases), intraductal papillary mucinous neoplasm of the salivary gland (IPMN, 6 cases), squamous papilloma (7 cases), and verrucous carcinoma (7 cases). We directly sequenced mutation hotspots in five genes (*BRAF, AKT1, HRAS, PIK3CA,* and *GNAS*) using Sanger sequencing. When *BRAF* mutation was detected, immunohistochemical staining for BRAF V600E was also performed.

Results: The patients were 63–80 years old, and the male/female ratio was 3:7. Seven SP cases (70%) harbored the *BRAF* V600E mutation. Of the tumors used for comparison, none exhibited this mutation except for one cystadenoma, which showed double-layered intraductal papillary proliferation, which is reminiscent of SP, but lacked surface squamous papillary growth. In the SP cases, BRAF V600E immunostaining was positive in both surface squamous and intraductal papillary luminal cells. On the other hand, *AKT1* mutations were observed only in IPMNs (5 cases [83.3%]). *HRAS* mutations were detected in one SP (10%), one cystadenoma (20%), and four IPMNs (66.7%), whereas no tumors harbored *PIK3CA* or*GNAS* mutations.

Conclusions: *BRAF* V600E mutation is a frequent mutation in, and highly specific to, SP compared with its histologically mimicking tumors. The immunohistochemical results suggest that the surface squamous proliferation and intraductal components of SP are of the same origin. Additionally, IPMN differed from SP in terms of the presence of *AKT1* mutations.

1204 Mucoepidermoid Carcinoma of the Base of the Tongue: A Tumor type with a Propensity for Lymph Node Metastases Unrelated to Histologic Grade

Pooja Navale[1], Lisa Rooper[2], Justin Bishop[3], William Westra[1]
[1]Icahn School of Medicine at Mount Sinai, New York, NY, [2]Johns Hopkins Hospital, Baltimore, MD, [3]University of Texas Southwestern Medical Center, Dallas, TX

Disclosures: Pooja Navale: None; Lisa Rooper: None; Justin Bishop: None; William Westra: None

Background: The designation “mucoepidermoid tumor” is a historic one used in reference to a form of mucoepidermoid carcinoma (MEC) that was believed to be benign. This bygone notion was based on a legitimate observation that the vast majority of MECs arising from the intraoral minor salivary glands behave in a benign fashion, particularly when they do not exhibit high grade features. There has been a recent move to partition the oral vault into the oral cavity (OC) proper and the oropharynx (OP) based on an awareness that these compartments are anatomically and histologically distinct, and that similar tumor types arising from these compartments may behave in dramatically different ways (e.g. OC squamous cell carcinoma vs. OP squamous cell carcinoma). The purpose of this study was to determine whether MECs of the OP behaved in the same benign fashion as the counterpart in the OC.

Design: The pathology data bases from three large academic medical centers were searched for cases of MECs arising in the OP. Relevant clinical and pathological information was collected from the medical records.

Results: Twenty-six cases were identified. They were from 18 females (69%) and 8 males (31%), ranging in age from 31 to 80 years (median, 62). Twenty (77%) were classified as low (n=5) or intermediate (n=15) grade, and 6 (23%) as high grade. Most arose from the base of tongue (n=25), but 1 arose from the lateral pharyngeal wall. The median tumor size was 2.1 cm. Twenty patients underwent neck node dissections. Of these 20 cases, 14 (70%) had histologically documented lymph node metastases. MECs that lacked high grade features were just as likely to metastasize as those with high grade features (55% vs 50%, p=1.0, Fischer exact). Of 3 metastases tested, 2 harbored the MAML2 gene fusion.

Conclusions: MECs arising from the base of tongue are associated with an alarmingly high rate of nodal metastases. This behavior radically departs from the indolent behavior of those MECs arising in the oral cavity proper. This behavior cannot be predicted on the bases of histologic grading. This propensity to regionally metastasize may to some degree reflect the unique microenvironment of the oropharynx.

1205 HPV+ Oropharyngeal Squamous Cell Carcinomas Immune Microenvironment in Metropolitan and West Indies Populations According to HPV RNA Hybridization in situ Stratification

Marine Nervo[1], Marion Mandavit[2], Cassandre Gasne[1], Jeremy Augustin[3], Ophélie Foléa[4], Sophie Outh-Gauer[5], Hélène Péré[5], Eric Tartour[5], Cecile Badoual[6]
[1]INSERM U970, Université Paris Descartes Sorbonne Paris-Cité, Paris, France, [2]Inserm U970, Paris, France, [3]Paris, France, [4]INSERM U970, Université Paris Descartes Sorbonne Paris-Cité, Noisy le sec, France, [5]Hôpital Européen Georges Pompidou, APHP, Paris, France, [6]G Pompidou Hospital, Paris, France

Disclosures: Marine Nervo: None; Marion Mandavit: None; Cassandre Gasne: None; Jeremy Augustin: None; Ophélie Foléa: None; Sophie Outh-Gauer: None; Hélène Péré: None; Eric Tartour: None; Cecile Badoual: None

Background: It's now well established that papillomavirus (HPV) infection is one of the main risk factors of oropharyngeal squamous cell carcinomas (COPs). Different subtypes (subT) of HPV can be involved in the carcinogenesis. HPV16 and HPV18 are the major subT found in COPs, nevertheless differences in HPV subT distribution have been observed depending on the geographical origin of the patients. In France, differences have been reported between metropolitan and West Indies patients. The clinical relevance of the HPV subT regarding survival is not well known. COPs are known to be associated with a better prognosis. Interestingly, some data show the impact of the HPV replication in the outcome of the HPV-related COPs. Indeed, among HPV+ COPs, high levels of viral replication seem to be associated with a better prognosis. The microenvironment could play a particular role. Our project was to correlate HPV replication levels with various HPV subtypes and with microenvironment features.

Design: In a cohort of 32 patients, including 16 Martiniquan and 16 Metropolitan French patients with HPV+ COPs, we have performed an *in situ* hybridization targeting 18 different HPV RNA subT. The replication signal (% of the stained cells and % of staining in the cell) was assessed in a semi-quantitative way (+/++). In the same cohort, a spectral digital analysis was obtained using the TSA technic. An immunostaining set including CD3, PD1, PD-L1, CD68 and cytokeratin immunostaining was performed. DNA PCR allowed the determination of the HPV subT.

Results: The cohort appeared quite homogenous in terms of HPV subtypes with HPV16 as the most represented (94%). A high expression of HPV RNA (++) was present in 69% of Martiniquan patients *versus* 44% of Metropolitan ones. The immune cells infiltration was not significantly different between the two populations. A strong expression of HPV RNA was associated with a more dense infiltration of overall macrophages (p= 0,038) and of PD-L1+ macrophages (p= 0,004). It was also associated with a higher expression of PD-L1 on both macrophages and tumour cells (p= 0,004). No association was found with the expression of PD-1 or with the density of T cells.

Figure 1 - 1205

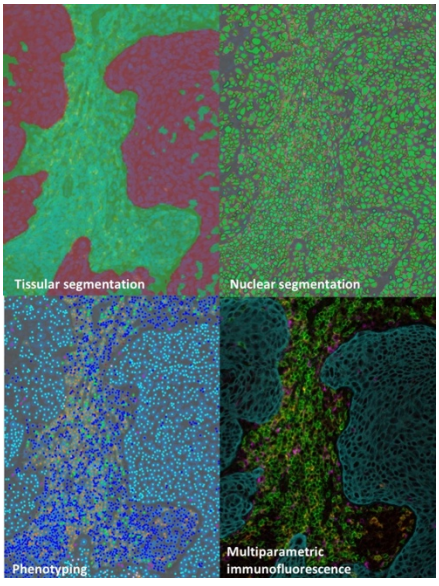

Figure 2 - 1205

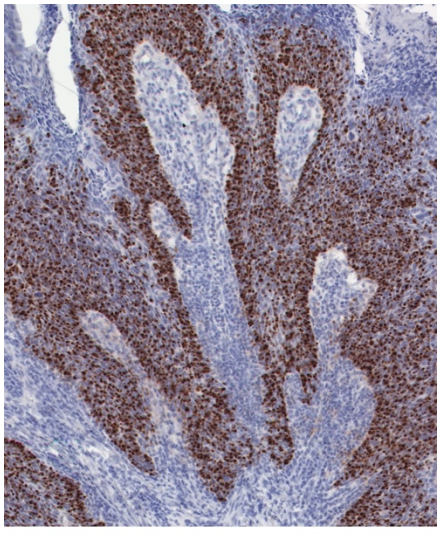

***In situ* hybridization targeting 18 HPV RNA subtypes x20**

Conclusions: These first results allow us to highlight that HPV plays a role in modulating tumour microenvironment. An extension of the cohort is needed to confirm these first data.

1206 Differentiated Papillary Thyroid Carcinoma with Early Distant Metastasis: A Comparative Study with a Non-Metastatic Cohort

Palgun Nisarga[1], Swapnil Rane[2], Asawari Patil[2], Neha Mittal[3], Munita Bal[2]
[1]Tata Memorial Hospital, Mumbai, India, [2]Tata Memorial Centre, Mumbai, India, [3]Tata Memorial Hospital, Mumbai, Maharashtra, India

Disclosures: Palgun Nisarga: None; Swapnil Rane: None; Asawari Patil: None; Neha Mittal: None; Munita Bal: None

Background: Papillary thyroid carcinoma (PTC) is the commonest differentiated thyroid cancer with indolent course and excellent survival rates. However, a small proportion of PTC patients develop early distant metastasis and endure poorer outcomes. Factors associated with early metastasis in PTC are currently poorly understood.

Design: Clinical profiles and pathologic features of primary tumors of 55 PTC cases with distant metastasis at, or occurring within 6 months, of presentation (MPTC) were reviewed and compared with a control group of 134 cases of PTC without distant metastasis for a minimum period of 5 years (NMPTC). Follicular, poorly differentiated (as per Turin's criteria), anaplastic and medullary thyroid carcinoma cases were excluded. The analysis was undertaken using SPSS v23.0.

Results: Among MPTC patients, the median age was 50 years; male-to-female ratio was 1:1.8. The commonest sites of metastasis were bone (58%) and lung (35%). MPTC patients were older (median age, 50 vs. 36 years, $p<0.001$) and had larger tumors than NMPTC patients ($p<0.001$). Bilobar involvement ($p=0.04$), solid ($p=0.004$) and encapsulated tumors ($p=0.02$) were more frequent in the MPTC group. Dominant histology among MPTC and NMPTC cohorts was the follicular-variant (58%) and classic type (52%), respectively. Presence of a non-papillary pattern ($p<0.0001$), clear cell morphology (30% vs. 2%, $p<0.001$), vascular invasion (71% vs. 29%, $p<0.001$), mitotic rate (2.5 vs. 0.3/10 high-power-fields, $p <.001$), and bilateral nodal metastasis ($p=0.03$) were significantly more common in MPTC group. On multivariate analysis, presence of nested/trabecular patterns ($p=0.004$), clear cell morphology ($p<0.001$), high mitotic rate ($p<0.001$) and necrosis ($p=0.01$) in primary tumors showed significant association with distant metastasis.

Conclusions: Distinctive clinicopathologic differences exist between tumors of PTC patients with early metastasis and those without long-term distant metastasis. Presence of nested/trabecular architecture, clear cell morphology, higher mitotic rate and necrosis in primary tumors are significantly associated with early distant metastasis.

1207 The Immunohistochemical Features of Ectopic Hamartomatous "Thymoma" are Different from Those of Spindle Cell Thymoma

Yuki Okumura[1], Jun Matsubayashi[2], Hayao Nakanishi[3], Toshitaka Nagao[4], Shigeo Nakamura[5], Masato Nakaguro
[1]Nagoya University Hospital, Nagoya city, Japan, [2]Tokyo Medical University, Shinjuku-ku, Japan, [3]Aichi Cancer Center Aichi Hospital, Okazaki, Japan, [4]Tokyo Medical University, Tokyo, Japan, [5]Nagoya University Hospital, Nagoya-shi, Japan

Disclosures: Yuki Okumura: None; Jun Matsubayashi: None; Hayao Nakanishi: None; Toshitaka Nagao: None; Shigeo Nakamura: None; Masato Nakaguro: None

Background: Ectopic hamartomatous thymoma (EHT) is a benign tumor that occurs mainly in the lower neck. Histologically, EHT exhibits fascicular proliferation of bland spindle cells intermingled with adipose tissue and squamous and/or ductal epithelium. Spindle cells in EHT are morphologically similar to those of spindle cell thymoma, which is the reason EHT was named as "thymoma". However, the immunohistochemical characteristics of EHT have not been well compared with those of spindle cell thymoma, and the origin of EHT has not been elucidated.

Design: 5 cases of EHT and 13 cases of thymoma (3 type A and 10 type AB cases) were selected from institutional case files. The diagnosis of EHT was reconfirmed by authors. Immunohistochemical staining of AE1/AE3, SMA, calponin, p63, and CD34 was performed. To investigate the possibility of a myoepithelial origin, we assessed *EWSR1* gene rearrangement by fluorescence *in situ* hybridization.

Results: Clinical information was available in four out of five cases. The four patients comprised four males aged 42–69 (mean age, 55) years. All EHTs showed typical histologic features of EHT. Immunohistochemically, spindle cells in the EHTs expressed AE1/AE3, SMA, p63, and CD34 in all cases (100%) and calponin in two cases (40%). Whereas spindle cells in some thymomas were positive for SMA (3 cases, 23.1%), calponin (1 case, 7.7%), and p63 (12 cases, 92.3%), CD34 positivity was not seen. The expression of SMA and CD34 was more commonly observed in EHT compared to spindle cell thymoma ($p=0.0065$ and $p=0.00018$, respectively). *EWSR1* gene rearrangement, which is observed in approximately 50% of myoepithelial tumors (myoepithelioma and myoepithelial carcinoma), was not detected in any of the EHT cases.

Percentage of marker-positive EHT cases compared with Thymoma

Antibody	Positive cases (%)		p-value
	EHT	Thymoma	
SMA	100	23.1	p=0.0065
Calponin	40	7.7	n.s.
p63	100	92.3	n.s.
CD34	100	0	p=0.00018

EHT: ectopic hamartomatous thymoma

n.s.: not significant

Conclusions: The immunohistochemical features of EHT were different from those of spindle cell thymoma. Our results suggest that EHT is not a genuine thymoma and, apart from its misleading terminology, may originate from a different cell type. Although the mixture of various histologic components and expression of myoepithelial markers (SMA, p63, and calponin) found in our EHT cases are indicative of a myoepithelial origin, the CD34 expression and lack of *EWSR1* gene rearrangement are not consistent with a myoepithelial origin.

1208 AZGP1 is a Novel Biomarkers in HPV-positive Oropharyngeal Squamous Cell Carcinoma

Kate Poropatich[1], Tatjana Paunesku[2], Gayle Woloschak[2], Bharat Mittal[3]
[1]Chicago, IL, [2]Northwestern University, Chicago, IL, [3]McGaw Medical Center of Northwestern University, Chicago, IL

Disclosures: Kate Poropatich: None; Tatjana Paunesku: None; Gayle Woloschak: None; Bharat Mittal: None

Background: HPV status is a known positive prognostic variable for patients with oropharyngeal squamous cell carcinoma (OPSCC) and is biologically distinct from HPV-negative OPSCC. Little is known, however, as to what are defining tumor intrinsic characteristics of HPV-positive OPSCC.

Design: We retrospectively analyzed the health records of patients with squamous cell carcinoma of the oropharynx at a tertiary academic health care institution from the years 2009-2018. Clinical endpoints for survival analysis included length of follow-up, recurrence-free survival (RFS) and overall survival. High-risk HPV testing was performed on all cases using DNA and RNA in situ hybridization. Laser capture microdissection was performed for tumor isolation for downstream mass spectroscopy and proteomic studies. Immunohistochemistry (IHC) was performed on FFPE specimens using anti-human AZGP1 antibody (Atlas Antibodies, HPA012582, 1:500). AZGP1 staining was scored as tumor cytoplasmic staining with a score of 1 to 3 (1 being lowest and 3 being highest expression). Correlations between IHC scores and HPV status were calculated using a linear regression model. The Kaplan-Meier method was used for survival outcome.

Results: Tumor tissue and matched histologically-normal squamous mucosa was obtained from 68 patients with OPSCC, including 45 HPV-positive and 23 HPV-negative patients (see Fig 1). Mean follow-up time was 3.60 years. Mass spectroscopy on tumor from OPSCC patients (n= 2) revealed AZGP1 protein present in HPV-positive OPSCC tissue but not HPV-negative tumor tissue. AZGP1 staining by IHC was positively correlated with HPV positivity in tumor (r^2= 0.24, p<0.00001). The median AZGP1 staining score in HPV-positive patients was 2.0 (range: 1-2.5) and in HPV-negative patients was 1.5 (1-2.25). AZGP1 protein was overexpressed, based on a staining score of >2.25, in tumor tissue from 12 patients, all of whom were HPV-positive. Low or absent AZGP1 staining, based on a score of 1.25 or less, was detected in 15 patients, more commonly but not exclusively in HPV-negative patients (n= 10) compared to HPV positive patients (n= 5). An AZGP1 staining score of >2.25 ('AZGP1-hi') positively predicted RFS (p= 0.034); median RFS for 'AZGP1-hi' patients was 1325 days and for 'AZGP1-lo' patients was 847 days.

Figure 1 - 1208

	All cases	HPV-positive cases	HPV-negative cases
No. Cases (n)	68	45	23
Age at diagnosis (median)	58	57	59
Sex			
Male	59	42	17
Female	9	4	5
Follow-up, years (mean)	3.60	3.71	3.38
Recurrences, percent (n)	23.53 (16)	13.33 (6)	43.48 (10)
RFS, years (mean)	3.20	3.58	2.48
Dead from disease, percent (n)	8.82 (6)	6.67 (3)	13.04 (3)
Treatment, percent (n=66)			
Surgery	16.67 (11)	13.95 (6/43)	21.74 (5)
Surgery with radiation	16.67 (11)	18.60 (8)	13.04 (3)
Surgery with chemoradiation	50.0 (33)	53.49 (23)	43.48 (10)
Chemoradiation	12.12 (8)	6.98 (3)	21.74 (5)
Chemotherapy or radiation	4.55 (3)	6.98 (3)	0
Tobacco use, percent (n=64)			
Never	35.94 (23)	42.86 (18/42)	22.73 (5/22)
1-10 ppy	23.44 (15)	28.57 (12)	13.64 (3)
10-20 ppy	17.19 (11)	11.90 (5)	27.27 (6)
>20 ppy	23.44 (15)	16.67 (7)	36.36 (8)
T stage, percentage (n= 65)			
1-2	80.0 (52)	88.64 (39/44)	61.90 (13/21)
3-4	20.0 (13)	11.36 (5)	38.10 (8)
N stage, percentage (n= 67)			
0-1	37.31 (25)	36.36 (16/44)	39.13 (9)
2-3	62.69 (42)	63.64 (28)	60.87 (14)

Figure 2 - 1208

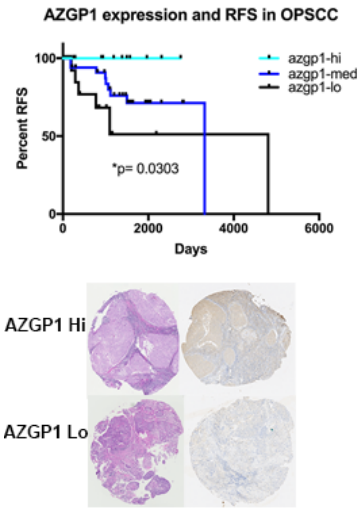

Conclusions: AZGP1 is correlated with HPV status in OPSCC and could represent a novel biomarker in HPV-related OPSCC, which currently remains enigmatic for its radiosensitivity and favorable clinical outcome.

1209 Metastatic Neuroendocrine Tumors to the Parotid Gland: A Retrospective Analysis

Josean Ramos[1], Paolo Gattuso[2]
[1]Rush University Medical Center, Chicago, IL, [2]Rush University Medical Center, Burr Ridge, IL

Disclosures: Josean Ramos: None; Paolo Gattuso: None

Background: Metastatic tumors to the parotid gland are not unusual clinical events, with squamous cell carcinoma and melanoma of the head and neck region being the most common malignancies encountered. However, primary or metastatic neuroendocrine carcinoma in the parotid gland is an uncommon clinical presentation, with only few case reports found in the literature. We performed a retrospective study to assess the incidence of metastatic neuroendocrine carcinomas to the parotid gland.

Design: The surgical/cytopathology pathology files at our institution were reviewed from 1995 to 2017 for metastatic neuroendocrine carcinomas to the parotid gland. The clinical and pathologic data was reviewed in detail.

Results: A total of 420 parotid gland neoplasms were recorded. 300 cases (71%) were benign neoplasms, with pleomorphic adenoma (194 cases) being the most common. 120 cases (29%) were malignant 70 primary, the most common being acinic cell carcinoma (28 cases) and 50 cases were metastatic neoplasms including melanoma. 13 of 50 metastatic neoplasm cases (26%) were neuroendocrine carcinomas, of which 9 were male (69%) and 4 were female (31%), with age ranging from 48-86y with a mean of 71y. 10 cases (77%) were located on the left parotid gland, and 3 cases (23%) were located on the right parotid gland.

6 cases (46%) were metastatic neuroendocrine carcinomas, small cell type originating from the lung (first manifestation in 4 cases and metachronous tumor in 2 cases), and 4 cases (31%) were metastatic Merkel cell carcinoma from the head/neck skin (3 cases synchronous, 1 case first manifestation). The remaining 3 cases (23%) were metastatic medullary thyroid carcinomas, two of them presenting 15 and 7 months later from the primary thyroid neoplasm diagnosis, and one case presenting as first manifestation.

Conclusions: Metastatic neuroendocrine carcinomas to the parotid gland account for 13 of 50 (26%) of all metastatic tumors seen in this region. Metastatic undifferentiated small cell carcinoma of the lung was the most common tumor encountered in this region (6/13 cases; 46%). It is not unusual for this tumor to present as a parotid mass, as a first sign of systemic clinical manifestation. Interesting enough, most of the metastatic tumors (77%) involved the left parotid gland.

1210 HPV-Related Squamous Cell Carcinoma of the Larynx and Oral Cavity: Clinicopathologic Characterization Including a Novel Warty Variant

Lisa Rooper[1], Melina Windon[2], Tahyna Hernandez[3], Brett Miles[4], Patrick Ha[5], William Ryan[6], Annemieke Van Zante[5], David Eisele[2], Gypsyamber D'Souza[2], Carole Fakhry[1], William Westra[4]
[1]Johns Hopkins Hospital, Baltimore, MD, [2]Johns Hopkins University, Baltimore, MD, [3]Mount Sinai Health System, New York, NY, [4]Icahn School of Medicine at Mount Sinai, New York, NY, [5]University of California, San Francisco, San Francisco, CA,[6]University of California, San Francisco, Mill Valley, CA

Disclosures: Lisa Rooper: None; Melina Windon: None; Tahyna Hernandez: None; Brett Miles: None; Patrick Ha: None; William Ryan: *Advisory Board Member*, Medtronic; *Advisory Board Member*, Olympus; *Consultant*, Ziteo; Annemieke Van Zante: None; David Eisele: None; Gypsyamber D'Souza: None; Carole Fakhry: None; William Westra: None

Background: Human papillomavirus (HPV) is well established as the predominant driver of squamous cell carcinoma (SCC) in the oropharynx, where it is associated with improved outcomes. Although HPV is also consistently identified in a small subset of SCC in the larynx and oral cavity, its pathogenic role and prognostic implications in these sites are not entirely clear. This study aims to characterize the histologic appearance and clinicopathologic features of HPV-related laryngeal and oral SCC.

Design: We identified all HPV-related laryngeal and oral SCC from the surgical pathology archives of three large academic medical centers, a subset of which were tested via an epidemiologic study. P16 immunohistochemistry and HPV-specific testing using high-risk HPV RNA in-situ hybridization (ISH), DNA ISH, or PCR-based genotyping was performed on all cases. Two head and neck pathologists reviewed all available histologic sections and classified the morphologic features of each case.

Results: The 51 HPV-related SCC included 30 larynx and 21 oral cavity primaries that arose in 35 men and 15 women with a mean age of 59 years (range 29-85). All tumors were positive for p16 and any HPV-specific testing performed, including RNA ISH in 26 cases. Among cases that underwent type-specific analysis, 29 (71%) were positive for HPV16. Thirty cases (63%) showed non-keratinizing morphology similar to oropharyngeal HPV-related SCC, and 6 (12%) had a conventional keratinizing appearance. However, 13 cases (25%) were best classified as a novel warty variant analogous to that seen in anogenital sites, with exophytic growth, prominent koilocytic change, multinucleation, marked nuclear pleomorphism, and abundant parakeratosis. Warty tumors tended to present at a lower stage than the other histologic types with no lymph node metastasis, local recurrence, or metastatic disease; they likewise showed a trend toward improved disease free survival at 3 years compared to other variants (100% vs. 64%, p=0.12).

Conclusions: The presence of transcriptionally active HPV in a subset of laryngeal and oral SCC as demonstrated by HPV RNA ISH confirms that HPV is a key pathogenic driver in this small group of tumors. There is a higher prevalence of non-HPV16 types in these sites than previously reported in the oropharynx. While most of these tumors are non-keratinizing with a prognosis similar to conventional SCC, this study highlights a warty variant previously unrecognized in the head and neck that shows a trend toward improved outcomes.

1211 Tumor-Associated Lymphoid Proliferation Creates an Immunomodulatory Environment that Facilitates Local Control in Acinic Cell Carcinoma

Lisa Rooper[1], Derek Allison[1], Rebecca Hammon[1], David Eisele[2], Hyunseok Kang[3]
[1]Johns Hopkins Hospital, Baltimore, MD, [2]Johns Hopkins University, Baltimore, MD, [3]University of California, San Francisco, San Francisco, CA

Disclosures: Lisa Rooper: None; Derek Allison: None; Rebecca Hammon: None; David Eisele: None; Hyunseok Kang: None

Background: Acinic cell carcinomas (AciCC) are frequently associated with prominent peritumoral inflammation known as tumor-associated lymphoid proliferation (TALP). Although TALP has long been hypothesized to play an anti-tumor role in salivary carcinomas, the immune constituents and prognostic correlates of this phenomenon have never been formally evaluated. This study aims to characterize the immune microenvironment of AciCC with an emphasis on the potential immunomodulatory role of TALP.

Design: We created a tissue microarray to include 43 primary, 9 locally recurrent, and 4 metastatic AciCC. Three 1 mm cores of each tumor were sampled to account for tumor and microenvironment heterogeneity. We performed immunohistochemistry for CD4, CD8, CD20, CD68, FOXP3, PD1, and PD-L1. Lymphocyte subsets were automatically quantified using the Halo image analysis platform; the percentage of tumor cells and tumor infiltrating lymphocytes (TILs) expressing PD-L1 was estimated manually.

Results: TALP from primary AciCC varied widely in density between tumors but consisted of an average 276 CD20+ B cells, 108 CD8+ cytotoxic T cells, 163 CD4+ T-helper cells, 131 CD68+ macrophages, and 67 FOXP3+ T-regulatory cells per mm2. There were also an average 180 activated PD1+ TILs per mm2 with tumor PD-L1 expression in 22 cases (51%) and TIL PD-L1 expression in 19 cases (44%). Among primary tumors, lymphocyte subsets and PD-L1 expression were not associated with risk for tumor progression (all p>0.05). However, recurrent and metastatic AciCC had significantly lower levels of most immune constituents compared to primary tumors, including an average 10 CD20+ B cells, 6 CD8+ cytotoxic T cells, 8 CD4+ T-helper cells, and FOXP3+ T-regulatory cells per mm2 (all p<0.001).

While there was not a significant difference in tumor PD-L1 expression, recurrent/metastatic tumors also showed a significantly lower population of 10 activated PD1+ TILS per mm2 and no TIL PD-L1 expression compared to primary tumors (all p<0.001).

Conclusions: TALP in AciCC consists of a mix of B cells, T cells, and macrophages. The presence of dense CD8+ cytotoxic T-cells, FOXP3+ T-regulatory cells, activated PD1+ TILs, and PD-L1+ TILs confirms that TALP may play an immunomodulatory role in AciCC. Furthermore, the low levels of immune constituents in recurrent and metastatic AciCC suggests that TALP may play an important role in local control of AciCC, with immune escape potentially facilitating tumor progression.

1212 Limited Sinonasal Rosai-Dorfman Disease Masquerading as Chronic Sinusitis: An Under-Recognized Variant

Lisa Rooper[1], Marissa White[1], Elizabeth Montgomery[2], Justin Bishop[3]
[1]Johns Hopkins Hospital, Baltimore, MD, [2]Johns Hopkins Medical Institutions, Baltimore, MD, [3]University of Texas Southwestern Medical Center, Dallas, TX

Disclosures: Lisa Rooper: None; Marissa White: None; Elizabeth Montgomery: None; Justin Bishop: None

Background: The sinonasal tract is one of the most common extranodal sites for involvement by Rosai-Dorfman Disease (RDD), which can occur as an isolated process or as part of systemic disease. However, most reported patients with RDD in this location have presented with prominent mass effect or locally destructive disease. Recently, we have unexpectedly encountered several cases with histologic and immunohistochemical features of RDD in the clinical setting of chronic sinusitis. In this study, we aim to systematically characterize the prevalence and significance of this phenomenon.

Design: We reviewed 403 sinus contents specimens taken for clinical symptoms of chronic sinusitis at a large academic medical center over a two-year period. All of these cases also had original pathologic diagnoses of sinusitis. We selected 25 cases with a prominent histiocytic infiltrate on H&E for further evaluation and performed immunostains for S100 protein, CD1a, and langerin. We also reviewed previous and subsequent sinus contents specimens taken from the same patients.

Results: There were 14 cases (3.5% of all sinus contents specimens) that demonstrated diagnostic histologic features of RDD on H&E, including epithelioid to spindled eosinophilic histiocytes with prominent emperiopolesis intermixed with scattered lymphoplasmacytic aggregates. The histiocytes were positive for S100 protein and negative for CD1a and langerin in all cases. All 14 patients with these findings presented with severe chronic sinusitis with polyposis; no discrete mass lesions or systemic symptoms were noted. Most of these patients (8/14; 57%) experienced recurrent sinus symptoms necessitating repeat surgery compared with a smaller subset of other chronic sinusitis patients (43/389; 11%); histologic findings of RDD were also present in their additional specimens.

Conclusions: A small but significant proportion of sinus contents removed for chronic sinusitis demonstrate diagnostic features of RDD. While a uniform lack of systemic involvement or tumefactive growth suggests that this is a limited variant of the disease, the concomitant presence of characteristic morphology and immunophenotype in the context of local symptoms supports classification of these cases within the RDD spectrum. The disproportionately high recurrence rate in these patients suggests that recognition of this phenomenon is clinically relevant; diagnosis as RDD could also help expand potential therapeutic options for refractory disease.

1213 Clinicopathological implications of Trk family expression in adenoid cystic carcinoma

Hyang Joo Ryu[1], Sun Och Yoon[2]
[1]Yonsei University College of Medicine, Seoul, Korea, Republic of South Korea, [2]Seoul, Korea, Republic of South Korea

Disclosures: Hyang Joo Ryu: None; Sun Och Yoon: None

Background: Adenoid cystic carcinoma (AdCC) is a salivary gland tumor, mostly occuring in head and neck area. Despite the bland-looking histologic morphology, AdCC is characterized frequent perineural invasion resulting in frequent recurrences. The frequent perineural invasion may be related to the biologic features of AdCC, and this can be therapeutic target. Tropomyosin-related kinase (Trk) receptor includes TrkA, TrkB, and TrkC subtype, and Trk is currently being evaluated as a biomarker for target therapy in several cancer types. And also Trk is related to neuronal signal-related factors, but their biological meaning related to neural invasion in AdCC has not been studied.

Design: A total of 126 consecutive AdCC cases were included, which was surgically resected and underwent histologic confirmation. The immunohistochemical expression of TrkA, TrkB, and TrkC was evaluated through H-score analysis (0-300 scale).

Results: In normal brain control tissue, expression of TrkA, TrkB, and TrkC protein was observed. However, TrkB and TrkC protein expression was not observed in AdCC. TrkA were variably expressed with the median H-score of 88.7; and low expression (<100 H-score) of TrkA was noted in 48.4% (61/126) of tested cases. Low TrkA expression revealed a tendency related to more advanced pT stages. In

the survival analysis, low expression of TrkA has the tendency of shorter event free survival rate, and low TrkA expression was significantly related to inferior overall survival rate.

Conclusions: In the present study, we evaluated the relation of neuronal signal-related factors, Trk family, especially TrkA to AdCC. Low expression of TrkA revealed an association with poor prognostic factors of AdCC patients. This result may suggest that dysregulated signals of neuronal factors, TrkA, may occur in AdCC, and such dysregulation may involve in the aggressiveness of AdCC. Although further in depth studies should be followed, the present finding could propose the potential of therapeutic targets in the aspect of dysregulated neuronal factors of AdCC.

1214 Evaluation of Histologic Risk Scoring Model, Tumor Budding and Depth of Invasion with Respect To Pathologic Stage and P16INK4A Immunostatus in Oral Squamous Cell Carcinoma

Priya Sahu[1], Andleeb Abrari[2]
[1]PGIMER, New Delhi, India, [2]Max Super Specialty Hospital, Saket, New Delhi, India

Disclosures: Priya Sahu: None; Andleeb Abrari: None

Background: Oral squamous cell carcinomas (OSCC) constitute a major health problem especially in developing countries. It's uncertain biological behavior has provoked vigorous multipronged research on factors that may predict disease outcome, and modify judgments on determining the best method of management. This study evaluated histologic risk scoring (HRS) model {worst pattern of invasion (WPOI), lymphohistiocytic reaction (LHR) and perineural infiltration (PNI)}, tumor budding and depth of invasion in OSCC cases and tried to assess impact of the preceding on the pathologic stage and relation if any to $p16^{ink4a}$ immunostatus.

Design: We studied 160 cases of OSCC retrospectively and prospectively over the period of two years. Histomorphologic parameters were assessed on their first resected specimen slides and categorized based on histologic risk scoring model. Impact of the preceding on the pathologic (pTN) stage and relation to $p16^{INK4A}$ immunostatus were evaluated by computing chi square test for each parameter. The level of significance was 5% and the calculation was done by SPSS 16 software.

Results: Most of the cases in this study were noted in 5^{th} and 6^{th} decade. Tongue was the most common primary subsite (42.5%) followed by buccal mucosa (28.1%). Our data supported highly significant association of pT category with perineural invasion (p-value <0.001) amongst all other parameters. Histologic risk scores, perineural invasion and tumor budding (p-value <0.001) were also highly predictive of nodal disease. The association of tumor $p16^{ink4a}$ immunostatus with respect to risk categories, WPOI and LHR were also significant.

Conclusions: These findings, as evident in our study, make a strong point in favor of assigning these or similar risk stratifying parameters, as essential data component of pathology reporting of oral squamous cell carcinoma and also make a strong point for striving to seek and report perineural invasion status in all such cases. Inclusion of multiparametric morphologic information in histology reporting helps in triaging high risk cases without adding an extra cost.

1215 Re-assessment of Common Surgical Pathology Practice: Is Histologic Examination of Sinonasal Excisions for Routine Chronic Rhinosinusitis Really Necessary?

Abeer Salama[1], Tahyna Hernandez[2], Mena Mansour[3], William Westra[1]
[1]Icahn School of Medicine at Mount Sinai, New York, NY, [2]Mount Sinai Health System, New York, NY, [3]Washington University Medical Center, St. Louis, MO

Disclosures: Abeer Salama: None; Tahyna Hernandez: None; Mena Mansour: None; William Westra: None

Background: Chronic rhinosinusitis (CRS) is a common disease with 26.9 million adults diagnosed in the United States in 2016. Accordingly, sinonasal excisions for CRS are very common specimens that may place an unnecessary strain on surgical pathology services if routine microscopic examination is unwarranted. The purpose of this study was to review the pathologic findings in routine CRS excisions from a high volume sinonasal surgical practice to determine the incidence and nature of unsuspected and clinically relevant pathologic findings.

Design: We retrospectively reviewed the surgical pathology reports of CRC excisions performed over a 7 year period (2012-2018). Cases were included only if the provided clinical information on the requisition form indicated CRS. For cases with an unsuspected finding, the medical records were reviewed to better define the clinical context.

Results: 883 cases were reviewed. 15 (1.5%) had unsuspected pathologic findings including Schneiderian papilloma (n=12, 1.4%) and invasive fungal sinusitis (n=3, 0.3%). Further review of the medical records revealed that 2 patients with invasive fungal sinusitis were severely immunocompromised, 10 patients with Schneiderian papillomas had a clinical suspicion of papilloma (prior biopsy or suggestive

imaging findings) and 3 patients had no available medical records. 565 cases included nasal septal excisions, and none of these specimens were found to harbor pathologic findings.

Conclusions: The likelihood of uncovering a pathologic process of clinical relevance during histopathologic evaluation of routine excisions for CRS is very low and practically non-existent for nasal septal excisions. Importantly, the incidence of unexpected findings can be even further reduced when relevant clinical findings (immunosuppression, prior history of a neoplastic process, unilateral nasal polyposis and/or unilateral sinus opacification) are communicated to the pathologists at the time of specimen submission. These observations should help guide the discussion of the need for routine histologic assessment of routine CRS specimens in an era of medicine where best surgical pathology practices are must take into account financial constraints. Gross only examinations sinonasal excisions for routine CRS specimens could result in significant cost savings.

1216 Biomarker Immunoprofile and Molecular Characteristics in Salivary Duct Carcinoma: Clinicopathologic and Prognostic Implications

Thalita Santana Conceição[1], Andrle Pavel[2], Petr Martinek[3], Petr Steiner[4], Alena Skalova[5]
[1]University of Sao Paulo, São Paulo, SP, Brazil, [2]Department of Maxillofacial Surgery, Clinic of Dentistry, Faculty of Medicine in Plzen, Plzen, Czech Republic, [3]Biopticka Laborator SRO, Plzen, Czech Republic, [4]Biopticka Laborator SRO, Pilsen, Czech Republic, [5]Charles University, Faculty of Medicine in Plzen, Plzen, Czech Republic

Disclosures: Thalita Santana Conceição: None; Andrle Pavel: None; Petr Martinek: None; Petr Steiner: None; Alena Skalova: None

Background: Salivary duct carcinoma (SDC) is one of the most aggressive salivary gland tumors, with current treatment choice including radical surgical resection followed by radio and/or chemotherapy. However, prognosis remains poor for most patients. SDC often presents overexpression of androgen receptors (AR), HER-2/*neu* and EGFR.

Design: Clinicopathological and follow-up information of 29 cases of SDC were collected. Immunoexpression of AR, HER-2/*neu,* GATA3, CK5/6 and MIB1 was analyzed, and *ERBB2 (HER-2/Neu*) gene amplification was investigated by FISH. Five cases were analyzed by NGS using the Fusion Plex Solid Tumor and Comprehensive Thyroid and Lung kits (ArcherDX). Overall (OS) and disease-free survival (DFS) were analyzed with Kaplan-Meier curves and Cox regression.

Results: Most cases (25/86.2%) occurred in male patients, with a mean age of 66.3 years. Eighteen (62.1%) cases occurred in the parotid gland, 10 (34.5%) in submandibular gland and 1 (3.4%) in minor salivary gland. Mean time of follow-up was 31.4 months. Most cases expressed AR, HER-2/*neu,* GATA3, and CK5/6. *ERBB2* gene amplification was proven by FISH in 9/15 (60%) cases. Lack of AR and GATA3 expression was associated with lower OS and DFS ($p < 0.05$). Thirteen cases were diagnosed as SDC ex pleomorphic adenoma (PA), one case as a high-grade not otherwise specified (NOS) ex PA and one case as a high-grade anaplastic carcinoma. Twenty-six cases were classified according to the SDC revised classification into five subtypes (table 1). Apocrine HER2 and HER2 enriched subtypes were significantly associated with lower OS ($p < 0.05$). NGS analysis revealed one case harboring an *ETV6-NTRK3* fusion, therefore it was reclassified as a high-grade secretory carcinoma. Three likely pathogenic mutations were detected in three cases (*HRAS*: c.182A>G p.Gln61Arg, *HRAS*: c.37G>C p.Gly13Arg, *AKT1*: c.49G>A p.Glu17Lys). Two cases were positive for amplification of *ERBB2* gene using FISH probes and corresponding over-expression using NGS was detected. Homozygous deletion of locus 9p21 (*CDKN2A*) was detected in one case. All four cases were negative for *MDM2* amplification, or break in genes *MYB, MYBL1, NFIB, NTRK1, RET*, and *PLAG1*.

Table 1 - Results of univariate survival analysis for SDC revised classification

SDC revised classification	Number of cases (%)	Median survival time	OS	p	DFS	p
			HR + 95% CI		HR + 95% CI	
Apocrine A[a]	3 (11.5%)	48 months	2.25 [0.22 – 22.08]	0.49	1.46 [0.15 – 14.39]	0.74
Apocrine B	4 (15.4%)	30.67 months	1.78 [0.22 – 14.32]	0.59	1.52 [0.18 – 12.27]	0.69
Apocrine HER2	16 (61.5%)	36.05 months	21.92 [1.05 – 457.46]	**0.04***	12.81 [0.65 –228.53]	0.09
HER2 enriched	1 (3.8%)	5.50 months	12.86 [0.95 – 174.85]	**0.05***	7.89 [0.63 – 98.25]	0.10
Double negative	2 (7.7%)	6.50 months	4.98 [0.29 – 85.57]	0.26	5.01 [0.29 – 85.07]	0.26

[a] Comparison factor; * Statistically significant; HR = Hazard ratio; CI = Confidence interval.

OS = Overall survival; DFS = Disease-free survival.

Conclusions: Herein we identified mutations of *HRAS* and *AKT1* genes in three cases of SDC, also a homozygous locus deletion in *CDKN2A* was observed in one case harboring a *HRAS* mutation. Our findings emphasize the importance of genetic profiling in understanding oncogenesis and molecular diagnosis of rare salivary gland malignancies.

1217 HPV Genotyping in Head and Neck Squamous Cell Carcinoma (HNSC) as a Function of Anatomic Subsite

Simran Sekhon[1], Pooja Navale[1], William Westra[1]
[1]*Icahn School of Medicine at Mount Sinai, New York, NY*

Disclosures: Simran Sekhon: None; Pooja Navale: None; William Westra: None

Background: In HNSC, high-risk HPV primarily targets the oropharynx. HPV16 is found in >90% of these HPV-oropharyngeal carcinomas, whereas only <5% harbor other high-risk types. Virtually everything known about HPV-HNSC is dominated by these HPV16-related cases. Assumptions regarding the equivalency of HPV genotypes, however, may not be valid. More insight into the epidemiology and behavior of HPV-HNSC requires precise distribution of HPV genotypes. The purpose of this study was to provide fine precision HPV genotype mapping for HNSCs across various anatomic subsites of the head and neck.

Design: Our pathology database was searched for all HNSCs that had undergone HPV testing from 2012-2018. HPV analysis used a multistep real-time PCR strategy that: 1)utilizes general consensus probes to discern the presence of more than 23 HPV genotypes, 2)applies both DNA melting point analysis and type specific hybridization to confirm presence of HPV 16, and 3)resorts to Sangers sequencing to type all HPV+ cases caused by non-16 genotypes. Relevant clinical information was collected including the site of tumor origin.

Results: Of the 800 HNSCs tested, the site of tumor origin was the oropharynx(n=522), larynx(n=89), oral cavity(n=66), hypopharynx(n=30), sinonasal tract(n=41), nasopharynx(n=14), and lymph node metastases of unknown primary origin(n=38). Overall, 551(69%) were HPV +. HPV16 was by far the most commonly detected genotype (85.3%), followed by 35(5.5%), 33(4.3%), 18(2.5%), 45(1.1%), 56(0.5%), 67(0.4%), 59(0.2%) and 69(0.2%). There were, however, sharp differences in the distribution of genotypes based on tumor site(Table). In the sinonasal tract, the percentage of HPV16 cases was outnumbered by variant genotype cases. The difference in distribution of HPV16 for HPV-HNSCs of the sinonasal tract and oropharynx was significant(41% vs 90%, $p < 0.00001$)(Figure).

Table. Distribution of HPV genotypes in head and neck squamous cell carcinoma by anatomic subsite

Anatomic subsite	HPV genotype									
	16	18	33	35	45	56	59	67	69	Total
oropharynx	418	7	17	23	0	0	0	2	0	467
larynx	3	0	0	1	1	1	0	0	0	6
oral cavity	4	0	1	1	0	0	0	0	0	6
hypopharynx	3	0	1	0	0	0	1	0	0	5
sinonasal tract	11	4	5	1	3	2	0	0	1	27
nasopharynx	3	3	0	0	2	0	0	0	0	8
unknown primary	28	0	0	4	0	0	0	0	0	32
Total	470	14	24	30	6	3	1	2	1	551

Figure 1 - 1217

Figure. Comparison of HPV genotype distribution for HNSCs arising in the oropharynx and sinonasal tract

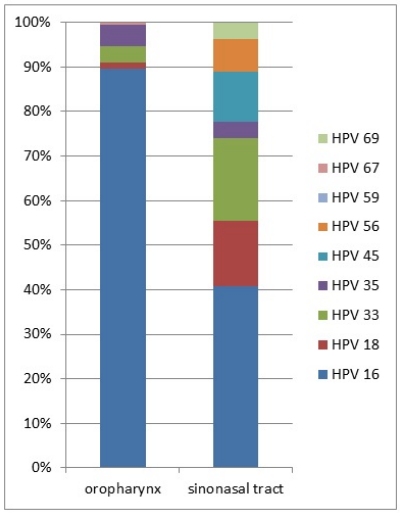

Conclusions: For HNSC, HPV genotypes are not evenly distributed across anatomic subsites. HPV-sinonasal carcinomas are more likely to harbor non-16 variant forms. The biologic principles underlying this observation remain to be elucidated, but they may reflect differences in viral exposure, tissue susceptibilities, and immunologic microenvironments. The application of HPV genotyping strategies to clinical practices will facilitate accrual of sufficiently powered studies needed to understand the impact of genotype variants on clinical outcomes, epidemiologic trends, and HPV vaccines that are currently focused on type 16 antigens.

1218 Cystathionine-Beta-Synthase is Increased in Thyroid Cancers

Rodney Shackelford[1], Matthew Kilpatrick[2], Andrew Meram[1], James Cotelingam[3], Ghali Ghali[1], Elba Turbat-Herrera[4]
[1]LSU Health Shreveport, Shreveport, LA, [2]LSU Health Sciences Center, Baton Rouge, LA, [3]Louisiana State University Shreveport, Shreveport, LA, [4]University of South Alabama, Mobile, AL

Disclosures: Rodney Shackelford: None; Matthew Kilpatrick: None; Andrew Meram: None; James Cotelingam: None; Elba Turbat-Herrera: None

Background: Cystathionine-beta-synthase (CBS) catalyses the conversion of homocysteine and cysteine to hydrogen sulfide (H_2S) and cystathione, via the transsulfuration pathway. CBS in increased in several human malignancies, including colon, ovarian, breast, renal, and oral squamous cell carcinomas. In these malignancies CBS-synthesized H_2S increases tumor growth, clinical aggressivity, invasiveness, metastatic potential, and chemotherapy resistance. CBS expression has not been examined in thyroid carcinomas. We examined CBS expression in thyroid follicular (FC), papillary (PC), medullarly (MC), and anaplastic (AC) carcinomas, compared to benign thyroid, thyroid follicular adenomas (FA), and oncocytomas (OCs).

Design: Tissue microarray technology from US Biomax was used to examine CBS protein expression in benign thyroid tissue and FA, OC, FC, PC, MC, and AC (26,4, 12, 29, 70, 6, and 6 samples each, respectively). We also examined nicotinamide phosphoribosyl transferase (Nampt) protein expression in benign thyroid, PC, FC, AC, and FAs (12 samples of each).

Results: CBS expression was significantly increased in all the thyroid carcinoma types compared to benign thyroid tissue. Compared to benign thyroid, FAs on average did not show increased CBS protein expression, while thyroid OCs showed only a minor increased in CBS expression. Nampt protein expression was increased in thyroid FCs and PCs compared to benign thyroid, while Nampt expression was the same between FAs and benign thyroid.

Conclusions: CBS is increased in several human malignancies, however a role for CBS and H_2S has not been found in thyroid malignancies. We show for the first time that CBS is increased in all the major common thyroid carcinoma types. Additionally, histologically FAs and FCs show very similar features and cannot cytologically be distinguished. They are differentiated by capsular invasion and/or vascular invasion, extrathyroidal tumor extension, and lymph node or systemic metastases seen with FCs and not in FAs. We show that CBS and Nampt protein expression differentiates between these lesions, demonstrating that the expression levels of these proteins can separate these lesions. This finding could have value in the differential diagnosis of FA vs. FC were tissue is limiting.

1219 SMARCB1-Deficient Adenocarcinoma of the Sinonasal Tract: A Potentially Under-Recognized Form of Sinonasal Adenocarcinoma

Akeesha Shah[1], Deepali Jain[2], Emad Ababneh[3], Abbas Agaimy[4], Aaron Hoschar[1], Bruce Wenig[5], Justin Bishop[6]
[1]Cleveland Clinic, Cleveland, OH, [2]All India Institute of Medical Sciences, New Delhi, India, [3]Cleveland Clinic Foundation, Cleveland Heights, OH, [4]Erlangen, Germany, [5]Moffitt Cancer Center, Tampa, FL, [6]University of Texas Southwestern Medical Center, Dallas, TX

Disclosures: Akeesha Shah: None; Deepali Jain: None; Emad Ababneh: None; Abbas Agaimy: None; Aaron Hoschar: None; Bruce Wenig: None; Justin Bishop: None

Background: Classifying sinonasal adenocarcinoma (SNAC) is complex. In addition to salivary-type SNACs, there are surface-type ACs further classified by grade and the presence/absence of intestinal differentiation. The high-grade non-intestinal SNAC group is particularly heterogeneous, with tumors showing quite variable morphology. SMARCB1-deficient sinonasal carcinoma is a newly described, aggressive tumor that usually resembles sinonasal undifferentiated carcinoma (SNUC) or squamous cell carcinoma; however, glandular differentiation has been rarely reported and this feature may be under-recognized. We present a dedicated series of SMARCB1-deficient SNACs.

Design: All cases of SMARCB1-differentiation with glandular differentiation were retrieved from the authors' archives. 5 cases were previously published. Histologic and immunohistochemical features were recorded.

Results: Nine cases of SMARCB1-deficient SNAC were found. They occurred in 7 men and 2 women ranging from 39-82 years (mean 59) and arose in the nasal cavity (n=5), maxillary sinus (n=1), or multiple subsites (n=3). Glandular differentiation ranged from 5-100% (mean 52%) of tumor volume, consisting of tubules and cribriform structures with foci of intracellular or intraluminal mucin. Myxoid stromal changes were seen in 5 of 9. All tumors demonstrated prominent oncocytoid/plasmacytoid cytomorphology in both glandular and non-glandular areas; 1 also exhibited foci of basaloid and spindled morphology. No cases had a component of a better differentiated tumor. The tumors were uniformly high-grade, with nuclear pleomorphism, elevated mitotic rates, and frequent necrosis. By immunohistochemistry, all tumors were entirely SMARCB1-deficient, and 8 of 9 were CK7-positive. Occasional expression of CK20 (2 of 9), CDX2 (1 of 9), and p40 (1 of 9) was seen, and some exhibited variable expression of yolk sac markers: glypican-3 (7 of 8), SALL4 (4 of 8), HepPar1 (3 of 8), PLAP (1 of 7), and AFP (1 of 8). Four cases were prospectively identified as SMARCB1-deficient carcinoma, while 4 were diagnosed as high-grade non-intestinal AC, and 1 diagnosed as SNUC.

Conclusions: SMARCB1-deficient sinonasal carcinoma, particularly the oncocytoid/plasmacytoid form, can demonstrate a variable degree of glandular differentiation. This unexpected morphology combined with variable immunohistochemical results may lead to misdiagnoses of high-grade intestinal or non-intestinal SNAC, myoepithelial carcinoma, or even yolk sac tumor or metastatic hepatocellular carcinoma.

1220 Salivary secretory carcinoma with a novel VIM-RET fusion: NGS based molecular profiling of 49 cases revealed an expanding molecular spectrum of a recently described entity

Alena Skalova[1], Thalita Santana Conceição[2], Tomas Vanecek[3], Luka Brcic[4], Martin Hyrcza[5], Roderick Simpson[6], Martina Baneckova[7], Marketa Horakova[8], Michal Michal[9]
[1]Charles University, Faculty of Medicine in Plzen, Plzen, Czech Republic, [2]University of Sao Paulo, São Paulo, SP, Brazil, [3]Biopticka laborator s.r.o., Plzen, Czech Republic, [4]Medical University of Graz, Graz, Austria, [5]University of Calgary/Calgary Laboratory Services, Calgary, AB, [6]University of Calgary, Calgary, AB, [7]Charles University, Faculty of Medicine in Plzen, Pilsen, Czech Republic, [8]Charles University, Plzen, Czech Republic, [9]Biopticka Laborator SRO, Plzen, Czech Republic

Disclosures: Alena Skalova: None; Thalita Santana Conceição: None; Tomas Vanecek: None; Luka Brcic: None; Martin Hyrcza: None; Roderick Simpson: None; Martina Baneckova: None; Marketa Horakova: None; Michal Michal: None

Background: Secretory carcinoma (SC), originally described as mammary analogue secretory carcinoma, is a predominantly low-grade salivary gland neoplasm characterized by a recurrent t(12;15)(p13;q25) translocation, resulting in *ETV6-NTRK3* gene fusion. Recently, novel *ETV6-RET* and *ETV6-MET* fusions were found in a subset of SCs lacking the classical *ETV6-NTRK3* fusion transcript, but harboring *ETV6* gene rearrangements.

Design: Forty nine cases of SC revealing typical morphology and immunoprofile were analyzed by NGS using the Fusion Plex Solid Tumor kit (ArcherDX). All 49 cases of SC were also tested for *ETV6* break by FISH and for common *ETV6-NTRK3*fusions using RT PCR.

Results: Among the 49 studied cases, 37 (76%) occurred in the parotid gland, 7 (14%) in the submandibular gland, 2 (4%) in minor salivary glands, 1 (2%) in nasal mucosa, 1 (2%) in facial skin and 1 (2%) in the thyroid gland. Most cases were diagnosed in males (27/55%). Patient age at diagnosis varied from 15 to 80 years, with a mean age of 49.9 years. Regarding molecular analysis, 38 cases (78%) presented the classical *ETV6-NTRK3* fusion, 9 cases (18%) were negative for the *ETV6-NTRK3* fusion and 2 cases (4%) were not analyzable. Among the 9 negative cases for *ETV6-NTRK3* fusion, 8 cases presented *ETV6-RET* fusion. Using NGS analysis, a novel *VIM-RET* fusion transcript was identified in one case of SC of parotid gland. In addition, one recurrent high grade SC of submandibular gland was simultaneously positive for *ETV6-NTRK3* and *MYB-SMR3B* fusion transcripts.

Conclusions: A novel finding in our study has been a discovery of a *VIM-RET* fusion in one patient with SC of parotid gland who could possibly benefit from *RET*-targeted therapy. In addition, in one SC two different fusions *ETV6-NTRK3* and *MYB-SMR3B* were found. The expanded molecular spectrum of SC provides a novel insight into oncogenesis, histopathology, and molecular diagnosis of this recently described entity.

1221 Biallelic PTCH1 Inactivation Is a Dominant Genomic Change in Sporadic Keratocystic Odontogenic Tumors

Ivan Stojanov[1], Inga-Marie Schaefer[2], Reshma Menon[3], Elizabeth Garcia[2], Hamza Gokozan[4], Jay Wasman[4], Dale Baur[1], Lynette Sholl[2]
[1]Case Western Reserve University, Cleveland, OH, [2]Brigham and Women's Hospital, Boston, MA, [3]Harvard School of Dental Medicine, Malden, MA, [4]University Hospitals Cleveland Medical Center, Cleveland, OH

Disclosures: Ivan Stojanov: None; Inga-Marie Schaefer: None; Reshma Menon: None; Elizabeth Garcia: None; Hamza Gokozan: None; Jay Wasman: None; Dale Baur: None; Lynette Sholl: *Consultant*, Foghorn Therapeutics; *Speaker*, Astra Zeneca Pharmaceuticals; *Advisory Board Member*, Loxo Oncology

Background: Keratocystic odontogenic tumors (KCOTs) are locally aggressive odontogenic neoplasms with recurrence rates up to 60%. Less than 10% of KCOTs are associated with nevoid basal cell carcinoma (Gorlin) syndrome and up to 85% of these show *PTCH1* inactivation. Sporadic KCOTs show *PTCH1* mutations in ~30% of cases but previous studies have been limited by low DNA yield. The absence of consistent genomic alterations prompted reclassification to odontogenic keratocyst in 2017 by the WHO. The aim of this study was to analyze sporadic KCOT for recurrent genomic aberrations, specifically those impacting the SHH signaling pathway.

Design: 18 KCOTs diagnosed between 2013-2018 and containing at least 30% neoplastic cells were retrieved from institutional archives. DNA extracted from FFPE tissue was subjected to targeted next-generation sequencing (NGS) interrogating the exonic sequences of 447 cancer-associated genes for mutations and copy number variations, and 191 introns across 60 genes for gene rearrangements.

Results: Sporadic KCOTs occurred in 10 male and 8 female patients with a median age of 59 (range, 11-82) years. 14 cases were located in the mandible, 4 in the maxilla. NGS identified loss of function *PTCH1* mutations in 17/18 (94%) cases; 9 cases harbored 2 concurrent *PTCH1* mutations and 5 cases showed 9q copy neutral loss of heterozygosity involving the *PTCH1* locus, for a total of 14 (78%) cases with evidence for *PTCH1* biallelic inactivation. 1 case showed a pathogenic *SMO*missense mutation; no mutations were detected in *SUFU* or *GLI*. No other copy number alterations or translocations were identified.

Conclusions: We identify inactivating *PTCH1* mutations in 94% of sporadic KCOTs, indicating that SHH pathway alterations are a near-universal event in these benign but locally aggressive tumors. The high frequency of biallelic *PTCH1* loss of function may provide a rational target for SHH pathway inhibitors to be explored in future studies.

1222 Diagnostic and Grading Challenges in Oncocytic Cell (OC) and Clear Cell (CC) of Mucoepidermoid Carcinoma (MEC)

Carolina Strosberg[1], Juan Hernandez-Prera[2], Brittany Holmes[3], Flávio Moreira[4], Bruce Wenig[2]
[1]H. Lee Moffitt Cancer Center & Research Institute, University of South Florida, Tampa, FL, [2]Moffitt Cancer Center, Tampa, FL, [3]Stanford University School of Medicine, Los Altos, CA, [4]São Paulo, SP, Brazil

Disclosures: Carolina Strosberg: None; Juan Hernandez-Prera: None; Brittany Holmes: None; Flávio Moreira: None; Bruce Wenig: None

Background: OC-MEC and CC-MEC are uncommon variants that can be diagnostically challenging. We present a series of OC-MECs and CC-MECs detailing their histologic features and grading, as well documenting the utility of *MAML2* gene rearrangement in their diagnosis.

Design: 37 cases of OC-MED and CC-MEC were identified in our files. The clinicopathologic features were documented. FISH for *MAML2* dual-color break-apart probe was performed in cases with available material (n=19). All cases were graded using the Armed Forces Institute of Pathology (AFIP) as well as the Brandwein grading systems. The level of agreement among the examiners was documented for both systems.

Results: 22 OC-MECs and 15 CC-MECs were identified. OC-MECs were more common in women and occurred in patients aged 26-73 (mean, 44 yrs); CC-MEC were more common in women occurring over ages ranging from 17-48 (mean 33 yrs). OC-MECs were most common in the parotid gland (82%); CC-MECs were most common in the oral cavity (67%). Histologically, tumors were circumscribed to infiltrative predominantly comprised of solid nests of OC and/or CC, and variably included epidermoid cells and mucocytes. Histochemical staining (mucicarmine and DPAS) and immunohistochemistry (MUC5) assisted in identifying mucocytes. 4 cases had perineural invasion. By AFIP grading the majority of tumors was low-grade; by Brandwein grading the majority of tumors was high-grade. The overall agreement by AFIP grading was 85.63%, with substantial free-marginal kappa of 0.78 (0.67-0.90, 95% CI); the overall agreement by

Brandwein grading was 61.56%, with a moderate free-marginal kappa of 0.42 (0.28-0.57, 95% CI). FISH testing showed 6 of 10 OC-MECs and 5 of 9 CC-MECs to harbor *MAML2* gene rearrangements. Clinical follow up was available in 7 patients all of whom were alive with no disease over periods ranging from 1-34 months (median, 5 months).

Conclusions: Our study contributes to the clinical and pathologic characterization of OC-MEC and CC-MEC variants. The presence of characteristic cytomorphologic findings, often limited in extent, including epidermoid cells and mucocytes should prompt consideration of MEC. *MAML2* gene rearrangement affirms the diagnosis in these cases. Using the AFIP grading resulted in better interobserver agreement and correlated to the majority of tumors being histologically low-grade. Clinically, the neoplasms had indolent biologic behavior.

1223 Correlation of Thyroid Molecular Alterations with 2017 ACR Thyroid Imaging Reporting and Data System (TI-RADS) Scoring

Wei Sun[1], Joseph Yee[2], Yan Shi[1], Melissa Yee-Chang[3], Xiao-Jun Wei[4], Aylin Simsir[5], Joan Cangiarella[6], Tamar Brandler[7]
[1]New York University Langone Medical Center, New York, NY, [2]New York University Langone Medical Center, Woodside, NY, [3]NYU Langone Health, New York City, NY, [4]NYU Langone Health, Long Island City, NY, [5]New York University School of Medicine, Edison, NJ, [6]New York University Medical Center, New York, NY, [7]NYU Langone Health, Highland Park, NJ

Disclosures: Wei Sun: None; Joseph Yee: None; Yan Shi: None; Melissa Yee-Chang: None; Xiao-Jun Wei: None; Joan Cangiarella: None; Tamar Brandler: None

Background: Molecular studies play an important role in the therapeutic triage of thyroid lesions. The 2017 TI-RADS added a new risk stratification system for classifying thyroid nodules based on sonographic appearance. Through this system radiologists guide clinicians in selecting which thyroid nodules necessitate fine needle aspiration (FNA) biopsy evaluation. Our study aimed to examine the molecular profiles of thyroid nodules broken down by TI-RADS categories.

Design: We performed a retrospective review of cases from 1/1/2016 to 4/1/2018 in our pathology database. Cases with in-house ultrasound (US), FNA Bethesda System (TBS) cytology diagnoses, molecular testing, and surgery were included. The USs from these cases were retrospectively reviewed and assigned TI-RADS scores (TR1-TR5) by a board certified radiologist.

Results: 90 cases (male=21, female=69, mean age=50.9 years, mean nodule size=2.49 cm) were included in this study. All cases fell into The Bethesda System for Reporting Thyroid Cytopathology (TBSRTC) indeterminate categories (III, IV, and V). The most common mutation across all TI-RADS categories was RAS (TR3 17/29, TR4 9/35, and TR5 8/21). Only TR4 and TR5 categories displayed more aggressive mutations such as BRAF and TERT. The most common surgical diagnosis was non-invasive follicular thyroid neoplasm with papillary-like nuclear features (NIFTP) (27.8%) followed by follicular adenoma (25.6%) (Table 1).

Table 1: Molecular Alterations in Thyroid Nodules Assessed by TI-RADS, The Bethesda System for Reporting Thyroid Cytopathology (TBS) and Surgical Pathology

Molecular Test (Total 90 cases)	TI-RADS				Bethesda System			Surgical Pathology Diagnoses					
	TR2 n=5 (5.6%)	TR3 n=29 (32.2%)	TR4 n=35 (38.9%)	TR5 n=21 (23.3%)	TBS III n=60 (66.7%)	TBS IV n=26 (28.8%)	TBS V n=4 (4.4%)	Benign-other n=19 (21.1%)	Follicular Adenoma n=23 (25.6%)	Follicular Carcinoma n=3(3.3%)	NIFTP n=25 (27.8%)	FV-PTC* n=10 (11.1%)	Classical PTC** n=10 (11.1%)
Negative n=22 (24.4%)	1	4	11	6	16	6		10	7		1	1	3
RAS n=34 (37.8%)		17	9	8	26	7	1	5	8		16	3	2
BRAF n=6 (6.7%)	1		2	3	3	3					1	2	3
PPARG n=6 (6.7%)	1	2	1	2	3	1	2				4	2	
TP53 n=4 (4.4%)		2	2		2	2		1	2	1			
MET n=3 (3.3%)		2	1		3			1	1				1
EIF1AX n=3 (3.3%)		2	1		3				2		1		
TERT n=2 (2.2%)			1	1		1	1			2			
NTRK1/ NTRK3 n=2 (2.2%)			2		1	1						1	1
Others n=8 (8.8%)	2		5	1	3	5		2	3		2	1	

** Follicular Variant Papillary Thyroid Carcinoma*

*** Papillary Thyroid Carcinoma*

Conclusions: While the majority of TR3, TR4 and TR5 thyroid nodules displayed molecular alterations, a large number were still negative for a molecular alteration, despite the indeterminate cytology diagnoses present in all cases. Knowledge of a nodule's TI-RADS score in combination with its molecular profile can aid in surgical decision making. While RAS occurred in both benign and malignant surgical entities in our study, more aggressive mutations occurred almost exclusively in malignant entities.

1224 Evaluation of Prognostic Impact of p53 Mutant Expression in HPV-Positive and HPV-Negative Head & Neck Squamous cell Carcinomas

Prerna Tewari[1], Prithi Raguraman[2], Robbie Woods[3], Niamh Kernan[4], Imogen Sharkey Ochoa[2], Jacqui Barry O'Crowley[4], Esther O'Regan[5], Cara Martin[6], John O'Leary[2]
[1]Trinity College, Dublin, Ireland, [2]Trinity College Dublin, Dublin, Ireland, [3]Beaumont Hospital, Dublin, Ireland, [4]Coombe Women & Infants University Hospital, Dublin, Ireland, [5]st. James Hospital, Dublin, Ireland, [6]Trinity St. James's Cancer Institute, Dublin, Ireland

Disclosures: Prerna Tewari: None; Prithi Raguraman: None; Robbie Woods: None; Niamh Kernan: None; Imogen Sharkey Ochoa: None; Jacqui Barry O'Crowley: None; Esther O'Regan: None; Cara Martin: None; John O'Leary: None

Background: Oropharyngeal Squamous Cell Carcinomas (OPSCCs) are associated with two distinct mechanisms of carcinogenesis: one related to smoking and alcohol and the other linked to Human Papilloma Virus (HPV) infections. HPV related OPSCC patients display a better overall survival than HPV negative patients. Overexpression of p16 is associated with an active HPV infection and is considered a surrogate marker for HPV infection, while p53 mutant expression is related to intrinsic p53 mutations indicative of tobacco and alcohol related carcinogenesis. This study was carried out to determine the frequency of p53 mutant expression as well as to determine the impact of p53 mutant expression on overall survival in a cohort of HPV positive and negative OPSCC patients.

Design: A retrospective study was carried out on 89 FFPE OPSCC tumour blocks. HPV testing and genotyping was carried out using the INNO-LiPA HPV Genotyping Extra test. Immunohistochemical staining was performed on 5um thick sections with the CINtec p16 antibody and p53 DO-7 antibody on the Ventana BenchMark Ultra immunostainer. For p16 immune expression, cases with diffuse nuclear and cytoplasmic staining in >70% of tumour cells were considered positive. P53 expression was scored as mutant overexpressed, null expression and wild type. Kaplan–Meier Survival analysis was carried out for overall survival based on p16 status, p53 expression and smoking history. Differences between groups were assessed using the log-rank test. SPSS was used for statistical analysis and a p value < 0.05 was considered significant.

Results: 51.0% (45/89) samples were HPV positive of which 93.3% displayed HPV 16 genotype. p16 immunostaining results were available for 83 cases. 42.0% of the cases displayed p16 positivity. P53 mutant expression was observed in 42.0% of the total cases. 37.0% of p16 positive cases displayed p53 mutant expression. Current smokers with p53 mutant expression and negative p16 expression had worst overall survival, while non-smokers displaying p16 overexpression and wild type p53 expression had the best overall survival ($p = 0.001$).

Conclusions: OPSCC patients displaying p53 mutant expression have a worse overall survival than patients with a wild type p53 expression pattern.

1225 Histopathologic and Molecular Analyses of Mucosal Melanomas: An Experience from a Single Academic Medical Center Spanning 15 Years

Aimi Toyama[1], Andrew Nelson[2], LaRue Rebecca[1], Christine Henzler[1], Alessio Giubellino[1], Faqian Li[1]
[1]University of Minnesota, Minneapolis, MN, [2]University of Minnesota, Saint Paul, MN

Disclosures: Aimi Toyama: None; Andrew Nelson: None; LaRue Rebecca: None; Christine Henzler: None; Alessio Giubellino: None; Faqian Li: None

Background: Mucosal melanoma is a rare diagnosis, known to have a different molecular profile than cutaneous melanomas, but with similar immunohistochemical staining patterns. Due to the poor prognosis of these tumors, determining the molecular profiles and pathologic features are crucial in considering personalized and rationale treatments targeting actionable genetic alterations.

Design: We searched our institution database from 2003 to 2018 and found 29 cases from different patients diagnosed as primary mucosal melanomas. We reviewed available pathology slides and medical records, as well as diagnostic and subsequent pathology reports. Clinical data was analyzed and correlated with histopathologic features and molecular profile.

Results: Among the 29 patients, the mean age of diagnosis was 67.6, ranging from 36 to 91. Primary sites included sinonasal (17), anorectal (7), genitourinary (4), and oropharyngeal (1). The overall two-year survival for all cases was 56.5% (13/23). Gastrointestinal primary mucosal melanomas had the lowest survival rate of 40.0% (2/5) while genitourinary cases had the highest two-year survival (75.0%, 3/4). The most common histopathologic cell type was epithelioid (18), followed by spindle cell (6) among 24 cases with available H&E slides. Of the epithelioid-predominant cases, rhabdoid features were found in 5/18 cases, while plasmacytoid features were seen in 2/18 cases. Notably, tumors with rhabdoid features had 0% two-year survival (0/3). Among the most commonly performed stains for characterization of the tumor, S100 was positive in 100% (28/28) of cases, HMB45 in 22/25 cases, Melan-A in 21/24 cases, and Tyrosinase in 14/17 cases. Of the 17 cases with molecular testing results, the most commonly mutated gene was NRAS (3/10 cases tested), while no BRAF mutations were detected (0/14 cases tested). Out of the 11 patients tested for presence of a KIT mutation, one

case was positive for a mutation, and the same case was also concurrently positive for NRAS and HRAS mutations. Patients with NRAS mutations had worse two-year survival (0%) compared to those without NRAS mutations (40.0%).

Conclusions: In our case series, we observed gastrointestinal mucosal melanomas to have a worse prognosis relative to other primary sites. Additionally, the presence of rhabdoid features within a tumor as well as the presence of an NRAS mutation appears associated with a poor two-year survival.

1226 Diagnostic Yield of HRAS Mutations in Epithelial–Myoepithelial Carcinoma Exhibiting a Broad Histopathological Spectrum

Makoto Urano[1], Masato Nakaguro[2], Hideaki Hirai[3], Maki Tanigawa[3], Kiyoaki Tsukahara[4], Yuichiro Tada[5], Toshitaka Nagao[4]
[1]Fujita Health University, Toyoake, Japan, [2]Nagoya University Hospital, Nagoya City, Japan, [3]Tokyo Medical University, Shinjuku-Ku, Japan, [4]Tokyo Medical University, Tokyo, Japan, [5]International University of Health and Welfare, Mita Hospital, Tokyo, Japan

Disclosures: Makoto Urano: None; Masato Nakaguro: None; Hideaki Hirai: None; Maki Tanigawa: None; Kiyoaki Tsukahara: None; Yuichiro Tada: None; Toshitaka Nagao: None

Background: Epithelial–myoepithelial carcinoma (EMEC) is a rare salivary gland tumor histologically defined as biphasic differentiation and comprising ductal and clear myoepithelial cells. Although EMECs basically present these classical features, they demonstrate histological variety with respect to cytoplasmic characteristics, cytologic atypia, or the proportions of ductal and myoepithelial cells. Thus the disease concept of EMEC is still unclear, and the accurate diagnosis is not always straightforward. Since many tumor entities display morphologic and immunophenotypic overlap with EMEC, a useful diagnostic tool is needed. Recently, *HRAS* mutations in EMEC were reported in a relatively small case series. The purpose of the present study was to investigate the mutation status of certain key genes, including *HRAS*, in a large number of EMEC cases and to determine the diagnostic utility.

Design: Totally 88 EMEC cases were enrolled. Direct Sanger sequencing of the *HRAS*, *PIK3CA*, *AKT1*, *KRAS*, *BRAF*, and *CTNNB1* genes was performed in 83 cases of EMEC. We also examined *HRAS* mutations in 19 adenoid cystic carcinomas, 14 basal cell adenomas, 12 pleomorphic adenomas, 9 myoepithelial carcinomas, 6 basal cell adenocarcinomas, and 1 myoepithelioma, all of which share certain histological patterns with classic EMEC.

Results: The EMECs showed a diverse histology, ranging from a benign-looking appearance to highly atypical features. Additionally, a subset of tumors displayed sebaceous, squamous, oncocytic, or apocrine differentiation and ex pleomorphic adenoma. *HRAS* mutations were found in 62 of the 83 EMECs (75.9%) and were mostly located in codon 61 (57 cases [90.5%]) of *HRAS*. There was no significant correlation between *HRAS* mutation status and the histological findings, including the grade and Ki-67 proliferation index. Sebaceous and apocrine histological variants also harbored *HRAS* mutations. Other less frequent mutations were detected in *PIK3CA* (20.5%), *AKT1* (6.49%), and *BRAF* (1.22%). *PIK3CA* mutations almost consistently co-occurred with *HRAS* mutations. No *KRAS* or *CTNNB1* mutations were identified. In contrast, no *HRAS* mutations were observed in tumors sharing histological features with EMEC. Detection of *HRAS* mutations was 100% specific to diagnosing EMEC.

Conclusions: EMEC harbors frequent *HRAS* mutations despite its wide histological spectrum. Our results suggest that *HRAS* mutations are commonly involved in the tumorigenesis of EMEC and provide a useful indicator aiding the differential diagnosis.

1227 Utility of p16 Expression for Distinction of HPV-Related Multiphenotypic Sinonasal Carcinoma from Adenoid Cystic Carcinoma

Annemieke Van Zante[1], Shweta Agarwal[2], Lucy Han[1], Patrick Ha[1]
[1]University of California, San Francisco, San Francisco, CA, [2]University of Tennessee Health Science Center, Memphis, TN

Disclosures: Annemieke Van Zante: None; Shweta Agarwal: None; Lucy Han: None; Patrick Ha: None

Background: Human papilloma virus-related multiphenotypic sinonasal carcinoma (HMSC) is an HPV-related carcinoma with histologic features that mimic adenoid cystic carcinoma (ACC). As originally described, HMSC is limited to the sinonasal tract, shows a myoepithelial immunophenotype and exhibits cribriform, tubular and solid architectures. However, HMSC includes a wider morphologic spectrum than ACC and lacks the characteristic MYB translocation. HMSC is diffusely positive for high risk HPV (hrHPV) and its immunohistochemical surrogate p16. This study investigates whether cases of ACC originally diagnosed based purely on histomorphology are in fact HMSC and establishes the utility of p16 expression pattern in differentiating HMSC from ACC.

Design: A total of 82 cases originally diagnosed as ACC of the head and neck based on histomorphologic features were evaluated. A tissue microarray was constructed and MYB and p16 immunohistochemistry (IHC) as well as hrHPV RNA in situ hybridization (ISH) were performed and analyzed on all cases. IHC for MYB was considered positive if staining was moderate to strong in >50% of tumor cells. The p16 IHC was evaluated for extent of staining, intensity and pattern; both nuclear and cytoplasmic staining were regarded as positive. The ISH for hrHPV was considered as positive if there was any dot-like staining.

Results: MYB upregulation was present in 48% of cases of ACC (39/80), consistent with previous reports. Three cases of HMSC were positive for hrHPV by ISH and showed strong diffuse staining with p16 as previously reported. hrHPV ISH was negative in all cases of ACC; however, p16 showed some degree of staining in 98% of cases (80/82). p16 was positive in 10-80% of tumor cells with variable intensity, ranging from weak to strong. The staining pattern for p16 showed ductular accentuation in 13% of cases (11/82) and contiguous patchy staining in 84% of cases (69/82). No strong diffuse (block positive) staining was present in the 82 cases of ACC.

Conclusions: All 82 cases of ACC tested were negative for hrHPV by ISH; thus, no cases of HMSC were misclassified as ACC based on histologic assessment despite the morphologic overlap of these two tumors. Nearly all cases of ACC had some degree of staining for p16, however this staining was variable and patchy, a pattern distinct from the strong diffuse staining seen in the HPV-associated HMSC. Thus, p16 can serve as diagnostic marker to exclude the diagnosis of HMSC on small specimens histologically resembling ACC.

1228 Recurrent and Novel Fusions Detected in Adenoid Cystic Carcinoma by a Custom-Designed Next-Generation Sequencing-Based Assay and Correlation with MYB Immunohistochemistry

Sagar Vishal[1], Natalya Guseva[2], Ava Bhattarai[3], Aaron Stence[4], Ramakrishna Sompallae[4], Krishnaveni Sompallae[4], Aaron Bossler[2], Robert Robinson[4], Deqin Ma[4]
[1]Coralville, IA, [2]University of Iowa, Iowa City, IA, [3]University of Tennessee Health Science Center, Memphis, TN, [4]University of Iowa Hospitals and Clinics, Iowa City, IA

Disclosures: Sagar Vishal: None; Natalya Guseva: None; Ava Bhattarai: None; Aaron Stence: None; Ramakrishna Sompallae: None; Krishnaveni Sompallae: None; Aaron Bossler: None; Robert Robinson: None; Deqin Ma: None

Background: Adenoid cystic carcinoma (AdCC) is an indolent but aggressive salivary gland carcinoma with a potential for local recurrence and distal metastasis. Recurrent t(6;9) or t(8;9) translocations resulting in *MYB/NFIB* or *MYBL1/NFIB* fusion is the major genomic aberration in AdCC. The diversity of fusions was also reported. We evaluated 18 cases of AdCC using a custom-designed, next generation sequencing (NGS)-based assay, which allows simultaneously detection of multiple fusions without prior knowledge of the partners. The NGS findings were correlated with immunohistochemistry (IHC) result for MYB.

Design: Fourteen genes (*ETV6, EWSR1, HMGA2, HRAS, MAML2, MYB, MYBL1, NFIB, NTRK3, NUTM1, PLAG1, PRKD1, PRKD2, PRKD3)* were selected based on extensive literature review. An RNA-based panel was designed using the Archer Assay Designer. Eighteen AdCCs from different organs including salivary gland, lung, orbital, and breast were tested. Total RNA was used togenerate NGS libraries and sequencing was performed on Illumina MiSeq. Data were analyzed using the Archer Analysis platform. Novel fusion was confirmed by RT-PCR and Sanger sequencing. IHC for MYB was performed using rabbit monoclonal antibody (EP769Y, Abcam) at a dilution of 1:400 and scored based on intensity of 0 to 3 (negative to strongly positive) with a cutoff of 10% tumor nuclear staining to be considered positive staining.

Results: Gene fusions were detected in 14 cases (74%): *MYB/NFIB* in 13 cases including one with a novel *MYB/PALLD* fusion and *MYLB1/NFIB* in 1 case. IHC studies for MYB were performed on 13 cases with additional unstained slides. Ten cases had concordant NGS and IHC results (8 positive for fusion and MYB expression and 2 negative for fusion and MYB IHC). Two cases were positive for MYB by IHC but negative for fusion by NGS. One case was positive for fusion but negative for MYB by IHC.

Conclusions: Recurrent *MYB* fusion in AdCC was detected at a frequency similar to that reported in the literature using our custom-designed NGS assay. Novel fusion was detected without prior knowledge of partners, which would expand our understanding of genomic aberrations in AdCC and help with diagnosis of challenging cases. The mechanism underlying the 3 cases with discordant NGS and IHC results warrants further investigation.

1229 Metastasizing Pleomorphic Adenoma: Recurrent PLAG1/HMGA2 Rearrangements and Identification of a Novel HMGA2-TMCT2 Fusion

Jason Wasserman[1], Brendan Dickson[2], Adam Smith[3], Bibianna Purgina[4], Ilan Weinreb[5]
[1]University of Ottawa, Ottawa, ON, [2]Mount Sinai Health System, Toronto, ON, [3]University Health Network, University of Toronto, Toronto, ON, [4]University of Ottawa/The Ottawa Hospital, Ottawa, ON, [5]University Health Network, Toronto, ON

Disclosures: Jason Wasserman: None; Brendan Dickson: None; Adam Smith: None; Bibianna Purgina: None; Ilan Weinreb: None

Background: Pleomorphic adenoma (PA) is the most common salivary gland neoplasm. On a molecular level PA is typically characterized by a translocation involving *PLAG1* or *HMGA2*. PA is considered to be a benign tumor although it can undergo malignant transformation. Alternatively, cases of histologically benign appearing PA “metastasizing” to lymph nodes or distant body sites are well documented. Several theories have been proposed to explain this behavior. 1. Metastasizing PAs (MPA) represent a similar but unrelated tumor to conventional PA. 2. MPAs represent a variant of PA with different genetics than the canonical *PLAG1/HMGA2* fusions, and have a greater risk of malignant behavior. 3. Surgical manipulation of the primary PA causes vascular permeation and increases the risk of metastasis of an otherwise benign PA. 4. All PAs have a minimal risk of malignant behavior only realized in a small subset of tumors. There is a lack of

molecular data available to assess the relationship of MPAs and their benign counterparts. In this study we describe five cases of MPAs and perform the first molecular study linking them to conventional PA.

Design: The index case was identified in routine clinical practice while the other cases were retrieved from the archives of the contributing authors. The original slides were reviewed to confirm the diagnosis of both the primary/recurrent tumor and the metastasis. Fluorescence in-situ hybridization (FISH) was performed in 4 of 5 cases and next generation sequencing (NGS) was performed on the index case.

Results: In all cases there was a history of recurrent PA involving the parotid. The average age at diagnosis was 40 years (range 28-59). Lymph node metastases were identified in 3 of 5 cases; non-lymph node metastases were also identified in 3 of 5 cases. In all cases reviewed, the metastases were histologically benign and morphologically resembled the primary tumor. NGS performed on the index case demonstrated a novel *HMGA2-TMCT2* translocation, which was subsequently confirmed by separate FISH break-apart assays for both genes. FISH performed on the remaining cases demonstrated a rearrangement of *PLAG1* in all 3 cases. *TMCT2* rearrangement was not recurrent.

Conclusions: So-called "metastasizing" PAs harbor the molecular hallmarks of their benign counterparts and represent part of the same family of tumors. All four tested cases showed *PLAG1* or *HMGA2* rearrangement with one harboring a novel *HMGA2-TMCT2* fusion.

1230 Inter-Observer Variation in the Histologic Classification of Polymorphous Adenocarcinoma (PAC) and Cribriform Adenocarcinoma of Salivary Gland (CASG)

Ilan Weinreb[1], Andrea Barbieri[2], Justin Bishop[3], Simon Chiosea[4], Snjezana Dogan[5], William Faquin[6], Ronald Ghossein[5], Martin Hyrcza[7], Vickie Jo[8], James Lewis[9], John Lozada[5], Michal Michal[10], Bayardo Perez-Ordonez[1], Manju Prasad[11], Bibianna Purgina[12], Jorge Reis-Filho[5], Theresa Scognamiglio[13], Ana Paula Martins Sebastiao[5], Raja Seethala[14], Alena Skalova[15], Stephen Smith[16], Lester Thompson[17], Jason Wasserman[18], Bruce Wenig[19], Bin Xu[5], Nora Katabi[5]
[1]University Health Network, Toronto, ON, [2]Yale University, New Haven, CT, [3]University of Texas Southwestern Medical Center, Dallas, TX, [4]University of Pittsburgh, Pittsburgh, PA, [5]Memorial Sloan Kettering Cancer Center, New York, NY,[6]Massachusetts General Hospital, Harvard Medical School, Boston, MA, [7]University of Calgary/Calgary Laboratory Services, Calgary, AB, [8]Brigham and Women's Hospital, Harvard Medical School, Boston, MA, [9]Vanderbilt University Medical Center, Nashville, TN, [10]Biopticka Laborator SRO, Plzen, Czech Republic, [11]Yale University School of Medicine, New Haven, CT, [12]University of Ottawa/The Ottawa Hospital, Ottawa, ON, [13]Weill Cornell Medicine, New York, NY, [14]University of Pittsburgh School of Medicine, Pittsburgh, PA, [15]Charles University, Faculty of Medicine in Plzen, Plzen, Czech Republic, [16]The Ohio State University Wexner Medical Center, Columbus, OH, [17]Southern California Permanente Medical Group, Woodland Hills, CA, [18]University of Ottawa, Ottawa, ON, [19]Moffitt Cancer Center, Tampa, FL

Disclosures: Ilan Weinreb: None; Andrea Barbieri: None; Justin Bishop: None; Simon Chiosea: None; Snjezana Dogan: None; William Faquin: None; Ronald Ghossein: None; Martin Hyrcza: None; Vickie Jo: None; James Lewis: None; John Lozada: None; Michal Michal: None; Bayardo Perez-Ordonez: None; Manju Prasad: None; Bibianna Purgina: None; Jorge Reis-Filho: *Advisory Board Member*, VolitionRx; *Advisory Board Member*, Paige.AI; *Consultant*, Goldman Sachs; Theresa Scognamiglio: None; Ana Paula Martins Sebastiao: None; Raja Seethala: None; Alena Skalova: None; Stephen Smith: None; Lester Thompson: None; Jason Wasserman: None; Bruce Wenig: None; Bin Xu: None; Nora Katabi: None

Background: PAC shows histologic diversity with fascicular and targetoid features; whereas CASG demonstrates predominant cribriform and solid patterns with glomeruloid appearance and optical clear nuclei. It remains controversial whether CASG represents a separate entity or a variant of PAC. Moreover, there is an ongoing dispute regarding the diagnosis of PAC with significant papillary architecture. In this study, we aimed to assess the level of agreement among expert Head and Neck (HN) pathologists in classifying PAC, CASG and their morphologic spectrum.

Design: Scanned Aperio slides of 48 cases of PAC/CASG were evaluated independently by 23 HN pathologists (US n=15; Canada n=6, Europe n=2), and were classified as: 1) PAC, 2) CASG, 3) tumors with ≥50% of papillary architecture (PAP) and 4) tumors with indeterminate features (IND). The consensus diagnosis was determined using the classification agreed upon by at least 50% of pathologists, or as IND when a predominant diagnosis cannot be reached. Interobserver agreement was calculated using Fleiss' Kappa test.

Results: The consensus diagnoses were PAC (17/48), CASG (16/48), PAP (3/48), and IND (12/48, Figure 1). Overall, there was a fair interobserver agreement among all participants in classifying the tumors (k=0.369). Full consensus was achieved in 3 (6%) cases, all of which were classified as PAC. A moderate agreement was achieved for PAC (k=0.511) and PAP (k=0.550) and a fair agreement for CASG (k=0.387). In contrast, tumors with indeterminate features had a completely nonsignificant diagnostic concordance among expert pathologists (k=0.084). The interobserver concordance was not significantly altered based on country of practice (US: k=0.381, Canada: k=0.366, Europe: k=0.639), years of practice (less than 5 years: k=0.359, 5 to 10 years: k=0.385, more than 10 years: k=0.382), practice pattern (less than 50% of HN specialty sign out k=0.351; more than 50%: k=0.372), and perception of CASG/PAC and their morphologic spectrum prior to the study (independent entities: k=0.323; variant: k=0.414, other: k=0.343).

Figure 1 - 1230

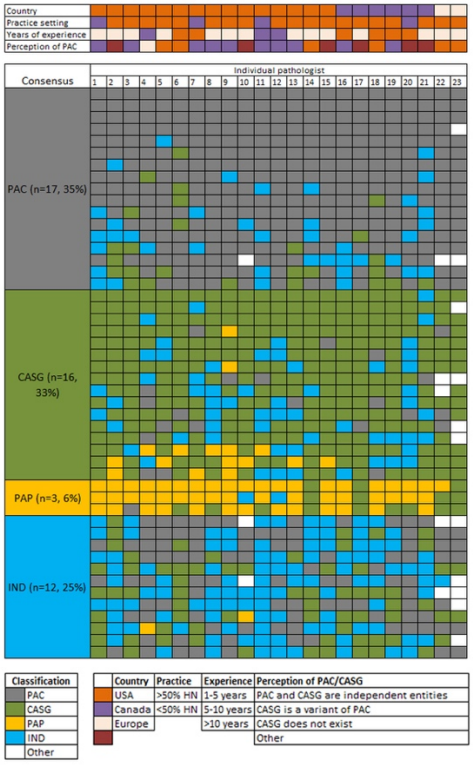

Conclusions: Overall, a fair to moderate interobserver agreement can be achieved in classifying the morphologic spectrum of PAC/CASG. However, a subset of tumors (25%) showed indeterminate features and was difficult to be classified even among expert HN pathologists. This may explain the controversy in classifying these tumors, which results in diagnostic uncertainty and poor interobserver agreement in this subgroup of tumors.

1231 Integrative Clinical and Genomic Analysis of Tonsillar Squamous Cell Carcinoma (T-SCC)

Bin Xu[1], Mohsin Jamal[1], Chad Vanderbilt[2], Sumit Middha[1], Anita Bowman[3], Venkatraman E. Seshan[1], Sean M. McBride[1], Michael Berger[1], Lara Dunn[1], Ian Ganly[1], Snjezana Dogan[1]
[1]Memorial Sloan Kettering Cancer Center, New York, NY, [2]Memorial Sloan Kettering Cancer Center, Denver, CO, [3]Memorial Sloan Kettering Cancer Center, Yeadon, PA

Disclosures: Bin Xu: None; Mohsin Jamal: None; Chad Vanderbilt: None; Sumit Middha: None; Anita Bowman: None; Venkatraman E. Seshan: None; Sean M. McBride: *Consultant*, Bristol-Myers Squibb; *Grant or Research Support*, Janssen; Michael Berger: *Consultant*, Roche; *Grant or Research Support*, Illumina; Lara Dunn: None; Ian Ganly: None; Snjezana Dogan: None

Background: The incidence of oropharyngeal SCC, especially those related to high risk papillomavirus (HPV), has been increasing over the past few decades. The oropharynx encompasses the palatine tonsil, base of tongue, posterior pharyngeal wall, and soft palate. To date, all published studies have grouped all these sites together. Large-scale studies focusing on a specific oropharyngeal subsite are lacking. In this study, we aimed to characterize the clinical behavior and molecular profile of a large cohort of T-SCC.

Design: Hybridization capture-based next generation sequencing (NGS) of 341-468 genes was performed using MSK-IMPACT™ platform in 103 T-SCCs, including 47 research and 56 clinical cases. The HPV/p16 status was determined using p16 immunohistochemistry, HPV *in situ* hybridization, and/or by HPV sequence reads detection in profiled samples. Clinical features and overall survival (OS) were collected.

Results: Eighty (78%) T-SCCs were HPV/p16-positive, whereas the remaining 23 (22%) were HPV/p16-negative. The frequency of HPV in T-SCC increased from 62% prior to 2010 to 92% after 2010. HPV-related T-SCC was associated with male gender (90% vs. 57%), non-smoker status (39% vs. 5%), and improved 5-year OS (64% vs. 47%, p<0.05). Compared with HPV-positive T-SCC, HPV-negative tumors were associated with a higher mutation burden, frequent *TP53*, *FGF3/FGF4/FGF19/CCND1*, *KMT2D*, and *NOTCH1* mutations (Figure 1), and recurrent alterations in p53, RB, cell cycle control and RTK signaling pathways (p<0.05). The most commonly altered genes in HPV-positive T-SCC were *PIK3CA* (24%), *TP63* (21%), *SOX2* (19%), *EP300* (16%), *FOXA1* (11%), *KMT2C* (10%), *RB1* (9%), *CREBBP* (9%), and *BCL6* (9%). The PI3K/Akt/mTOR and NOTCH pathways were commonly altered in HPV-positive TSCC: the frequency was 43% and 36% respectively.

Figure 1. Genetic alterations in T-SCC according to HPV/p16 status. * There was a significant difference between HPV/p16-positive and HPV/p16-negative group (Student's t test or Fisher's exact test, p<0.05).

Figure 1 - 1231

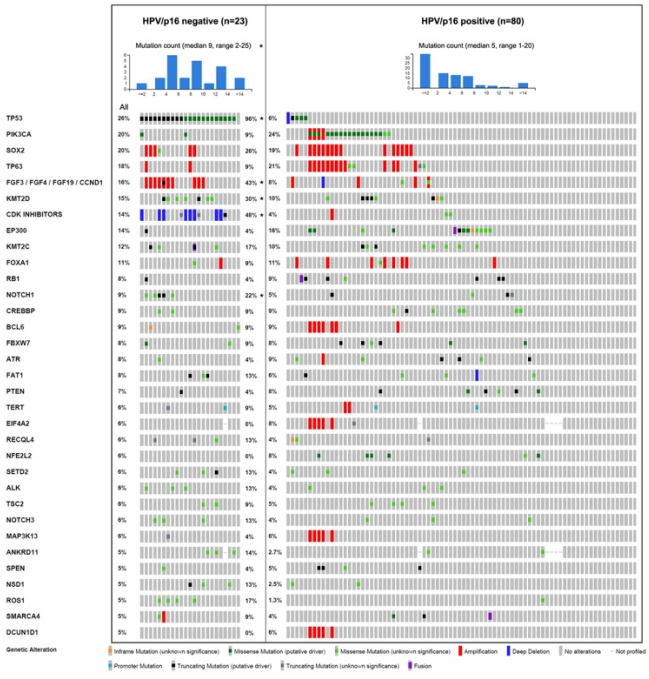

Conclusions: Here we present a comprehensive clinical and molecular analysis of the largest cohort of T-SCC. A high frequency of HPV is detected in T-SCC (especially in recent years), and is associated with a non-smoker status, male sex, and improved OS. HPV-related T-SCC is characterized by high frequency of alterations in PI3K/Akt/mTOR and NOTCH pathways.

1232 Semaphorin 4D Expression in Tumor Associated Inflammatory Cells in Oral and Mobile Tongue with Implications of Tumor Immune Suppression

Rania Younis[1], Sonia Sanadhya[2], Ioana Ghita[2], Manar Moustafa Helmy Elnaggar[3]
[1]UMB, Baltimore, MD, [2]University of Maryland Baltimore, School of Dentistry, Baltimore, MD, [3]University of Baltimore, Baltimore, MD

Disclosures: Rania Younis: None; Sonia Sanadhya: None; Ioana Ghita: None

Background: Tumor associated inflammatory cells (TAIs) play a critical role in tumor development and progression. Several molecules expressed by TAIs, have significant diagnostic, prognostic and therapeutic implications. The immune regulatory protein, Semaphorin 4D (Sema4D) represents an emerging prognostic biomarker and immunotherapeutic target. We have previously showed in an in vitro model the role of Sema4D produced by oral squamous cell carcinoma (OSCC) cell lines in inducing myeloid derived suppressor cells and upregulating signature immune suppressive enzymes and cytokines. SCC of the oral and mobile tongue represent a specific subset of head and neck squamous cell carcinoma that is induced mostly by smoking as well as other factors.

Design: Here we investigated Sema4D expression in TAIs of SCC of the oral and mobile tongue in a tissue microarray (TMA) of 50 cases, and 10 cases of normal adjacent to tumor using immunofluorescence.

Results: Sections showed Sema4D strong cytoplasmic granular positivity in inflammatory cells in the peri-tumoral stroma and infiltrating into the tumor island in 20 out of the 49 tumor cores (41%). The inflammatory cells had abundant cytoplasm with eccentric nucleus which prompted us to stain with the monocyte/macrophage marker CD163. We showed that Sema4D showed strong cytoplasmic granular positivity in the CD163 positive cells in the tumor stroma. Interestingly, some of the Sema4D/CD163 positive cells were bi-nucleated ranging in size to 10um. Whether the bi-nucleated Sema4D/CD163 positive cells are eosinophils, and whether eosinophils can express the CD163 (also known as hemoglobin scavenger receptor, and macrophage marker biomarker for monocytes/macrophages) is still not clear.

Conclusions: Our work describes for the first time Sema4D expression by TAIs in SCC of the oral and mobile tongue. It suggests Sema4D as a immunotherapeutic target and an emerging tumor biomarker for immune suppression in SCC of the oral and mobile tongue.

1233 A Series of 100 Ameloblastomas with 4 cases of Ameloblastic Carcinoma and 2 Cases of Metastasizing Ameloblastomas

Rania Younis[1], Donita Dyalram[2], Joshua Lubek[2], Robert Ord[2]
[1]UMB, Baltimore, MD, [2]UMB, SOD, Baltimore, MD

Disclosures: Rania Younis: None

Background: Ameloblastoma is the most common odontogenic tumor of epithelial origin. The estimated annual incidence of malignant ameloblastoma in the US (Ameloblastic Carcinoma (AC) and metastasizing ameloblastoma (MA)) is 1.79 cases per 10 million. About one third of the AC patients develop pulmonary metastases, and rarely lymph node metastases, with the maxillary lesions more likely to cause death, with average median survival of 5 years. While the overall 5 year survival for metastasizing ameloblastoma is 70%, although it depends on the site of metastases and surgical accessibility.

Design: Here we present a retrospective study of 100 ameloblastoma cases, with emphasis on the clinicopathological analysis, of 6 malignant cases.

Results: This study showed a higher rate of incidence of malignant ameloblstoma (6%) (6 out of 100 cases). The malignancy occurred in 4 males and 2 females, with age range from 16 to 85 years old (median 42.8). 2 cases showed benign histological features with evidence of distant metastases, while 4 cases showed malignant cellular features whether in the primary site (one case) or in the metastatic sites (3cases). The line of treatment for all entailed surgical resection. Four out of the 6 cases received radiotherapy (RT) and 2 cases received chemotherapy. The follow up ranged from 3 months (mo) till 131 mo, with two deaths one at 74 mo and the other at 4 mo of follow up.

	Gender	Age	Race	Type	Meatstasis	?	Outcome
Case 1	M	62	B	Malignant Ameloblastoma	Lymph Node, Lung, Kidney	Surgery, RT, Chemotherapy	Died 74 mo
Case2	M	85	W	Ameloblastic Carcinoma	Lung	Surgery, RT	LFU 30 mo
Case 3	F		B	Ameloblastic Carcinoma	Lymph node, Lung, Brain, Skull	Surgery, RT	Died 4 mo
Case 4	M	57	ME	Malignant ameloblastoma	Lung	Surgery, RT, Chemotherapy	A + Disease 131 mo
Case 5	F	16	B	Ameloblastoma Secondary Type	None	Surgery	A+W 14 mo
Case 6	M	37	W	Ameloblastic Carcinoma	Lymph Node	Surgery	A+W 3 mo

Conclusions: Here we present a cohort of ameloblastoma with 6 % incidence of malignancy. We emphasis the significance of the awareness of the histological features of AC and the ability of ameloblastoma with benign cellular features to metastasis as well as the treatment modalities, specially and in the presented cohort death occurred in 2 out of the 6 malignant ameloblastoma cases.